Antimicrobial resistance: pharmacodynamic approaches for explicating PD changes for bacterial strains that are susceptible and resistant to the antimicrobial drug treatments of choice

by

Jessica R. Salas

B.S., Clarkson University, 2016

A THESIS

submitted in partial fulfillment of the requirements for the degree

MASTER OF SCIENCE

Department of Diagnostic Medicine/Pathobiology
College of Veterinary Medicine

KANSAS STATE UNIVERSITY
Manhattan, Kansas

2020

Approved by:

Major Professor
Dr. Victoriya Volkova

Copyright

Abstract

Bacterial pathogens of humans and animals are becoming increasingly resistant to an array of antimicrobial drugs of different classes. This is not easily remedied because the timeline for development of new and effective antimicrobials is uncertain. One way to extend the useful life of existing antimicrobial drugs could be by optimizing the treatment regimens, originally designed for fully susceptible bacterial pathogen strains, to be efficacious for less susceptible strains. The optimized regimens can be designed through the pharmacokinetic-pharmacodynamic (PK-PD) mathematical modeling of the probable antimicrobial drug concentrations (the PK component) and its effects on the pathogen population dynamics (the PD component) *in vivo*. This approach requires the initial *in vitro* PD data and data modeling to project the PD responses of strains that have acquired resistance to the antimicrobials of choice.

This thesis involves two studies to analyze and compare the PD of existing antimicrobials against different bacterial species depending on the pathogen population characteristics such as density, and within a species against strains with and without acquired resistance to the drugs. In both cases, we conducted *in vitro* microbiological experiments to generate the data and mathematically modelled the data to describe the antimicrobial PD.

In our first study, we investigated the relationships between the antimicrobial's minimum inhibitory concentration (MIC) and the bacterial pathogen density for Gram-negative *Escherichia coli* and nontyphoidal *Salmonella enterica* subsp. *enterica* and Gram-positive *Staphylococcus aureus* and *Streptococcus pneumonia* (for n=4 strains per (sub)species and across the densities 1 to 8 $\log_{10}$(colony forming units (CFU)/mL)), for antimicrobial classes with bactericidal activity against the (sub)species. This study was focused on bacterial strains susceptible to the studied antimicrobials. We fit six candidate mathematical models to the

$\log_2$(MIC) *vs.* $\log_{10}$(CFU/mL) curves but did not identify one model best capturing the relationships across the pathogen-antimicrobial combinations. Gompertz and logistic models (but not a previously proposed Michaelis-Menten model) most often captured the relationships. Based on the study results, we have reported for the first time that bacterial density after which the MIC sharply increases and the intra-(sub)species between-isolate range of that density may depend on the antimicrobial's mechanism of action. We termed that density the MIC advancement-point. Capturing these dependencies could help determine using the MICs for which bacterial densities is most informative for designing effective antimicrobial treatment regimens.

In our second study, we investigated whether there are predictable changes in the PD parameter values among nontyphoidal *Salmonella enterica* subsp. *enterica* strains that are susceptible and those that have reduced susceptibility (due to acquiring specific genes encoding resistance) to the first-line treatment choice antimicrobials for serious salmonellosis in adults. The antimicrobials are the fluoroquinolone ciprofloxacin and cephalosporin ceftriaxone. We generated the antimicrobial PD data, and used a combination of the data PD modeling and statistical analysis of the estimated PD parameter values to test whether the acquired resistance genotype or imposed phenotype (the drug's MIC) provide insight pertaining to the direction and degree of changes in the PD parameter values. The study results suggest there are statistically significant trends in the PD parameter values between the drug susceptible and resistant nontyphoidal *Salmonella* strains for both ciprofloxacin and ceftriaxone. With further studies, this research could continue towards designing modifications of the treatment regimens to achieve efficacy against the strains with reduced susceptibility

Table of Contents

List of Figures

fitted to the data using the least-squares method. Best-fit parameter values for each of the six models were estimated and used to make the model predictions of $\log_2$(MIC) for 1 to 12 $\log_{10}$(CFU/mL) bacterial densities. The predictions are shown by lines: blue – von Bertalanffy, dark green – Gompertz, red – logistic, pink – Hill, gray – Michaelis-Menten, and cyan – exponential model. The line increment indicates the relative fit of the six models (each with best-fit parameter values) to the data for the representative isolate. Specifically, predictions of the model with highest adjusted R^2 are shown by a solid line; predictions of the other models are shown in the order of decreasing adjusted R^2 of the model by a long dashed, short-long dashed, short dashed, dashed-dotted-dotted, and dotted lines. The cross shows the MIC advancement-point density estimated using the curvature analysis of the predicted curve for each of the three models with highest adjusted R^2; the cross is of the same color as the line showing the curve predicted by the model. MIC – minimum inhibitory concentration of the antimicrobial. CFU – colony forming units of the bacterial population. 84

List of Tables

Acknowledgements

I would like to thank my advisor, Dr. Victoriya Volkova, for supporting me through my time as a research assistant and my Masters research, and for helping to guide me through important career decisions. She was there for me as a mentor on both a personal and professional levels and was always looking for ways to help me improve as a scientist.

I would also like to thank the other members of my research group. Tara Gaire was invaluable in my training as a microbiologist and lending his expertise on statistical modelling. I would also like to thank all of the undergraduate students who assisted with the time-kill experiments. This thesis would not have been possible without them.

Chapter 1 - Overview of relevant scientific concepts

Objective

This thesis involves two studies to analyze and compare the PD of antimicrobial drugs of choice against different bacterial species and depending on the bacterial population characteristics such as density, and within-species against strains with and without acquired resistance to the drugs. The pharmacodynamic relationships were studied for *Escherichia coli*, nontyphoidal *Salmonella enterica* subsp. *enterica*, *Staphylococcus aureus*, and *Streptococcus pneumoniae*.

Purpose

Each year in the United States, over 2.8 million Americans experience diseases caused by infections by antimicrobial resistant (AMR) bacterial strains, and over 35,000 of those people succumb to the diseases due to a lack of effective treatment options (*1, 2*). Although these numbers appear to signal a decrease in the occurrence and impact of such diseases since 2013 (*3*), AMR infections is still a major public health concern in the U.S. and globally.

Bacterial pathogens of humans and animals are becoming increasingly resistant to existing antimicrobial drugs of different classes. This is not easily remedied, as the timeline for development of new and effective antimicrobials is unknown (*4-6*). Moreover, even when effective antimicrobials are developed, bacterial pathogens can rapidly evolve, acquire, and spread resistance (*5*). Therefore, it is imperative that the useful life of the existing antimicrobial drug classes is extended. One possibility is to modify the treatment regimens by existing antimicrobials so that the regimens are efficacious against strains with acquired resistance to the drugs (*7*). Then a recourse to newest antimicrobial drugs would be needed less often. The modified regimens could be designed using the pharmacokinetic-pharmacodynamic modeling (*2, 7, 8*). This requires *in vitro*

data on the PD of the antimicrobials against the pathogen strains with and without acquired resistance to the drugs. Through proper PD modelling of such data we could project the PD responses of strains that have acquired resistance to the antimicrobials (*9*).

The World Health Organization (WHO) defines a list of critically important antimicrobial drug classes for human medicine. Based on the 2019 list, the highest priority classes are: fluoroquinolones, 3rd and higher generation cephalosporins, macrolides and ketolides, glycopeptides, and polymyxins (*10*). Of particular interest to our studies are the classes of fluoroquinolones and cephalosporins, since these include antimicrobials recommended for treating serious salmonellosis in adults in the U.S., specifically, the fluoroquinolone ciprofloxacin and 3rd generation cephalosporin ceftriaxone. In the WHO's 2014 Antimicrobial Resistance: Global Report on Surveillance, nontyphoidal *Salmonellae* were listed as a "selected bacteria of international concern" (*11*). This is because of the emerging trends of rising occurrence of such *Salmonellae* resistant to fluoroquinolones, *e.g.*, in South-East Asia and the Western Pacific regions, while the pathogen remains a leading cause of gastroenteritis worldwide (*11*).

In a 2019 report, the U.S. CDC classified AMR patterns in bacterial pathogens into categories of "urgent", "serious", and "concerning" threats (*1*). Antimicrobial resistant nontyphoidal *Salmonella enterica* subsp. *enterica* is one of the "serious" threats, along with vancomycin-resistant *Enterococci* (VRE) and multidrug-resistant *Pseudomonas aeruginosa*. The priority is nontyphoidal *Salmonellae* which have become resistant to the first-line treatments of choice, which for adults in the U.S. are the cephalosporin ceftriaxone and fluoroquinolone ciprofloxacin. Nontyphoidal *Salmonellae* cause 1.35 million infections in the U.S. each year and approximately 420 deaths (*1, 3*). Antimicrobial resistant nontyphoidal *Salmonellae* are responsible for approximately 212,500 human infections and 70 deaths annually (*1, 12*). Prevalence of both

the types of infections have been on the rise since 2013 (*1, 3*). Nontyphoidal *Salmonella* spp. are the number one bacterial foodborne pathogen linked to hospitalizations in the U.S. and are also the leading cause of death from foodborne illness (*1, 12*). Common modes of infection with nontyphoidal *Salmonellae* are consuming contaminated food products and coming in contact with contaminated fecal matter of infected humans or animals (*1, 3, 12*). The U.S. population are at risk of diminishing treatment options for infections caused by Gram-negative bacteria, with that of AMR nontyphoidal *Salmonellae* as a prime example (*1, 3*).

Antimicrobial resistance: Definitions and control approaches

When humans and animals become ill due to a bacterial infection, the contemporary treatment of choice is an antimicrobial drug known to be effective against fully susceptible strains of the bacterial pathogen. As the result of the treatment, in some cases bacteriological cure is achieved, that is – the pathogen population is eradicated (*2, 13*). In other cases, the pathogen population is sufficiently reduced for the patient immune system to clear the infection (*2, 13*). Yet in other cases, a part of the bacterial population develops or acquires antimicrobial resistance. The term antimicrobial resistance (AMR) refers to the situation when a bacterial strain develops or acquires genes encoding resistance mechanisms that make the infection caused by the strain unamenable to treatment with that antimicrobial under the current treatment regimen for the disease (*1, 12*). This is different from yet another scenario of the pathogen population developing phenotypic non-susceptibility to the antimicrobial during the treatment, which is termed persistence and is discussed below. The genes encoding AMR can spread rapidly among bacterial strains and even across species (*1, 3*). To distinguish between intrinsic and acquired resistance, intrinsic resistance is when a bacterial species is naturally non-susceptible to the effects of the antimicrobial, *e.g.*, because of not containing the drug targets.

Conversely, acquired resistance is a phenomenon when a strain of a bacterial species naturally susceptible to the antimicrobial loses a degree of the susceptibility, due to a mutation in a gene or due to acquiring a gene from other strains through horizontal gene transfer, with the gene encoding a mechanism of resistance to the drug (*14*). Horizontal gene transfers occur via bacterial conjugation, transduction by bacteriophages, and transformation, which is a process when bacteria uptake foreign genetic material from their surrounding environment. Via conjugation, bacteria horizontally transfer mobile genetic elements, such as plasmids and transposons, and thus share the genetic material between otherwise unrelated clonal populations (*14*). Many of the fluoroquinolone and cephalosporin resistance genes are plasmidic and thus are spread among bacterial strains via plasmid conjugation (*15, 16*) .

Bacterial pathogens with acquired AMR (especially strains resistant to ≥3 antimicrobial drug classes, which are referred to as multi-drug resistant) are one of the most pressing public health concerns globally, according to the WHO (*11*). The WHO provides suggestions to remedy this global health problem. For example, some of the suggestions introduced in 2011 were to devise new monitoring and surveillance programs for antimicrobial drug use, tackle the sale and use of counterfeit antimicrobials, and develop funding opportunities and incentives for research regarding AMR (*17*). In the U.S., the Food and Drug Administration (FDA) has created funding mechanisms for projects collecting data needed to design antimicrobial use surveillance systems for human and animal populations. The U.S. FDA, along with Department of Health and Human Services, and Department of Agriculture also fund AMR monitoring efforts, including the National Antimicrobial Resistance Monitoring System (NARMS) established in 1996.

At a community level, it is imperative that healthcare professionals understand the guidelines for stewardship of prescribed antimicrobials, and the public understand the proper use

of the drugs. The misuse of antimicrobials for illnesses that do not require them contributes to the development of AMR worldwide (*17*). Furthermore, in some countries antimicrobial drugs can be accessed over the counter. Results of a systematic review of literature point out in Africa there can be up to 100% non-prescription use of antimicrobials by the public (*11, 18*). Within healthcare facilities, strict biosecurity, sanitation, and handwashing practices reduce spread of bacteria, including AMR bacteria, from patient-to-patient and between staff and patients (*1, 3, 11*). Another component approach of combatting AMR is limiting the usage of antimicrobials in food animals. This could bound the spread of AMR from food-animal production systems into the environment and the occupational exposure of workers in animal farms and slaughter and processing facilities (*1, 3, 11, 12*), as well as AMR transmission to general public via the food chain (*19*).

Ciprofloxacin: Mechanisms of action and bacterial resistance

Ciprofloxacin belongs to the class of drugs called fluoroquinolones. It was first approved for human use by the U.S. FDA in 1987 and has been used to treat a multitude of diseases (*20-23*). It is currently approved for the treatments of urinary tract infections, sexually transmitted diseases, gastrointestinal infections, salmonellosis, and other (*24*). It is one of the most widely used antimicrobial drugs in human populations world-wide (*20*). Ciprofloxacin is a broad spectrum antimicrobial, active against Gram-negative and select Gram-positive bacteria (*24*). Ciprofloxacin inhibits the bacterial population growth by targeting two bacterial enzymes: DNA gyrase and DNA topoisomerase IV (*20-22*). This leads to creation of the DNA/topoisomerase/drug ternary complex that leaves the bacteria unable to continue on in the replication process (*20, 25, 26*). Fluoroquinolones also increase the creation of reactive oxygen species in the bacteria, increasing the bacterial death rate (*20, 23*).

Bacteria can become resistant to a class of antimicrobial drugs through different mechanisms on a cellular level. For the class of quinolones, the major mechanisms are alterations in the target enzymes, drug deactivation intra-cellular, and activation of bacterial efflux pumps (*27*). The former two mechanisms are mediated by chromosomal and the third by plasmidic bacterial genes. In the case of the target alteration quinolone resistance, the most common mutations are in the genes encoding the DNA gyrase and topoisomerase IV, with the greatest level of resistance conferred when both the enzymes have been altered (*27-33*). This occurs through point mutations at a single or multiple amino acids, primary the serine or acidic residues that act to anchor the water-ion bridge of the subunits of these enzymes (*27, 28, 34-36*). A second family of genes that confers quinolone resistance is aac(6′)-Ib-cr. These encode a mutant aminoglycoside acetyltransferase that can work to deactivate ciprofloxacin in the bacteria, rendering it ineffective at killing the bacteria (*27, 37, 38*).

Plasmid-mediated antimicrobial resistance can be transmitted both vertically from generation to generation of the bacteria and horizontally. Through the horizontal gene transfer by mobile genetic elements, resistance to multiple classes of antimicrobials can co-spread (*15, 27, 39-41*). The first group of plasmidic genes conferring quinolone resistance is the *qnr* family of genes. Qnr genes encode different types of proteins, which protect the DNA gyrase and topoisomerase IV enzymes from inhibition by the drugs. They also can stop quinolones from being able to form cleavage complexes by binding to gyrase and topoisomerase IV, directly (*15, 27, 41-45*). Another group of plasmidic genes that contribute to quinolone resistance are genes encoding the bacterial efflux pump function, such as OqxAB, QepA1, and QepA2 (*15, 27, 46, 47*). The efflux pumps act to pump drug out of the bacteria before it has a chance to act on them.

Ceftriaxone: Mechanisms of action and bacterial resistance

Ceftriaxone is a third-generation cephalosporin drug. It is a broad-spectrum antimicrobial, active against most Gram-negative and select Gram-positive bacteria. It is commonly used to treat urinary tract infections, meningitis, bone and joint infections, septicemia, and other (*48*). Ceftriaxone inhibits bacterial cell wall synthesis during the replication process (*49*). Inhibition of this imperative synthesis leads to a weakening of the cell wall and death of the dividing bacteria, thus preventing the bacterial population growth. Notably, antimicrobials of this class are known to rarely cause adverse side effects in mammalian hosts, because the mammalian host cells do not contain the target peptidoglycan, rendering them resistant to the antimicrobial effects (*50*).

Cephalosporins are a class of *β*-lactam antimicrobials. In 1940, it was discovered that a culture of *Escherichia coli* deactivated penicillin, the first widely used *β*-lactam drug. This is based on the bacteria producing *β*-lactamases, which hydrolyze chemical bonds present in the ring structure of *β*-lactams, rendering them inactive (*51, 52*). Today, many different types of *β*-lactamases have been discovered, and have been divided amongst different classes based on their mechanism of drug inactivation (Bush–Jacoby system) or the amino acid structure of the enzyme itself (the Ambler system) (*51, 53-57*). Despite the classification systems, the nomenclature of >2,000 *β*-lactamases is somewhat arbitrary, with some of the enzymes named after the patients yielding the bacterial isolates, bacterial species the enzymes were first discovered in, the geographic location at which they were discovered, or chemical or physical properties/idiosyncrasies, for example (*58*). The drug hydrolysis by *β*-lactamases is the most common mechanism of bacterial resistance against *β*-lactam antimicrobials (*16, 59*). Other resistance mechanisms include alteration of target proteins to which the drugs bind, and partial

disablement or destruction of porin structures within the bacterial cell wall (*16, 59, 60*). These porin structures allow *β*-lactams to enter the bacteria to bind to penicillin-binding proteins to delay or stop the bacterial growth (*16, 59, 60*). Activation of the bacterial efflux pumps can also contribute to a reduced susceptibility to *β*-lactams (*16, 59, 60*).

Persisters

In 1944, Joseph Bigger performed an experiment where he exposed a culture of *Staphylococcus pyogenes* (*aureus*) to high concentrations of penicillin. He discovered that roughly 1 in a million of the *Staphylococcus pyogenes* cells were not eradicated by the antimicrobial, even at its high concentrations. Further evaluation showed these cells did not acquire mutations conferring resistance mechanisms to the antimicrobial, instead, the cells appeared to be phenotypic variants "tolerant" to the drug. Today, such variants phenotypically tolerant to the antimicrobial are termed persisters (*61, 62*). It has been hypothesized that different types of persisters can be present in a clonal bacterial population (*63, 64*). Two main types are coined as type I and type II persisters. Type I persisters are described as cells in the initial clonal population that are in a non-growing state due to reacting to a stress signal. Such persisters are tolerant to antimicrobials because of their dormant growth state, since many antimicrobials target structures in actively replicating bacteria (*62*). Type II persisters are characterized as cell subpopulations that randomly develop a low growth rate state during the exponential growth phase of the culture (*63, 65*). Different conditions can affect the collective antimicrobial tolerance of persisters and their rate of occurrence in a bacterial population. Some studies showed a bacterial culture maintained for a longer period of time has a larger proportion of persisters (*62, 66*). Others showed that cultures of a similar starting density but exposed to different antimicrobial drugs, in the concentrations lethal to the non-persister subpopulations,

have different densities of the remaining persisters (*67*). Others highlighted that merely being in the presence of minute antimicrobial concentrations will induce a stress response in the bacterial population, and the persister frequency will be higher compared to that in an antimicrobial free environment (*68*). What triggers persistence in a bacterial subpopulation is still not fully understood (*62, 64*).

Modeling antimicrobial pharmacodynamics

The field of antimicrobial pharmacodynamics (PD) aims to elucidate the dynamics of action of different antimicrobials on populations of bacterial pathogens, and hence the bacteriologic and clinical outcomes of antimicrobial drug treatments of diseases caused by the pathogens in hosts of interest (*2, 8, 69*). Data on the antimicrobial's PD against the pathogens could allow optimizing the treatment regimens for the diseases, to increase the likelihood of the bacteriological cure *in vivo* (*70-72*).

One of first approaches using the PD principles to optimize the antimicrobial treatment regimens was undertaken by Harry Eagle in the 1940's and 1950's. Eagle and his colleagues used a mouse model of a thigh infection with *β*-hemolytic streptococci and pneumococci treated with penicillin to evaluate how varying drug concentrations effected the pathogen population at the infection site. They found that a property of the drug concentration-time curve was predictive of the treatment efficacy. Specifically, the treatment efficacy was directly related to the duration of time when the drug concentration at the infection site remained above the drug's minimum inhibitory concentration (MIC) for the pathogen strain (*70, 73*). This has also been shown for other *β*-lactam drugs and bacterial pathogens, for the drug-susceptible strains, and is referred to as a "time-dependent" PD (*70*). In this case, the antimicrobial effect on the bacterial population levels off at the drug concentrations of low multiples of the MIC, with no further increase in the

effect even if the drug concentration further increases (*70, 73*). Other properties of the drug concentration-time curve are predictive of the treatment efficacy for antimicrobials of other classes. For quinolones, the PD is "concentration-dependent" for the drug-susceptible strains, that is, the antimicrobial effect on the bacterial population continues to increase as the drug concentration further increases (beyond low multiples of the MIC), as has been observed *in vitro* and *in vivo* (*9, 70*). In this case, the treatment efficacy is most correlated to the ratio of the area under the drug concentration-time curve (AUC) at the infection site to the MIC for the strain (AUC/MIC ratio), during each 24 hours of the treatment (*70*). Importantly, historically, these PD properties were defined based on the data for bacterial pathogen strains fully susceptible to the antimicrobials. Whether the PD of an antimicrobial changes between the susceptible strains and strains with acquired resistance to the drug is the focus of our second study.

Different PD models have been introduced to capture differences in the dynamics of interactions between antimicrobials and bacterial populations. One commonly used model is termed the E_{max} model (E_{max} – maximum effect), which can capture the relationship between the drug concentration and its effect on the bacterial population growth rate (*72*, *74*). Two formulations of this model are included below as examples. These are formulated with I_{max} – maximum inhibitory effect on the bacterial population growth.

Inhibitory baseline sigmoid I_{max} model

$$E(C) = E_0 - \frac{I_{\max} \times C^H}{IC^H_{50} + C^H}$$

Inhibitory fractional sigmoid I_{max} model

$$E = E_0 \times \frac{1 - I_{\max} \times C^H}{IC^H_{50} + C^H}$$

where:

E(C) – bacterial population growth rate ($\log_{10}$(colony forming units (CFU)/mL)/hour) when exposed to the antimicrobial concentration *C*

C – antimicrobial concentration (μg/mL)

E_0 – bacterial population growth rate in the absence of antimicrobial exposure (the baseline growth rate) ($\log_{10}$(CFU/mL)/hour)

H – Hill-coefficient reflecting steepness of the relationship between an increase in the antimicrobial concentration and an increase in the inhibition of the bacterial population growth (dimensionless)

IC_{50} – Drug concentration at which 50% of the maximal inhibition in the bacterial population growth occurs (μg/mL)

I_{max} – Maximal inhibition of the bacterial population growth at high antimicrobial concentrations (dimensionless)

To project the antimicrobial action against the pathogen populations *in vivo*, data are generated *in vitro* on the antimicrobial PD against similar strains of the pathogen and PD models capturing the data are identified. Then, the PD model projections are combined with the projections of the drug distribution in the treated host (that is, the drug PK projections), to perform the integrated PK-PD modeling of the efficacy of the treatment regimen in reducing the pathogen population at the infection site in the host (*75*). Thus, the PK-PD modeling can be used to project how effective different antimicrobial treatment regimens will be against the infection by a pathogen strain with specific characteristics, and giving the disease caused and PK of the drug in the treated host with its characteristics. It is through the PK-PD modelling that the treatment regimens could be optimized to ultimately improve the patient treatment outcomes.

Chapter 2-Modeling the antimicrobial pharmacodynamics for bacterial strains with vs. without acquired resistance to fluoroquinolones or cephalosporins

Jessica R. Salas[1], Tara Gaire[1,2], Victoria Quichocho[1], Emily Nicholson[1], Victoriya V. Volkova[1,2,*]

[1] Department of Diagnostic Medicine/Pathobiology,

[2] Center for Outcomes Research and Epidemiology,

College of Veterinary Medicine,

Kansas State University, Manhattan, KS 66506, USA

* Corresponding author

Phone: +1 (607) 220-8687. e-mail: vv88@vet.k-state.edu (Dr. Victoriya Volkova).

Abstract

Antimicrobial resistance is a threat to therapeutic options for human and animal bacterial diseases worldwide. The pipeline of new and effective antimicrobial drugs is uncertain. The current treatment regimens by existing antimicrobial drug classes were designed for bacterial pathogen strains that were fully susceptible to the drugs. It is pertinent that we expand the useable lifetime of the existing antimicrobial drug classes, for example, by optimizing the treatment regimens to achieve efficacy against pathogen strains that are no longer fully susceptible. This requires data on the pharmacodynamics (PD) of the antimicrobials against such strains. In this study, we generated the required data for the fluoroquinolone ciprofloxacin and cephalosporin ceftriaxone for nontyphoidal *Salmonella enterica* subsp. *enterica* strains with varying levels of acquired resistance to the drugs, as well as for fully susceptible strains. Strains of majority of genotypes of reduced susceptibility to fluoroquinolones or cephalosporins that have been reported in the U.S. were included. The strains have been isolated from human infections, food-animal products sold in retail, and food-animal production chains in the U.S. We compared the fit of six mathematical models to capture the PD for each antimicrobial and strain category. The inhibitory baseline sigmoid I_{max} (or E_{max}) model was best-fit for the PD of each antimicrobial against a majority of the strains, and yielded estimates of the PD parameter values for each antimicrobial and strain. There were statistically significant differences in the PD parameter values among the strain categories for each antimicrobial. The results suggest predictable multi-parameter changes in the PD of each of these first-line antimicrobials depending on the *Salmonella* strain's susceptibility phenotype (*i.e.* the antimicrobial's minimum inhibitory concentration for the strain), and potentially associated with the strain carrying specific genes conferring the reduced drug susceptibility. This warrants a future investigation of

whether the current treatment regimens could be safely modified to achieve efficacy in treating infections by strains of some of the reduced susceptibility pathogen types.

Introduction

Nontyphoidal *Salmonella enterica* subsp. *enterica* are the number one bacterial foodborne pathogen linked to hospitalizations and death in cases of foodborne illness in the U.S. (*1, 12*). Antimicrobial drug resistant (AMR) nontyphoidal *Salmonellae*, specifically, cause ~212,500 infections in the U.S. each year and are responsible for ~70 deaths (*1*). The challenge of treating infections by the AMR strains is not easily remedied, because the time-line for development of new effective antimicrobials is uncertain (*4-6*). Devising approaches to optimize the treatment regimens by existing antimicrobials is therefore of paramount importance, in order to expand the useable lifetime of the effective antimicrobials we have. Developing these approaches requires understanding through *in vitro* and *in vivo* studies of the antimicrobial pharmacokinetics in the target hosts, and the antimicrobial pharmacodynamics against the pathogen populations at the sites of infection in the hosts (*2, 8, 13, 69, 76*).

The minimum inhibitory concentration (MIC) of an antimicrobial for a bacterial strain is a measurement of the strain's phenotypic susceptibility. Currently, it is used as a single parameter of the antimicrobial pharmacodynamics (PD), along with modeling the drug pharmacokinetics (PK) in the target host, in the design of the treatment regimen. Specifically, in the integrated PK-PD models, the duration of time that the drug concentration at the site of infection remains above the MIC for the pathogen strain, or the area under the concentration-time curve (AUC) above the MIC, is projected (*2, 8, 9*). In this framework, the antimicrobial administration regimen is designed, that is, the drug dosage, length of time between the doses, and length of the overall course of treatment are optimized to achieve the desired duration or AUC above MIC (*2, 8*). Multi-parameter PD models, however, further capture the antimicrobial PD against the pathogen population depending on the drug concentration that inevitably varies at the site of infection during

the treatment, and thus are superior tools for the regimen design compared to the MIC alone (*7, 9, 72, 76, 77*). Another aspect is that the current antimicrobial treatment regimens have been designed using the PD parameter values (whether the MIC or those from multi-parameter PD models) for pathogen strains that were fully susceptible to the drugs. Less susceptible strains are considered to differ only by the MIC of the antimicrobial (*2, 72*). However, evidence is emerging that all the antimicrobial's PD parameter values, and not only the MIC, are changing between the fully susceptible strains and strains with acquired resistance to the drug (*7, 9, 78*). It is unknown whether the changes are predictable and how they relate to the strain's antimicrobial susceptibility phenotype or genotype. It is also unknown if for a given antimicrobial the same mathematical model captures the PD across the strain categories. Several models have been shown to capture various forms of the relationships between an antimicrobial drug concentration and its effects on the bacterial population (*72*, *74, 77*, *79*).

In this study, we investigated the PD against nontyphoidal *Salmonella* strains that are susceptible or have acquired resistance for the first-line treatment choices for serious salmonellosis in adults, the fluoroquinolone ciprofloxacin and cephalosporin ceftriaxone. Strains fully susceptible to fluoroquinolones or extended spectrum cephalosporins, and strains carrying majority of reported in the U.S. gene families conferring reduced susceptibility to these drug classes were included (**Tables 1-2**). We investigated whether the strain phenotypic susceptibility to the antimicrobial or specific drug resistance genes carried are associated with the ranges of the antimicrobial's PD parameter values.

Materials and methods

Bacterial strains. Fifty-three nontyphoidal *Salmonella enterica* subsp. *enterica* strains were used. The strains were isolated and shared by the U.S. National Antimicrobial Resistance Monitoring System (NARMS), Centers for Disease Control and Prevention (CDC), and colleagues at the University of Nebraska Medical Center (strains acquired within the NARMS activities in Nebraska). Along with the strains, those organizations shared data on the strain serotype and AMR gene content determined via the whole genome sequencing and annotation. Based on the data, strains with majority of reported in the U.S. gene families conferring reduced susceptibility to fluoroquinolones or extended spectrum cephalosporins were selected for the study (**Tables 1-2**). In the ciprofloxacin PD study, *n*=24 strains were used (**Table 1**). In the ceftriaxone PD study, *n*=29 strains were used (**Table 2**).

MIC estimation. We measured the phenotypic susceptibility of each strain to ciprofloxacin or ceftriaxone. The strains were stored in brucella broth with 15% glycerol (Remel^{TM}, Lenexa, KS, USA) at −80 °C. Tryptic soy agar supplemented with 5% sheep blood (BAP, Remel^{TM}, Lenexa, KS) was used for the strain streaking and plating between the experiments. High purity (analytical standards) forms of ceftriaxone and ciprofloxacin were purchased from Sigma-Aldrich, Inc. (St. Louis, MO, USA). The antimicrobial's MIC for a bacterial strain was determined by the broth microdilution assay aerobically in cation-adjusted Mueller-Hinton broth (CA-MHB, Remel^{TM}), following the procedures recommended by the Clinical and Laboratory Standards Institute (CLSI) (*80*). The standard CLSI recommended assay protocol is with a single starting drug concentration; this only returns the drug double-dilution interval within which the MIC is, with a double-dilution margin of error in both the directions. This was an insufficient precision of the MIC estimation to design informative time-kill

experiments with the antimicrobials. We used multiple approaches to get a more precise MIC estimate. First, for each antimicrobial and strain, the broth microdilution assay was performed with a variety of the starting drug concentrations and otherwise following the CLSI recommended procedures; the MIC was estimated from the data assuming that in each assay the strain's MIC was in the middle of the drug double-dilution interval identified (unpublished data). Second, we performed the E-test® in accordance with the manufacturer's recommendations (bioMérieux, Marcy-l'Étoile, France). After evaluating the precision and repeatability of the MIC estimates, we used the MIC estimate from the multiple broth microdilution assays coupled with the mid-point data analysis for a strain categorized as intermediately susceptible or resistant to ceftriaxone or ciprofloxacin. We used the E-test® MIC estimate for a susceptible strain. The categorization of a strain as susceptible, intermediately susceptible, or resistant was based on the CLSI recommended clinical interpretive breakpoints for ceftriaxone or ciprofloxacin MIC for nontyphoidal *Salmonellae* treatments in humans.

Time-kill experiments. Time-kill experiments were conducted for 24 bacterial isolates with ciprofloxacin and 29 with ceftriaxone, following previously described procedures (*9, 75*). A strain was plated from frozen culture on BAP and aerobically incubated overnight at 37 °C. From the overnight plate, several bacterial colonies were inoculated in Mueller Hinton 2 broth (MHB, Remel™), which was incubated aerobically at 37 °C with shaking (200 rpm) overnight. The overnight culture was diluted ~1:175 into fresh MHB and incubated at 37 °C with shaking (200 rpm) for 1 hour to allow the bacterial population to enter the exponential growth phase. The culture was then diluted 1:40 into each of the individual flasks containing MHB with a different concentration of ceftriaxone or ciprofloxacin (0.5, 0.75, 1, 2, 3, 5, 8, or 10 multiples of the drug's MIC for the strain) and into a control flask with fresh MHB (no drug added). The drug-free

control and drug-exposed cultures were incubated aerobically at 37 °C with shaking (200 rpm), and sampled at 0, 1, 2, 3, 4, 5, 6, 7, 8, 12, and 24 hours of incubation. Each sample of the cultures underwent 10-fold serial dilutions in a 0.9% sterile saline solution, and 3 to 4 of the dilutions were spread plated on BAP. These plates were incubated aerobically at 37 °C for 24 hours, at which time the colony counts were determined. The colony counts from all the dilutions plated from a given culture at a time-point were transformed as $\log_{10}$(CFU/mL); the transformed data were averaged providing an estimate of the bacterial population density (colony forming units (CFU)/mL) in the culture at the time-point in that experiment replicate. For each strain, a time-kill experiment on a given date was performed including the control culture (no drug added) and cultures with each 0.5, 0.75, 1, or 2 multiples of the MIC drug concentrations, or, including the control culture and cultures with each 3, 5, 8, or 10 multiples of the MIC drug concentrations. Experiments with each of the two arrangements for the strain-antimicrobial combination were performed in replicate (on different days).

Pharmacodynamic modeling and statistical analyses. The bacterial population density estimates for the strain, antimicrobial, MIC multiple drug concentration or no-drug control, and time-point were averaged between the replicates of the experiment. These mean estimates of the bacterial density were plotted against the experiment time in hours, for each drug concentration or no-drug control. The plotted curve reflected the strain's population density under that drug concentration or in the control throughout a 24-hour experiment. The maximal hourly slope of the curve during any time-period in the experiment was identified. For this, the hourly slope was estimated for each of time-windows from 1 to 23 hours, starting from the 0 hour of the experiment, and then for each of time-windows from 1 to 22 hours starting from the 1 hour time-point, and the maximal slope identified. This provided an estimate of the maximal hourly bacterial population

growth or decline rate when exposed to that drug concentration or in the absence of antimicrobial exposure (in the no-drug control case). These estimates were collated for the strain, yielding the antimicrobial concentration-bacterial population growth/decline rate data-set. Six candidate models were compared in capturing the antimicrobial's PD for the strain. Each model was fitted as a non-linear regression model using the least-squares method, by regressing the maximal hourly bacterial population growth/decline rate on the drug concentration (0 for the control) for the strain. The models were:

(1) Inhibitory baseline sigmoid I_{max} model – form 1:

$$E(C) = E_o - \frac{I_{\max} \times C^H}{IC_{50}^H + C^H}$$

(2) Inhibitory baseline sigmoid $I_{\max}$ model – form 2:

$$E = E_0 - \frac{I_{\max}}{IC^H{}_{50} + C^H}$$

(3) Inhibitory fractional model:

$$E = E_0 \times \frac{1 - C}{IC_{50} + C}$$

(4) Inhibitory fractional sigmoid model:

$$E(C) = E_0 \times \frac{1 - C^H}{IC^H{}_{50} + C^H}$$

(5) Inhibitory fractional I_{max} model:

$$E = E_0 \times \frac{1 - I_{\max} \times C}{IC_{50} + C}$$

(6) Inhibitory fractional sigmoid I_{max} model:

$$E = E_0 \times \frac{1 - I_{\max} \times C^H}{IC^H{}_{50} + C^H}$$

where:

E(C) – bacterial population growth rate ($\log_{10}$(CFU/mL)/hour) when exposed to the antimicrobial concentration *C*

C – antimicrobial concentration (μg/mL)

E_0 – bacterial population growth rate in the absence of antimicrobial exposure ($\log_{10}$(CFU/mL)/hour)

H – Hill-coefficient reflecting steepness of the relationship between an increase in the antimicrobial concentration and an increase in the inhibition of the bacterial population growth (dimensionless)

IC_{50} – Drug concentration at which 50% of the maximal inhibition in the bacterial population growth occurred (μg/mL)

I_{max} – Maximal inhibition of the bacterial population growth at high antimicrobial concentrations (dimensionless)

To identify the model that best fits to the PD data for each antimicrobial and strain (the antimicrobial concentration-maximal bacterial population hourly growth/decline rate data), the six models were ranked on their relative fit. The models were ranked based on the Akaike information criterion (AIC) values (with a lower AIC indicating a better fit model), and then based on the adjusted coefficient of determination, R^2, values (with a higher R^2 indicating a better fit model). The AIC is applicable for evaluating the relative fit to a dataset of non-linear regression models that contain different numbers of parameters. The results were summarized across the strains for each antimicrobial. For both ciprofloxacin and ceftriaxone, the PD model ranked "best" fit most often across the strains was identified, and the estimates of the model parameter values for

individual strains were extracted. Statistical analysis was performed to test for trends in the PD parameter values depending on the strain's phenotype or genotype of susceptibility to the antimicrobial. The PD modeling and statistical analyses were performed in the SAS® University Edition software for Windows (SAS Institute Inc., Cary, NC).

Results and discussion

Relative fit of candidate mathematical models to the pharmacodynamic data

Relative fit of the six candidate models to the antimicrobial concentration-maximal bacterial population hourly growth/decline rate data for individual strains of nontyphoidal *Salmonellae* is summarized for ciprofloxacin in the **Supplementary Table 1** and for ceftriaxone in **Supplementary Table 2**. For ciprofloxacin, the inhibitory baseline sigmoid I_{max} model – form 1 (equation (1) above) was best fit to the PD data for 96% of the strains (*i.e.*, for 23 out of 24 strains). The inhibitory fractional I_{max} model (equation (5) above) was best-fit for the other strain in the ciprofloxacin PD study. For ceftriaxone, the inhibitory baseline sigmoid I_{max} model – form 1 (equation (1) above) was best fit to the PD data for 86% of the strains (*i.e.*, for 25 out of 29 strains). The inhibitory fractional I_{max} model (equation (5) above) was best-fit for the other 4 strains in the ceftriaxone PD study. To enable statistical analysis of trends in the PD parameter values among the strain categories, the inhibitory baseline sigmoid I_{max} model – form 1 (equation (1) above) was accepted as the best fit model for all the strains in both ciprofloxacin PD and ceftriaxone PD.

Trends in the ciprofloxacin pharmacodynamics parameter values

The time-kill experiment results with ciprofloxacin are included in the **Supplementary Figures 1-2**. The results suggest the ciprofloxacin PD varies depending on the strain phenotypic (as reflected by the drug MIC) and genotypic (identities of the fluoroquinolone resistance genes carried) susceptibility to the antimicrobial. For all the strains, the PD parameter value estimates of the inhibitory baseline sigmoid I_{max} model – form 1 and the model fit statistics are shown in **Table 3**. The model projections are plotted against the antimicrobial concentration-bacterial population hourly growth/decline rate data for the individual strains in **Figures 3-5**.

The strain population growth rate in the absence of antimicrobial exposure, E_0, represents the strain fitness or intrinsic growth potential. This is also a parameter that impacts the PD of antimicrobials acting on the replicating bacterial cells, as has been shown by us for fluoroquinolones (*75*) and by others for β-lactams (*e.g.*, (*81*)). We categorized the *Salmonella* strains in their phenotypic ciprofloxacin susceptibility based on the ciprofloxacin MIC and the corresponding CLSI-set clinical interpretative breakpoints for salmonellosis treatment in humans. The categories were the susceptible, intermediately susceptible, and resistant to ciprofloxacin strains. The mean intrinsic growth rate of the ciprofloxacin resistant strains was statistically significantly lower, and less variable compared to that of the susceptible or intermediately susceptible strains (Kruskal-Wallis one way analysis of variance p-value=0.060, $n = 24$ strains; **Figure 1A**). The mean E_0 was lowest for the strains with chromosomal fluoroquinolone resistance genes, increasing for the strains with plasmidic fluoroquinolone resistance genes, and further increasing for the susceptible strains, but this trend was not statistically significant (Kruskal-Wallis one-way analysis of variance p-value=0.346, n=24; **Figure 1D**). The mean maximal inhibition of the bacterial population growth, I_{max}, was the

highest for the ciprofloxacin susceptible strains, decreasing for the intermediately susceptible, and further decreasing for the resistant strains (Kruskal-Wallis one way analysis of variance *p*-value=0.077, *n* =22; **Figure 1B**). However, the I_{max} was highly variable across the susceptible strains, while it was highly predictable across the resistant strains (**Figure 1B**). The mean Hill-coefficient estimate was lowest for the ciprofloxacin susceptible strains, increasing for the intermediately susceptible, and further increasing for the resistant strains (the Kruskal-Wallis one-way analysis of variance *p*-value=0.039, *n* =22; **Figure 1C**). As well, the Hill-coefficient was highly predictable for the susceptible strains, while it was highly variable across the intermediately susceptible and resistant strains (**Figure 1C**). Further analysis showed a stepwise increase in the Hill-coefficient from the susceptible strains to the strains with chromosomal to the strains with plasmidic genes conferring fluoroquinolone resistance (Kruskal-Wallis one-way analysis of variance *p*-value=0.010, *n*=20).

The ciprofloxacin PD was influenced by the strain's intrinsic growth potential. A higher intrinsic growth rate, E_0, was statistically significantly correlated with a lower Hill-coefficient for the strains (Spearman's nonparametric correlation coefficient ρ=-0.617, *p*-value=0.001, *n*=24; **Table 5**). Given that the intrinsic growth rate declines with the strain phenotypic susceptibility (**Figure 1A**), that correlation may be a contributing factor to that the ciprofloxacin PD is more often concentration-dependent for the susceptible strains, but trending towards time-dependency through the intermediately susceptible to resistant strains (**Figures 3-5**). However, the impacts of the intrinsic growth potential may be interacting with more direct influences of the strain susceptibility phenotype on the ciprofloxacin PD. Specifically, there were a statistically significant negative correlation between I_{max} and MIC:IC_{50} ratio (Spearman correlation

coefficient ρ=-0.659, p-value ≤0.001, n=24), and a statistically significant positive correlation between Hill-coefficient and MIC:IC_{50} ratio for the strains (ρ=0.538, p-value=0.010, n=24).

Trends in the ceftriaxone pharmacodynamics parameter values

The time-kill experiment results with ceftriaxone are included in the **Supplementary Figures 3-5**. The results suggested the ceftriaxone PD varies depending on the strain phenotypic cephalosporin susceptibility and the *bla*-gene family that confers the reduced susceptibility. For all the strains, the PD parameter value estimates of the inhibitory baseline sigmoid I_{max} model – form 1 and the model fit statistics are shown in **Table 4**. The model projections are plotted against the ceftriaxone concentration-maximal bacterial population hourly growth/decline rate data for the individual strains in **Figures 6-8**.

The strains were categorized by their phenotypic cephalosporin susceptibility based on the ceftriaxone MIC and the corresponding CLSI-set clinical interpretative breakpoints for salmonellosis treatment in humans. The categories were the susceptible and resistant to ceftriaxone strains. The mean intrinsic growth rate of the resistant strains was statistically significantly lower compared to that of the susceptible strains (Student's t-test p-value=0.005, n=27; **Figure 2A**). Interestingly, the intrinsic growth rate of the cephalosporin resistant strains was highly variable, in opposite to the highly predictable intrinsic growth rate of the fluoroquinolone resistant strains (**Figure 2A** vs. **Figure 1A**). A higher mean maximal inhibition of the bacterial population growth, I_{max}, was estimated for the ceftriaxone resistant strains compared to the susceptible strains (Welch's t-test p-value≤0.001, n = 26; **Figure 2B**). The mean Hill-coefficient estimates were similar between the ceftriaxone susceptible and resistant strains (Student's t-test p-value=0.156, n=26; **Figure 2C**).

The ceftriaxone PD is more often time-dependent for the susceptible strains, but trending towards concentration-dependent dynamics with the decreasing phenotypic susceptibility of the strains (**Figures 6-8**). This trend may be related to the strain's decreasing intrinsic growth rate with a lower phenotypic cephalosporin susceptibility (recall also the trend of the change from concentration-dependent to time-dependent fluoroquinolone PD is correlated to the strain's decreasing intrinsic growth rate with a lower phenotypic fluoroquinolone susceptibility). For the ceftriaxone PD, a lower intrinsic growth rate, E_0, was statistically significantly correlated with a higher I_{max} (Spearman's nonparametric correlation coefficient ρ=-0.448, p-value=0.020, n=25; **Table 6**), and with a lower MIC:IC_{50} ratio (ρ=0.414, p-value=0.040, n=25; **Table 6**) for the strains. Correspondingly, there was a negative correlation between I_{max} and MIC:IC_{50} ratio for the strains (ρ=-0.583, p-value=0.002, n=22; **Table 6**). Moreover, specific gene families conferring the reduced cephalosporin susceptibility may be predictive of the ceftriaxone PD parameter value ranges. There were statistically significant differences among the strain groups carrying individual *bla*-gene families in each the mean intrinsic growth rate, E_0 (Kruskal-Wallis one-way analysis of variance p-value=0.025, n=28); mean maximal inhibition of the bacterial population growth by ceftriaxone, I_{max} (p-value=0.003, n=26); and mean Hill-coefficient estimates for the ceftriaxone PD (p-value=0.028, n=27) (**Figure 2D-F**).

In conclusion, the results of this study strongly suggest there are predictable changes in the pharmacodynamics against nontyphoidal *Salmonellae* of each of the first-line antimicrobials, the fluoroquinolone ciprofloxacin and 3rd generation cephalosporin ceftriaxone, linked to the strain phenotypic susceptibility to the antimicrobial. The changes are at least partially related to the fitness cost for the strains associated with the reduced antimicrobial susceptibility. Furthermore, the PD changes may vary among the strains depending on the specific gene

families conferring the reduced antimicrobial susceptibility. The results justify pursuing a future investigation of whether the current treatment regimens by these antimicrobials for salmonellosis in adults could be safely modified to achieve efficacy to treat the infections caused by some of the reduced susceptibility strain types.

Acknowledgements

We thank microbiologists of the U.S. NARMS and CDC and colleagues at the University of Nebraska Medical Center for collecting and sharing the *Salmonella* strains used. The authors greatly appreciate the hard work of undergraduate student scholars who assisted in performing the time-kill experiments: John (Jack) Murray, Victoria Quichocho, Christine Rosa, Kirsten Novotny, Shelby Risner, Breanna Fox, Laura Sellers, Alexis Pedrow, and Boyd Roenne. Without their assistance completion of this project would not have been possible.

This work was supported by the National Institute of General Medical Sciences of the U.S. National Institutes of Health (NIH) under award number R15GM126503. The manuscript content is solely the responsibility of the authors and does not represent the NIH official views.

Conflicts of interest

None to declare.

Author contributions

VVV conceived and designed the study. JS, TG, VQ, and EN performed the experiments. JS, TG, VQ, EN, and VVV interpreted the microbiological results. JS and VVV performed and

interpreted the pharmacodynamic modeling and statistical analyses. JS and VVV wrote the manuscript.

Figure 1. Distributions of the parameter estimates of the inhibitory baseline sigmoid I_{max} model fitted to the time-kill data for nontyphoidal *Salmonella enterica* subsp. *enterica* strains (n=24) in the study of ciprofloxacin pharmacodynamics. Of six compared pharmacodynamic models, this model fitted the data best most often across the strains. **Top** (left to right): The strains are categorized by phenotypic ciprofloxacin susceptibility based on the ciprofloxacin MIC and the clinical interpretative breakpoints set by the Clinical and Laboratory Standards Institute for salmonellosis treatment in humans. **Bottom:** (left to right): The strains are categorized by carrying none, chromosomal, or plasmidic genes encoding reduced susceptibility to quinolones, based on the whole genome sequencing and annotation.

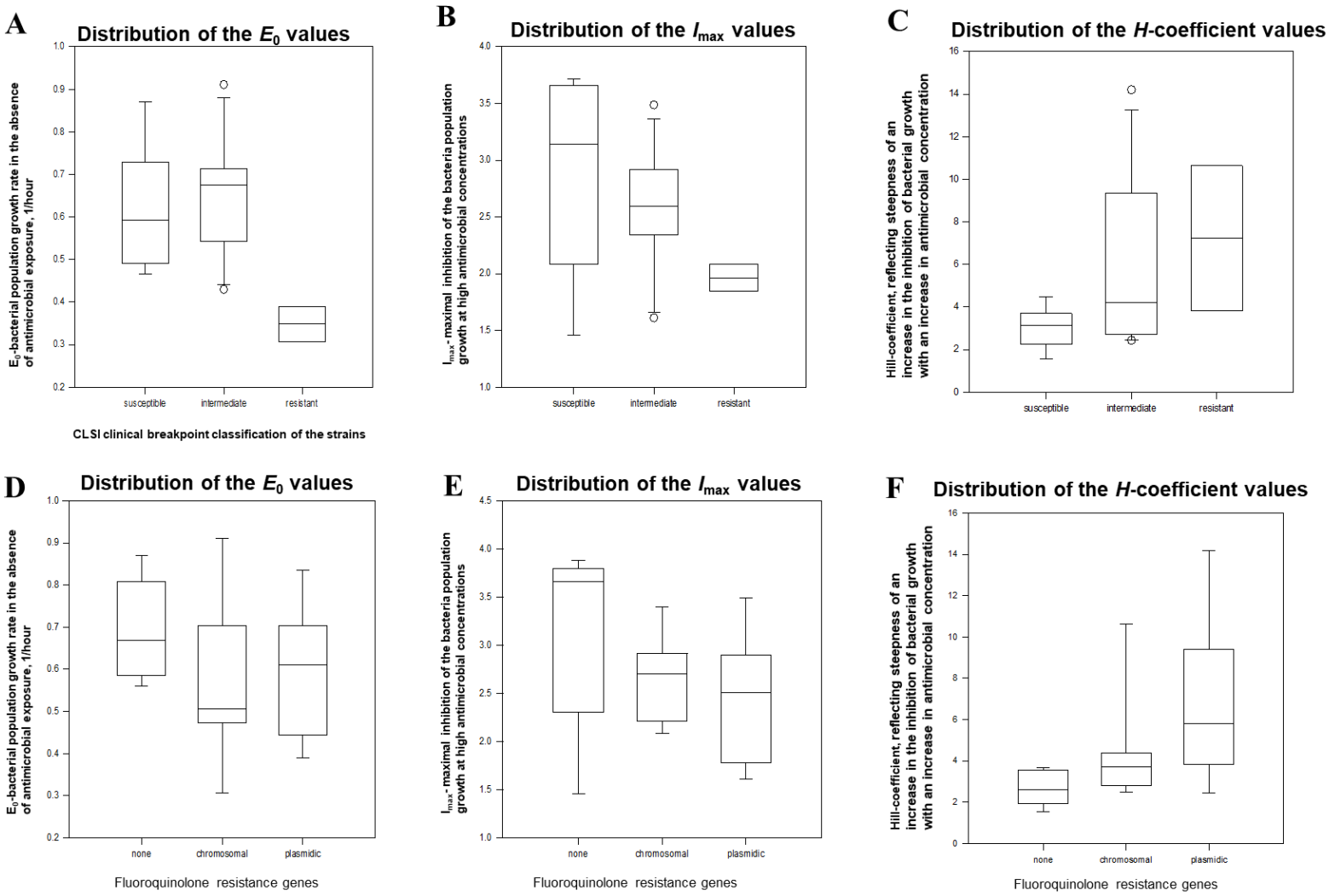

Figure 2. Distributions of the parameter estimates of the inhibitory baseline sigmoid I_{max} model fitted to the time-kill data for nontyphoidal *Salmonella enterica* subsp. *enterica* strains (n=29) in the study of ceftriaxone pharmacodynamics. Of six compared pharmacodynamic models, this model fitted the data best most often across the strains. **Top** (left to right): The strains are categorized by phenotypic ceftriaxone susceptibility based on the ceftriaxone MIC and the clinical interpretative breakpoints set by the Clinical and Laboratory Standards Institute for salmonellosis treatment in humans. **Bottom:** (left to right): The strains are categorized by the content of genes encoding reduced susceptibility to cephalosporins, based on the whole genome sequencing and annotation.

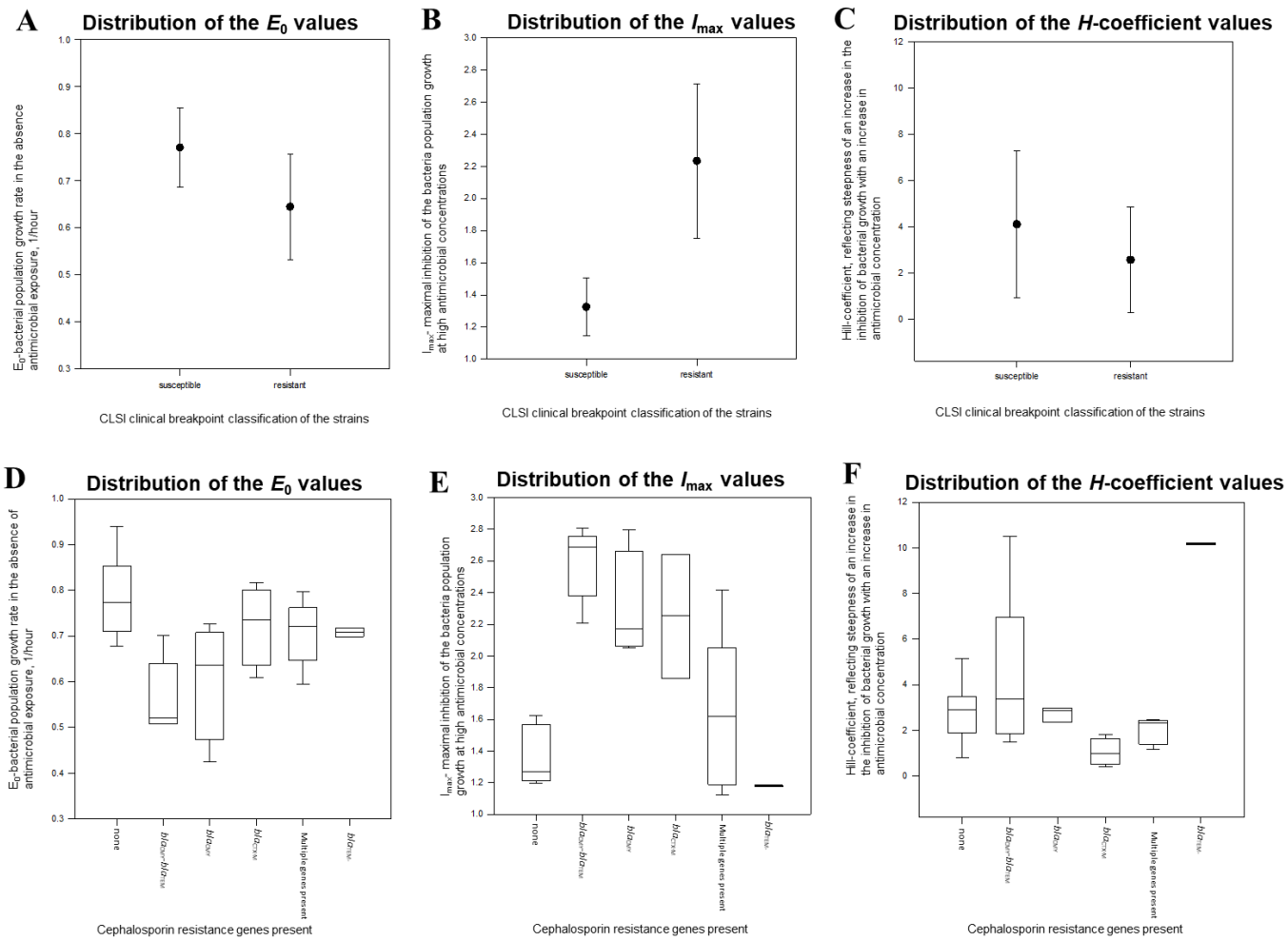

Figure 3. Projections of the bacterial population growth/decline rate depending on the ciprofloxacin concentration. The projections are of the inhibitory baseline sigmoid I_{max} model, which demonstrated best-fit out of six candidate modes to the time-kill data for nontyphoidal *Salmonella enterica* subsp. *enterica* strains investigated. The projections for the strains with the ciprofloxacin MIC 0.006 µg/mL to 0.012 µg/mL are plotted in the increasing order of the MIC (left to right, and top to bottom). These strains are categorized as susceptible to ciprofloxacin, based on the ciprofloxacin MIC clinical interpretative breakpoints set by the Clinical and Laboratory Standards Institute.

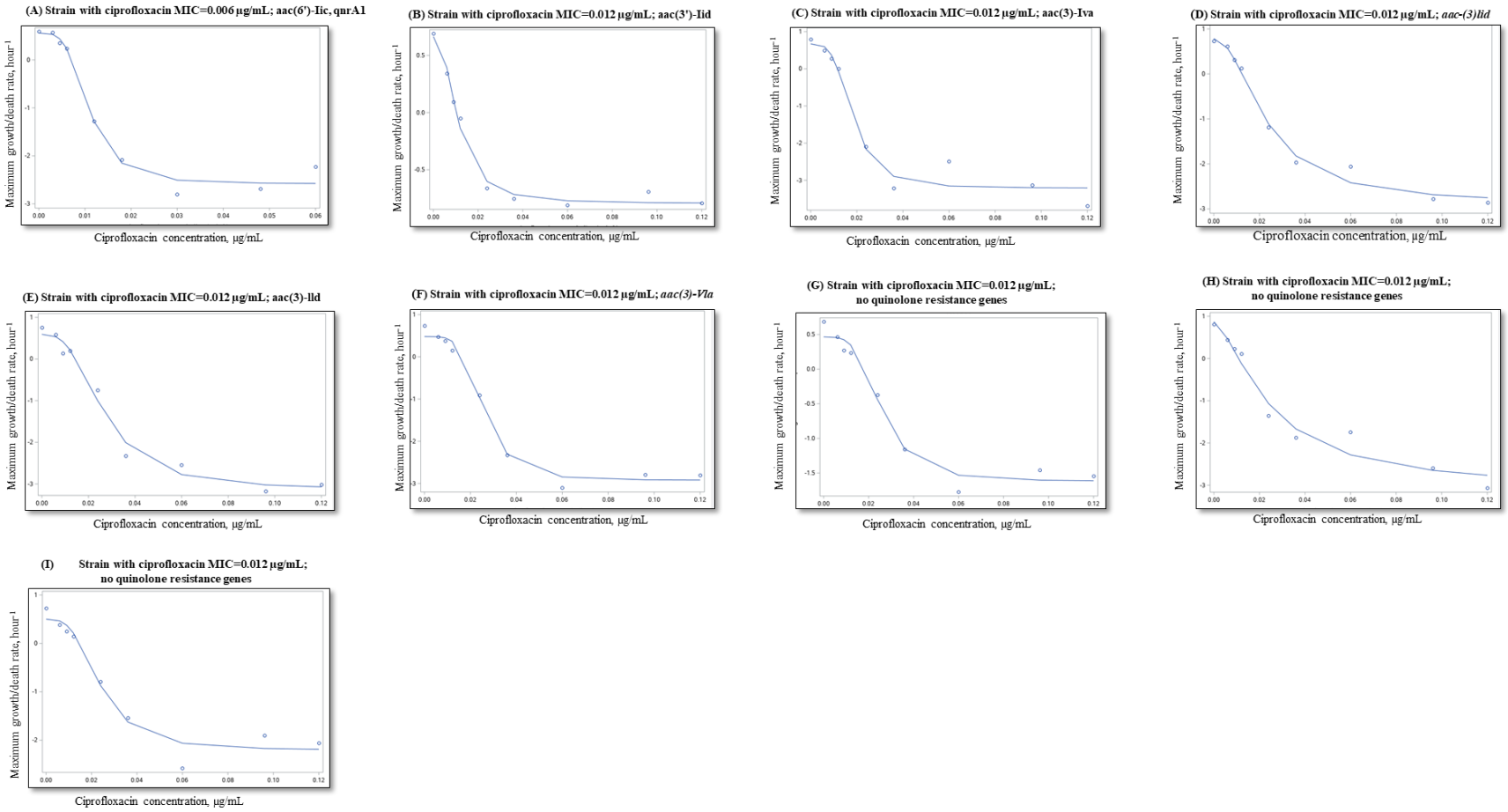

Figure 3. Projections of the bacterial population growth/decline rate depending on the ciprofloxacin concentration. The projections are of the inhibitory baseline sigmoid I_{max} model, which demonstrated best-fit out of six candidate modes to the time-kill data for nontyphoidal *Salmonella enterica* subsp. *enterica* strains investigated. The projections for the strains with the ciprofloxacin MIC 0.10 µg/mL to 0.45 µg/mL are plotted in the increasing order of the MIC (left to right, and top to bottom). These strains are categorized as intermediately susceptible to ciprofloxacin, based on the ciprofloxacin MIC clinical interpretative breakpoints set by the Clinical and Laboratory Standards Institute.

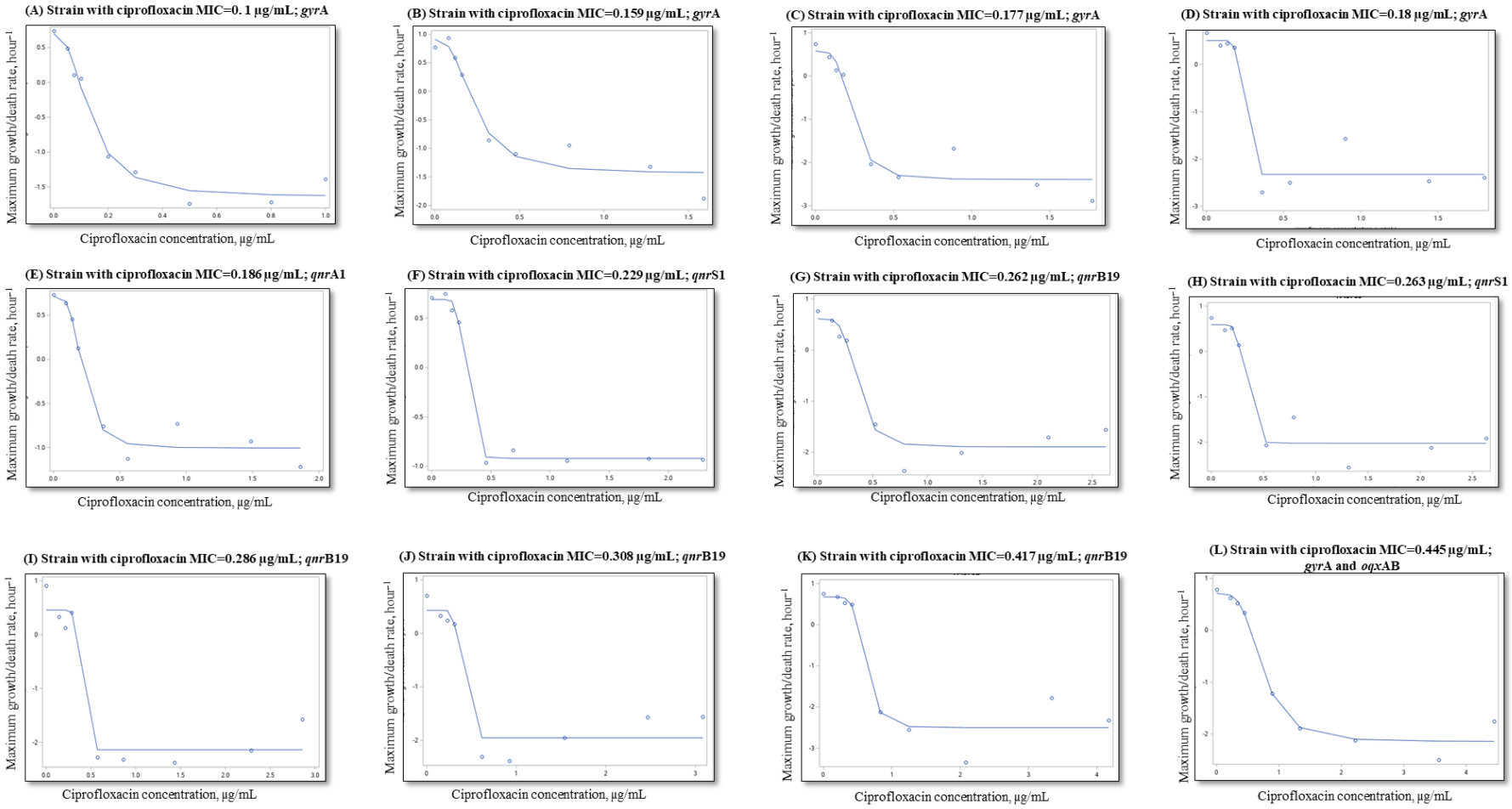

Figure 4. Projections of the bacterial population growth/decline rate depending on the ciprofloxacin concentration. The projections are of the inhibitory baseline sigmoid I_{max} model, which demonstrated best-fit out of six candidate modes to the time-kill data for nontyphoidal *Salmonella enterica* subsp. *enterica* strains investigated. The projections for the strains with the ciprofloxacin MIC 0.56 µg/mL to 25.78 µg/mL are plotted in the increasing order of the MIC (left to right, and top to bottom). These strains are categorized as intermediately susceptible or resistant to ciprofloxacin, based on the ciprofloxacin MIC clinical interpretative breakpoints set by the Clinical and Laboratory Standards Institute.

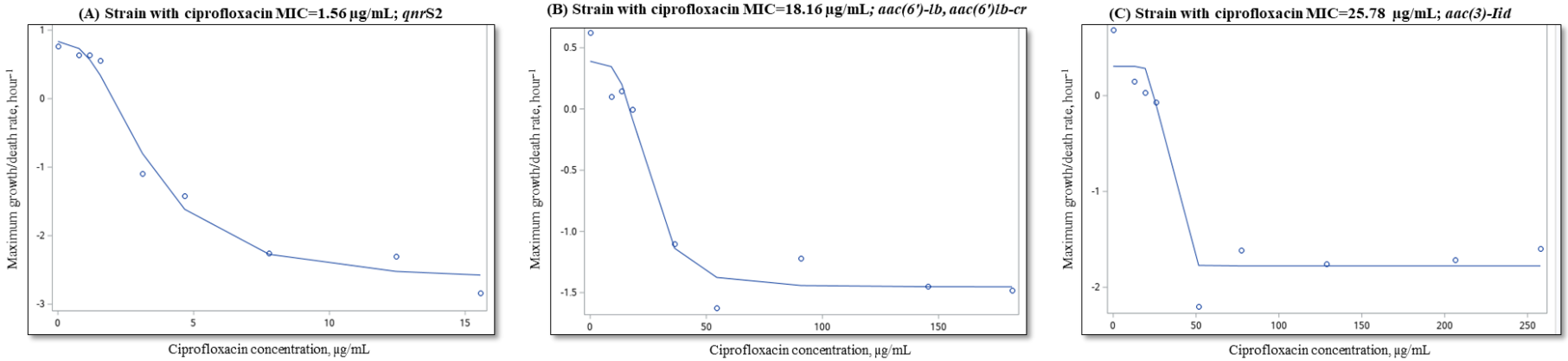

Figure 5. Projections of the bacterial population growth/decline rate depending on the ceftriaxone concentration. The projections are of the inhibitory baseline sigmoid I_{max} model, which demonstrated best-fit out of six candidate modes to the time-kill data for nontyphoidal *Salmonella enterica* subsp. *enterica* strains investigated. The projections for the strains with the ceftriaxone MIC 0.012 µg/mL to 2.98 µg/mL are plotted in the increasing order of the MIC (left to right, and top to bottom). These strains are categorized as susceptible or intermediately susceptible to ceftriaxone, based on the ceftriaxone MIC clinical interpretative breakpoints set by the Clinical and Laboratory Standards Institute.

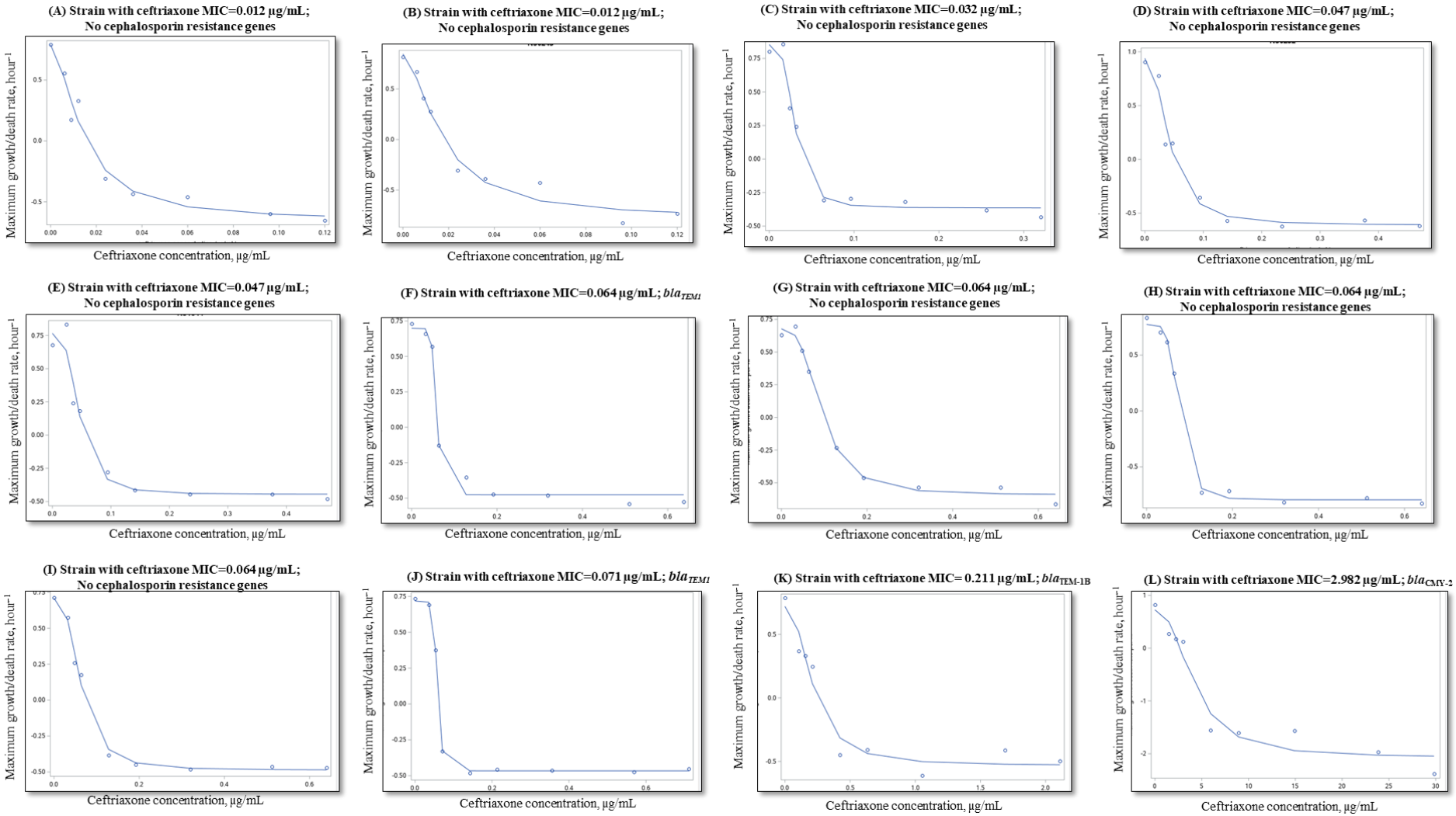

Figure 6. Projections of the bacterial population growth/decline rate depending on the ceftriaxone concentration. The projections are of the inhibitory baseline sigmoid I_{max} model, which demonstrated best-fit out of six candidate modes to the time-kill data for nontyphoidal *Salmonella enterica* subsp. *enterica* strains investigated. The projections for the strains with the ceftriaxone MIC 7.9 µg/mL to 211.9 µg/mL are plotted in the increasing order of the MIC (left to right, and top to bottom). These strains are categorized as intermediately susceptible or resistant to ceftriaxone, based on the ceftriaxone MIC clinical interpretative breakpoints set by the Clinical and Laboratory Standards Institute.

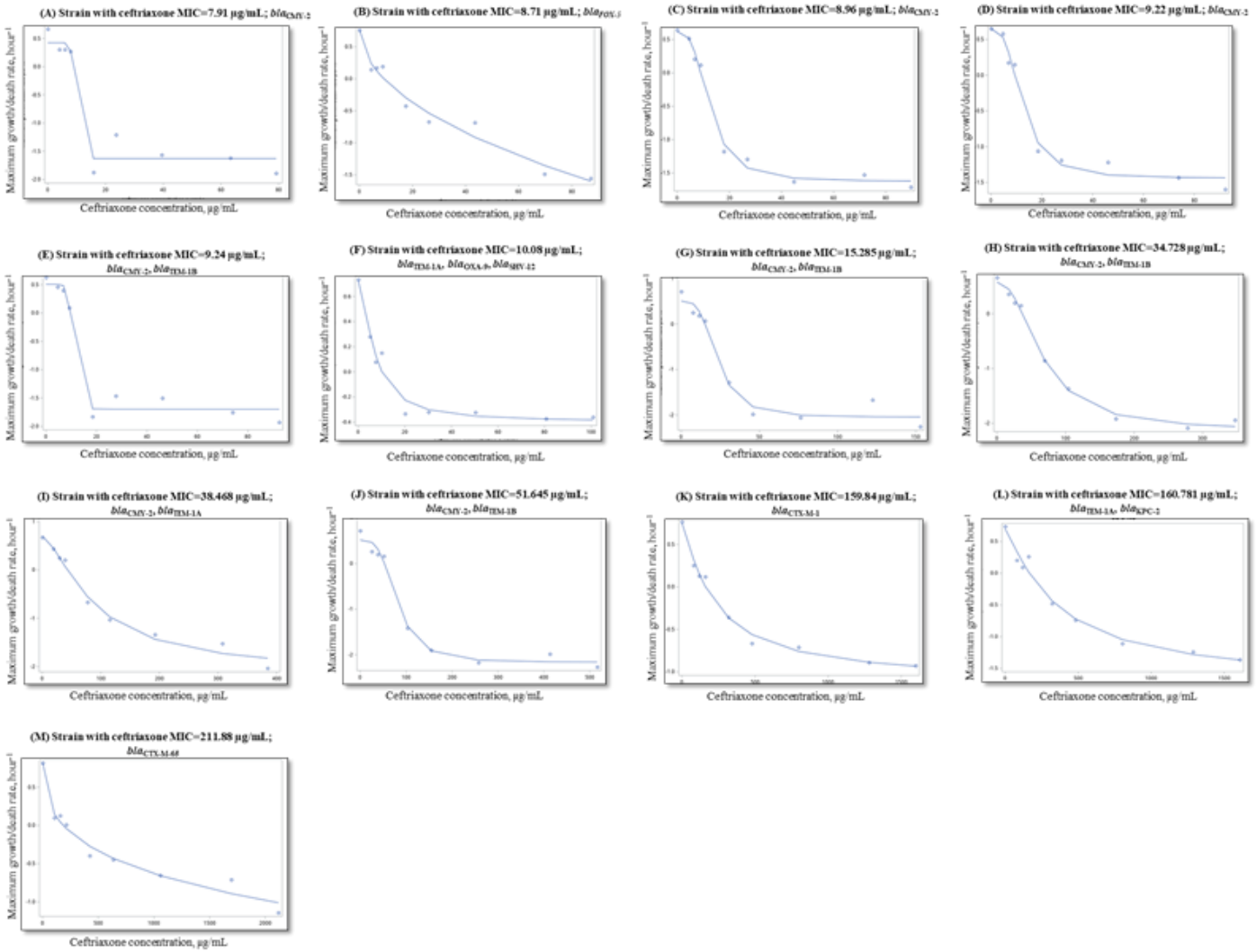

Figure 7. Projections of the bacterial population growth/decline rate depending on the ceftriaxone concentration. The projections are of the inhibitory baseline sigmoid I_{max} model, which demonstrated best-fit out of six candidate modes to the time-kill data for nontyphoidal *Salmonella enterica* subsp. *enterica* strains investigated. The projections for the strains with the ceftriaxone MIC 433 µg/mL to 1,260 µg/mL are plotted in the increasing order of the MIC (left to right, and top to bottom). These strains are categorized as resistant to ceftriaxone, based on the ceftriaxone MIC clinical interpretative breakpoints set by the Clinical and Laboratory Standards Institute.

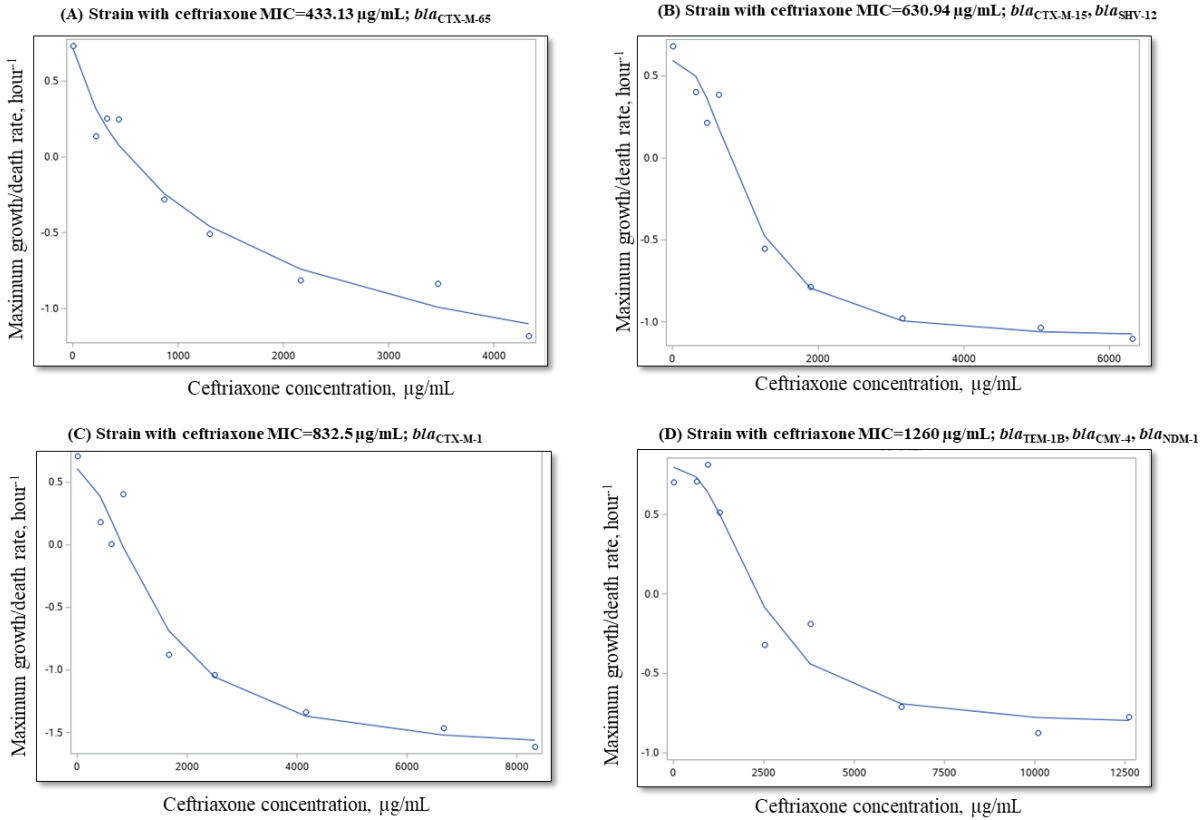

Table 1: Strains of nontyphoidal *Salmonella enterica* subsp. *enterica* (*n*=24) included in the study of ciprofloxacin pharmacodynamics.

Strain ID	Serotype	Ciprofloxacin minimum inhibitory concentration (µg/mL)	Fluoroquinolone resistance gene content based on the isolate whole genome sequencing and annotation
1	Senftenberg	25.781	*aac(3)-Iid*
2	Typhimirium	0.012	*aac(3')-Iid*
3	Derby	0.012	*aac(3)-Iva*
4	Saintpaul	0.012	*aac-(3)lid*
5	Anatum	0.012	*aac(3)-lld*
6	Newport	0.012	*aac(3)-Vla*
7	Concord	0.006	*aac(6')-Iic*, *qnr*A11
8	Senftenberg	18.164	*aac(6')-lb, aac(6')lb-cr*
9	Enteritidis	0.100	*gyr*A (D87N)
10	Saintpaul	0.177	*gyr*A (S83F)
11	Agona	0.180	*gyr*A (S83F)
12	Typhimurium	0.159	*gyr*A (S83Y)
13	Typhimirium	0.445	*gyr*A (s83Y), *oqx*AB
14	Litchfield	0.012	none
15	Agona	0.012	none
16	Enteritidis	0.012	none
17	Stanley	0.186	*qnr*A1
18	Derby	0.286	*qnr*B19
19	Typhimurium	0.262	*qnr*B19
20	Newport	0.417	*qnr*B19
21	Anatum	0.308	*qnr*B19
22	Saintpaul	0.263	*qnr*S1
23	Litchfield	0.229	*qnr*S1
24	Derby	1.556	*qnr*S2

Table 2: Strains of nontyphoidal *Salmonella enterica* subsp. *enterica* (*n*=29) included in the study of ceftriaxone pharmacodynamics.

Strain ID	Serotype	Ceftriaxone minimum inhibitory concentration (µg/mL)	Cephalosporin resistance gene content based on the isolate whole genome sequencing and annotation
25	Typhimurium var. 5	8.962	*bla*$_{\text{CMY-2}}$
26	Kentucky	2.982	*bla*$_{\text{CMY-2}}$
27	Typhimurium	9.218	*bla*$_{\text{CMY-2}}$
28	Dublin	7.909	*bla*$_{\text{CMY-2}}$
29	Heidelberg	38.468	*bla*$_{\text{CMY-2}}$, *bla*$_{\text{TEM-1A}}$
30	Typhimurium	34.728	*bla*$_{\text{CMY-2}}$, *bla*$_{\text{TEM-1B}}$
31	Heidelberg	15.285	*bla*$_{\text{CMY-2}}$, *bla*$_{\text{TEM-1B}}$
32	Saintpaul	51.645	*bla*$_{\text{CMY-2}}$, *bla*$_{\text{TEM-1B}}$
33	Typhimurium var. 5	9.239	*bla*$_{\text{CMY-2}}$, *bla*$_{\text{TEM-1B}}$
34	Heidelberg	159.844	*bla*$_{\text{CTX-M-1}}$
35	Albany	832.500	*bla*$_{\text{CTX-M-1}}$
7	Concord	630.938	*bla*$_{\text{CTX-M-15}}$, *bla*$_{\text{SHV-12}}$
36	Infantis	211.875	*bla*$_{\text{CTX-M-65}}$
37	Infantis	433.125	*bla*$_{\text{CTX-M-65}}$
38	Newport	8.714	*bla*$_{\text{FOX-5}}$
39	Cubana	160.781	*bla*$_{\text{TEM-1A}}$, *bla*$_{\text{KPC-2}}$
8	Senftenberg	10.078	*bla*$_{\text{TEM-1A}}$, *bla*$_{\text{OXA-9}}$, *bla*$_{\text{SHV-12}}$
40	Brandenburg	0.211	*bla*$_{\text{TEM-1B}}$
1	Senftenberg	1260	*bla*$_{\text{TEM-1B}}$,*bla*$_{\text{CMY-4}}$, *bla*$_{\text{NDM1}}$
41	Kentucky	0.032	none
42	Newport	0.047	none
43	Dublin	0.064	none
3	Derby	0.064	none
44	Saintpaul	0.064	none
2	Typhimirium	0.012	none
45	Heidelberg	0.047	none
15	Agona	0.012	none
46	Enteritidis	0.064	*bla*$_{\text{TEM-1}}$

47	Enteritidis	0.071	*bla*$_{\text{TEM-1}}$

Table 3: Parameter estimates and fit statistics for the inhibitory baseline sigmoid I_{max} model fitted to the data on ciprofloxacin pharmacodynamics for individual strains of nontyphoidal *Salmonella enterica* subsp. *enterica* (n=24). Of six compared pharmacodynamic models, this model fitted the data best most often across the strains. For each strain and parameter, the first row is the parameter estimate and its 95% confidence interval and the second row is the coefficient of variation CV (%) for the estimate. AIC – Akaike information criterion. R^2 – coefficient of variation.

Strain ID	I_{max}	E_0	Hill coefficient	IC_{50}	AIC	Adjusted R^2
6	1.46	0.67	2.43	0.01	-37.44	0.98
	(1.23, 1.69) 6.1%	(0.48, 0.85) 10.8%	(1.32, 3.53) 17.7%	(0.008, 0.013) 7.9%		
3	3.88	0.67	3.53	0.02	-10.62	0.9370
	(2.80, 4.97) 10.9%	(-0.13, 1.47) 46.5%	(0.35, 6.72) 35.1%	(0.01, 0.03) 14.8%		
15	3.95	0.87	1.54	0.02	-13.54	0.93
	(2.05, 5.85) 18.7%	(0.04, 1.70) 37.1%	(0.15, 2.94) 35.2%	(0.01, 0.04) 28.3%		
16	3.66	0.79	2.06	0.02	14.12	0.98
	(2.86, 4.45) 8.5%	(0.34, 1.23) 22.0%	(1.00, 3.12) 20.0%	(0.0165, 0.03) 11.0%		
14	3.72	0.59	2.78	0.03	-17.04	0.97
	(2.81, 4.63) 9.5%	(0.09, 1.09) 32.9%	(0.62, 4.94) 30.3%	(0.02, 0.03) 10.5%		
4	2.71	0.50	3.13	0.02	6.79	0.93
	(1.82, 3.59) 12.7%	(-0.05, 1.05) 42.7%	(-0.48, 6.74) 44.8%	(0.01, 0.03) 14.8%		
5	3.40	0.48	4.47	0.026	-21.12	0.98
	(2.92, 3.89) 5.6%	(0.18, 0.78) 24.2%	(1.34, 7.59) 27.2%	(0.02, 0.03) 5.6%		
2	2.084	0.47	3.72	0.026	-22.83	0.953
	(1.59, 2.57) 9.1%	(0.17, 0.76) 24.5%	(0.01, 7.42) 38.8%	(0.02, 0.03) 9.8%		
23	1.61	0.69	9.42	0.28	-38.73	0.99
	(1.46, 1.76) 3.6%	(0.58, 0.80) 6.2%	(-9.70, 28.54) 79.0%	(0.17, 0.38) 14.5%		
17	1.72	0.72	3.81	0.22	-23.74	0.94
	(1.25, 2.19) 10.6%	(0.35, 1.08) 19.8%	(0.09, 7.52) 37.9%	(0.15, 0.30) 13.2%		
12	2.35	0.91	2.70	0.23	-15.50	0.90

	(1.43, 3.26) 15.2%	(0.25, 1.57) 28.2%	(-0.14, 5.53) 40.9%	(0.10, 0.36) 20.9%		
24	3.49	0.83	2.42	3.28	-18.65	0.97
	(2.58, 4.39) 10.1%	(0.33, 1.34) 23.4%	(0.69, 4.17) 27.9%	(2.28, 4.28) 11.8%		
19	2.51	0.61	4.81	0.35	-14.33	0.92
	(1.75, 3.26) 11.7%	(0.03, 1.19) 36.9%	(-0.79, 10.41) 45.3%	(0.20, 0.51) 16.9%		
9	2.34	0.70	2.47	0.13	-24.12	0.96
	(1.79, 2.88) 9.1%	(0.30, 1.10) 22.3%	(0.98, 3.95) 23.5%	(0.09, 0.18) 12.8%		
20	3.18	0.68	6.83	0.62	-7.10	0.88
	(2.10, 4.26) 13.3%	(-0.15, 1.50) 47.4%	(-6.68, 20.34) 77.0%	(0.21, 1.03) 25.6%		
21	2.38	0.43	14.20	0.36	-11.70	0.89
	(1.54, 3.23) 13.9%	(-0.24, 1.10) 60.3%	(-733.40, 761.80) 2,047.5%	(-2.41, 3.13) 301.3%		
13	2.86	0.71	3.74	0.73	-18.88	0.96
	(2.23, 3.48) 8.5%	(0.26, 1.16) 24.6%	(0.74, 6.74) 31.2%	(0.52, 0.94) 11.3%		
18	2.60	0.46	19.79	0.35	-11.31	0.90
	(1.78, 3.41) 12.2%	(-0.14, 1.06) 50.8%	(-9,534.20, 9,573.80) 18,782.0%	(-33.89, 34.59) 3,802.4%		
22	2.62	0.59	9.34	0.31	-12.25	0.91
	(1.80, 3.43) 12.1%	(-0.02, 1.20) 40.5%	(-56.20, 74.81) 272.9%	(-0.05, 0.67) 45.5%		
11	2.83	0.51	21.04	0.21	-10.75	0.91
	(1.94, 3.72) 12.2%	(-0.23, 1.24) 56.3%	(-12,182.60, 12,224.70) 22,563.5%	(-16.45, 16.86) 3,131.7%		
8	1.84	0.39	3.82	24.04	-20.37	0.92
	(1.28, 2.41) 11.9%	(-0.04, 0.82) 43.3%	(-0.05, 7.69) 39.4%	(14.10, 33.99) 16.1%		
1	2.08	0.31	10.64	29.55	-14.88	0.90
	(1.38, 2.78) 13.1%	(-0.24, 0.85) 69.4%	(-116.20, 137.50) 463.9%	(-17.71, 76.81) 62.2%		
7	3.14	0.56	3.67	0.01	-20.26	0.97
	(2.56, 3.73) 7.3%	(0.17, 0.95) 27.4%	(0.94, 6.40) 29.0%	(0.01, 0.01) 8.9%		

10	2.97	0.58	4.19	0.23	-10.36	0.90
	(1.94, 4.01) 13.5%	(-0.21, 1.37) 52.9%	(-0.93, 9.31) 4.5%	(0.12, 0.35) 18.5%		

Table 4: Parameter estimates and fit statistics for the inhibitory baseline sigmoid I_{max} model fitted to the data on ceftriaxone pharmacodynamics for individual strains of nontyphoidal *Salmonella enterica* subsp. *enterica* (*n*=29). Of six compared pharmacodynamic models, this model fitted the data best most often across the strains. For each strain and parameter, the first row is the parameter estimate and its 95% confidence interval and the second row is the coefficient of variation CV (%) for the estimate. AIC – Akaike information criterion. R^2 – coefficient of variation.

Strain ID	I_{max}	E_0	**Hill coefficient**	IC_{50}	**AIC**	**Adjusted R^2**
15	1.63	0.85	1.70	0.02	-30.20	0.95
	(1.15, 2.10) 11.4%	(0.56, 1.14) 13.3%	(0.60, 2.80) 25.1%	(0.00, 0.02) 18.2%		
43	1.27	0.68	2.97	0.09	-41.50	0.99
	0.05, 1.11) 5.0%	(0.05, 0.56) 6.9%	(0.05, 1.88) 14.3%	(0.05, 0.08) 6.9%		
3	1.57	0.77	5.14	0.08	-42.07	0.99
	(1.44, 1.70) 3.3%	(0.67, 0.88) 5.1%	(2.93, 7.35) 16.7%	(0.07, 0.08) 4.3%		
2	0.08	1.44	0.79	1.71	-30.31	0.94
	(0.07, 0.08) 223.6%	(1.00, 1.88) 7.8%	(0.50, 1.08) 60.4%	(0.48, 2.94) 0.2%		
45	1.21	0.77	3.18	0.05	-29.07	0.93
	(0.84, 1.58) 11.83%	(0.47, 1.06) 15.2%	(-0.05, 6.41) 39.5%	(0.03, 0.06) 13.1%		
42	1.55	0.94	2.41	0.04	-29.69	0.95
	(1.17, 1.93) 9.4%	(0.64, 1.24) 12.5%	(0.70, 4.12) 27.6%	(0.03, 0.06) 12.2%		
41	1.22	0.85	3.57	0.03	-34.18	0.96
	(0.96, 1.48) 8.3%	(0.64, 1.07) 9.7%	(0.78, 6.36) 30.4%	(0.02, 0.04) 8.3%		
31	2.55	0.51	3.3698	22.9701	-18.39	0.95
	(1.88, 3.23) 10.3%	(0.01, 1.00) 38.1%	(0.60, 6.14) 32.0%	(14.72, 31.22) 14.0%		
33	2.21	0.51	10.5	10.60	-21.95	0.96

	(1.76, 2.65) 7.9%	(0.16, 0.85) 26.6%	(-61.41, 82.42) 266.4%	(0.81, 20.38) 35.9%		
29	2.81	0.70	1.50	88.87	-25.30	0.97
	(1.78, 3.84) 14.2%	(0.31, 1.09) 21.5%	(0.53, 2.46) 25.1%	(40.34, 137.40) 21.2%		
27	2.09	0.65	2.87	12.28	-26.07	0.97
	(1.65, 2.54) 8.3%	(0.32, 0.99) 20.0%	(1.165, 4.58) 23.1%	(8.70 15.86) 11.3%		
25	2.25	0.62	2.99	12.39	-29.52	0.98
	(1.90, 2.60) 6.1%	(0.36, 0.88) 16.5%	(1.66, 4.32) 17.3%	(9.74, 15.02) 8.3%		
28	2.05	0.42	16.34	9.23	-16.27	0.91
	(1.42, 2.69) 12.0%	(-0.07, 0.92) 45.7%	(-1,804.10, 1,836.79) 4,333.3%	(-148.22, 166.67) 663.8%		
38	31.09	0.76	0.53	10047.75	-23.96	0.94
	(-931.37, 993.55) 1204.3%	(0.32, 1.21) 22.8%	(-0.33, 1.39) 63.6%	(-701,910.56, 722,006.07) 2,756.5%		
30	2.70	0.58	2.22	66.13	-31.86	0.99
	(2.30, 3.10) 5.7%	(0.34, 0.81) 15.7%	(1.40, 3.04) 14.4%	(53.66, 78.60) 7.3%		
26	2.7978	0.7266	2.3667	4.1360	-14.6	0.91
	(1.77, 3.83) 14.3%	(-0.00, 1.46) 39.4%	(0.17, 4.56) 36.1%	(1.97, 6.30) 20.3%		
35	2.26	0.61	1.82	1413.66	- 18.426	0.90
	(1.21, 3.30) 18.0%	(0.01, 1.21) 38.2%	(-0.02, 3.65) 39.3%	(457.02, 2,370.30) 26.3%		
34	1.86	0.75	1.16	223.75	-36.39	0.98
	(1.38, 2.33) 9.9%	(0.55, 0.95) 10.3%	(0.59, 1.74) 19.3%	(107.53, 339.96) 20.2%		
37	2.64	0.72	0.84	1694.01	-26.83	0.94
	(-0.52, 5.81) 46.6%	(0.35, 1.09) 20.1%	(-0.09, 1.77) 42.9%	(-3,377.08, 6,765.11) 116.5%		
39	2.42	0.70	1.18	356.35	-27.59	0.96
	(1.28, 3.56) 18.3%	(0.35, 1.05) 19.4%	(0.33, 2.02) 27.9%	(35.80, 676.91) 35.0%		
36	7.17	0.82	0.40	30,752.62	-29.00	0.94
	(-58.55, 72.90) 356.4%	(0.49, 1.14) 15.4%	(-0.40, 1.21) 78.1%	(-1,062,959.34, 1,124,464.56)		

				1383.5%		
7	1.69	0.59	2.43	1006.08	-28.25	0.96
	(1.25, 2.13) 10.1%	(0.30, 0.89) 19.4%	(0.80, 4.06) 26.1%	(648.86, 1,363.30) 13.8%		
1	1.62	0.80	2.46	2344.39	-23.17	0.91
	(0.99, 2.25) 15.2%	(0.41, 1.19) 19.1%	(-0.16, 5.08) 41.4%	(1,184.74, 3504.03) 19.2%		
40	1.25	0.72	2.33	0.22	-27.84	0.91
	(0.82, 1.68) 13.4%	(0.39, 1.06) 18.1%	(0.13, 4.54) 36.7%	(0.11 0.32) 18.4%		
8	1.12	0.73	1.62	6.98	-34.64	0.94
	(0.82, 1.42) 10.4%	(0.50, 0.95) 12.0%	(0.22, 3.02) 33.6%	(3.92, 10.04) 17.1%		

Table 5: Pair-wise correlations between the ciprofloxacin pharmacodynamics parameter values based on the inhibitory baseline sigmoid I_{max} model fitted to the data on ciprofloxacin pharmacodynamics for individual strains of nontyphoidal *Salmonella enterica* subsp. *enterica* (*n*=24). Spearman correlation coefficient values, * indicates a correlation coefficient for which *p*-value ≤0.05.

Parameter	I_{max}	E_0	**Hill-coefficient**
I_{max}	-	0.258	-0.298
E_0	0.258	-	-0.617*
Hill-coefficient	-0.298	-0.617*	-
MIC:IC_{50} ratio	-0.659*	-0.249	0.538*
MIC	-0.318	-0.155	0.546

Table 6: Pair-wise correlations between the ceftriaxone pharmacodynamics parameter values based on the inhibitory baseline sigmoid I_{max} model fitted to the data on ceftriaxone pharmacodynamics for individual strains of nontyphoidal *Salmonella enterica* subsp. *enterica* (*n*=29). Spearman correlation coefficient values, * indicates a correlation coefficient for which *p*-value ≤0.05.

Parameter	I_{max}	E_0	**Hill-coefficient**
I_{max}	-	-0.448*	-0.354
E_0	-0.448*	-	-0.193
Hill-coefficient	-0.354	-0.193	-
MIC:IC_{50} ratio	-0.583*	0.414*	0.308
MIC	0.564*	-0.473*	-0.641*

Supplementary Figure 1. Time-kill data for the experiments with ciprofloxacin for nontyphoidal *Salmonella enterica* subsp. *enterica* strains. Each dot represents the mean of the data from two to three replicates of the experiment. The drug concentrations used in the experiments are shown by color: light blue – no antimicrobial or control; orange 0.5 MIC; gray 0.75 MIC; yellow 1 MIC; dark blue 2 MIC; green 3 MIC; navy blue 5 MIC; red 8 MIC; and dark gray 10 MIC. MIC – minimum inhibitory concentration of ciprofloxacin for the strain. Additional strain characteristics can be referenced in **Table 1**.

a) MIC=0.01 µg/mL; strain 2 **b)** MIC=0.01 µg/mL; strain 6 **c)** MIC=0.01 µg/mL; strain 4 **d)** MIC=0.01 µg/mL; strain 5 **e)** MIC=0.01 µg/mL; strain 6 **f)** MIC=0.01 µg/mL; strain 14 **g)** MIC=0.01 µg/mL; strain 15 **h)** MIC=0.01 µg/mL; strain 16 **i)** MIC=0.01 µg/mL; strain 7.

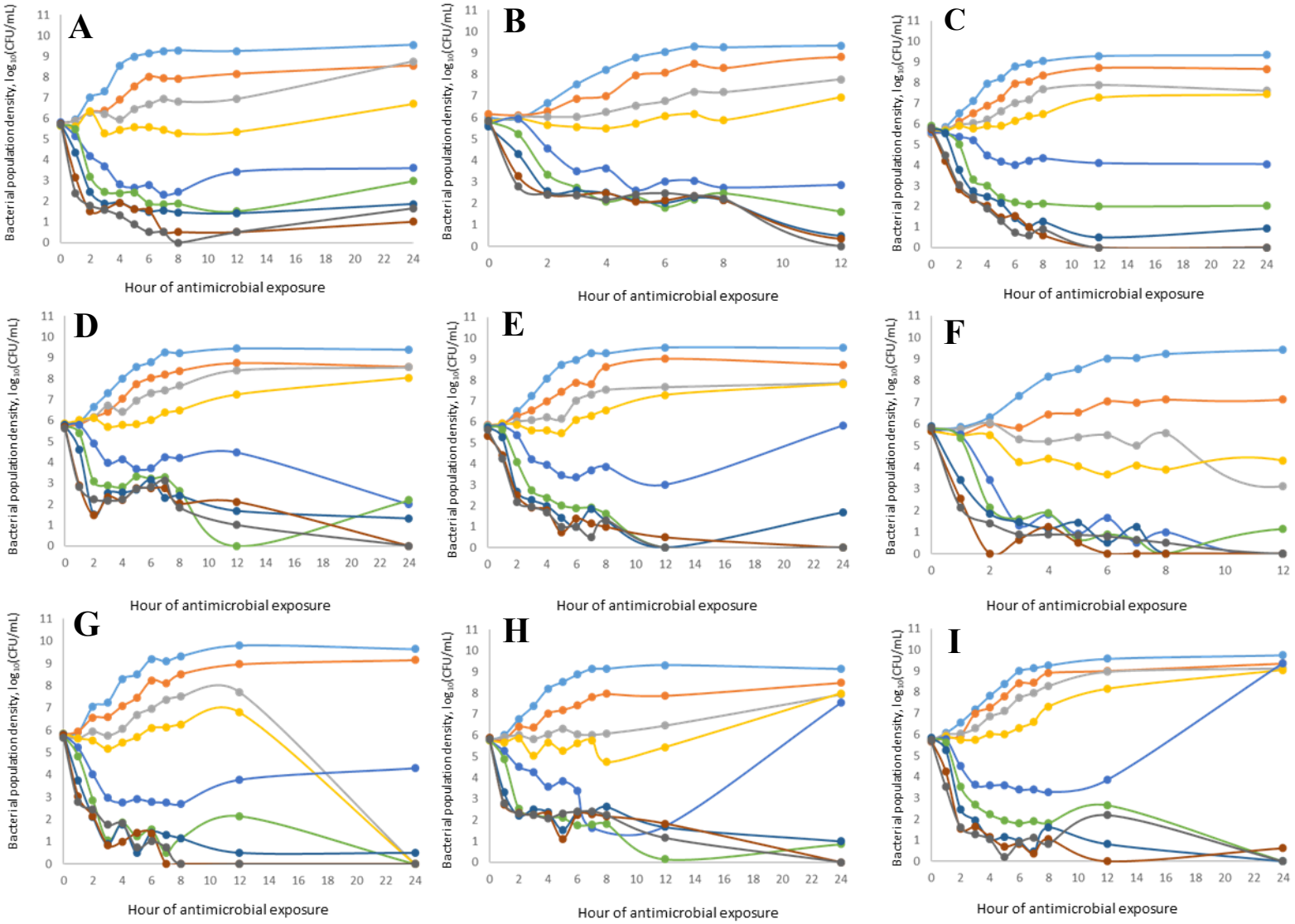
A
B
C
D
E
F
G
H
I
Bacterial population density, log10(CFU/mL)
Hour of antimicrobial exposure

Supplementary Figure 2. Time-kill data for the experiments with ciprofloxacin for nontyphoidal *Salmonella enterica* subsp. *enterica* strains. Each dot represents the mean of the data from two to three replicates of the experiment. The drug concentrations used in the experiments are shown by color: light blue – no antimicrobial or control; orange 0.5 MIC; gray 0.75 MIC; yellow 1 MIC; dark blue 2 MIC; green 3 MIC; navy blue 5 MIC; red 8 MIC; and dark gray 10 MIC. MIC – minimum inhibitory concentration of ciprofloxacin for the strain. Additional strain characteristics can be referenced in **Table 1**.

a) MIC=0.10 µg/mL; strain 9 **b)** MIC=0.16 µg/mL; strain 12 **c)** MIC=0.18 µg/mL; strain 10 **d)** MIC=0.18 µg/mL; strain 11 **e)** MIC=0.19 µg/mL; strain 17 **f)** MIC=0.23 µg/mL; strain 23 **g)** MIC=0.26 µg/mL; strain 19 **h)** MIC=0.26 µg/mL; strain 22 **i)** MIC=0.29 µg/mL; strain 18 **j)** MIC=0.31 µg/mL; strain 21 **k)** MIC=0.42 µg/mL; strain 20 **l)** MIC=0.45 µg/mL; strain 13 **m)** MIC=1.56 µg/mL; strain 16 **n)** MIC=18.16 µg/mL; strain 8 **o)** MIC=25.78 µg/mL; strain 1.

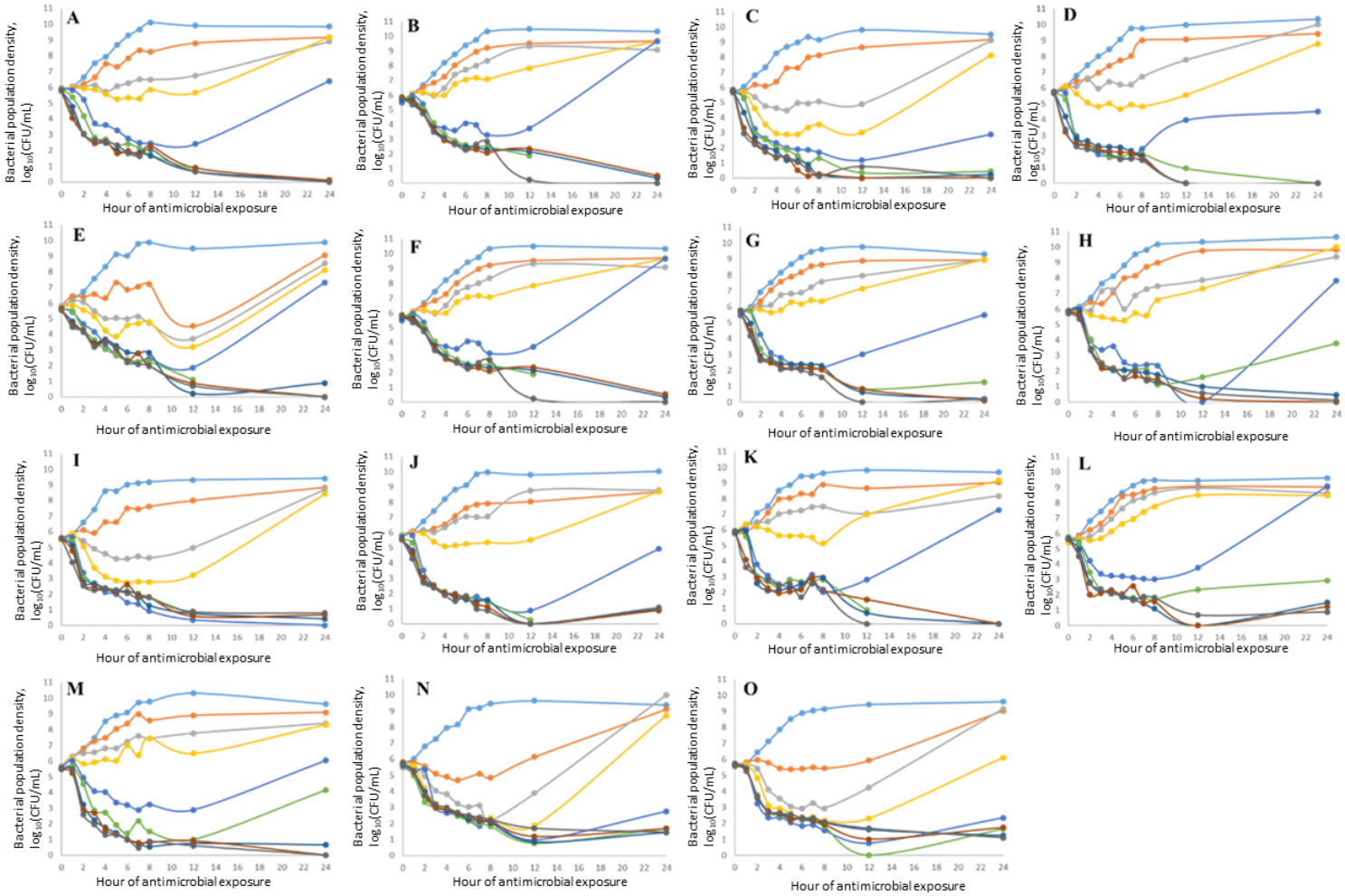
A
B
C
D
E
F
G
H
I
J
K
L
M
N
O
Bacterial population density, log10(CFU/mL)
Hour of antimicrobial exposure

Supplementary Figure 3. Time-kill data for the experiments with ceftriaxone for nontyphoidal *Salmonella enterica* subsp. *enterica* strains. Each dot represents the mean of the data from two to three replicates of the experiment. The drug concentrations used in the experiments are shown by color: light blue – no antimicrobial or control; orange 0.5 MIC; gray 0.75 MIC; yellow 1 MIC; dark blue 2 MIC; green 3 MIC; navy blue 5 MIC; red 8 MIC; and dark gray 10 MIC. MIC – minimum inhibitory concentration of ceftriaxone for the strain. Additional strain characteristics can be referenced in **Table 2**.

a) MIC=0.01 µg/mL; strain 2 **b)** MIC=0.01 µg/mL; strain 15 **c)** MIC=0.03 µg/mL; strain 41 **d)** MIC=0.05 µg/mL; strain42 **e)** MIC=0.05 µg/mL; strain 45 **f)** MIC=0.06 µg/mL; strain 46 **g)** MIC=0.06 µg/mL; strain 43 **h)** MIC=0.06 µg/mL; strain 3 **i)** MIC=0.06 µg/mL; strain 44 **j)** MIC=0.07 µg/mL; strain 47 **k)** MIC=0.21 µg/mL; strain 40.

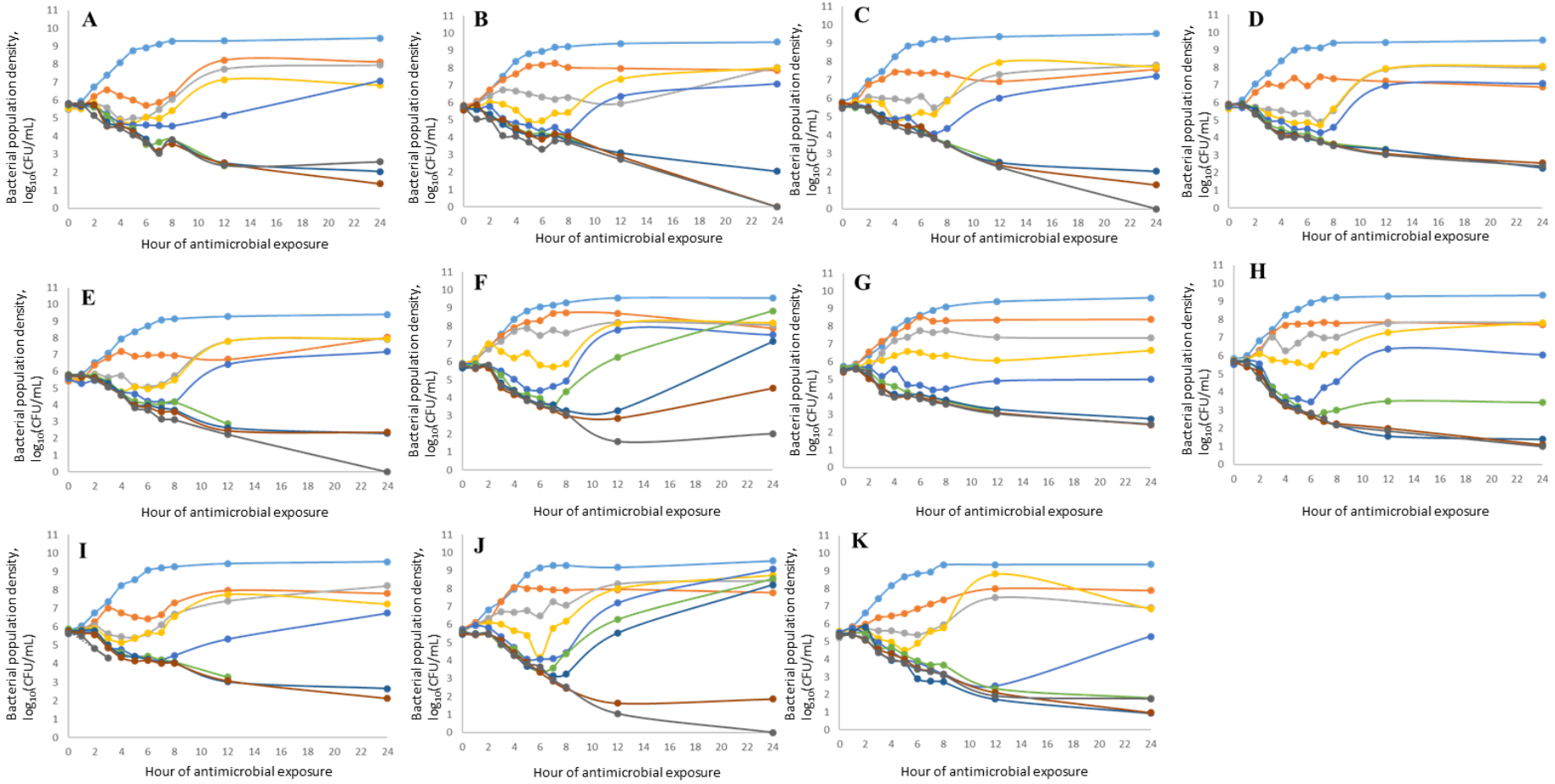

Supplementary Figure 4. Time-kill data for the experiments with ceftriaxone for nontyphoidal *Salmonella enterica* subsp. *enterica* strains. Each dot represents the mean of the data from two to three replicates of the experiment. The drug concentrations used in the experiments are shown by color: light blue – no antimicrobial or control; orange 0.5 MIC; gray 0.75 MIC; yellow 1 MIC; dark blue 2 MIC; green 3 MIC; navy blue 5 MIC; red 8 MIC; and dark gray 10 MIC. MIC – minimum inhibitory concentration of ceftriaxone for the strain. Additional strain characteristics can be referenced in **Table 2**.

a) MIC=2.98 µg/mL; strain 26 **b)** MIC=7.91 µg/mL; strain 28 **c)** MIC=8.71 µg/mL; strain 38 **d)** MIC=8.96 µg/mL; strain 25 **e)** MIC=9.22 µg/mL; strain 27 **f)** MIC=9.24 µg/mL; strain 33 **g)** MIC=10.08 µg/mL; strain 8 **h)** MIC=15.29 µg/mL; strain 31 **i)** MIC=34.73 µg/mL; strain 30.

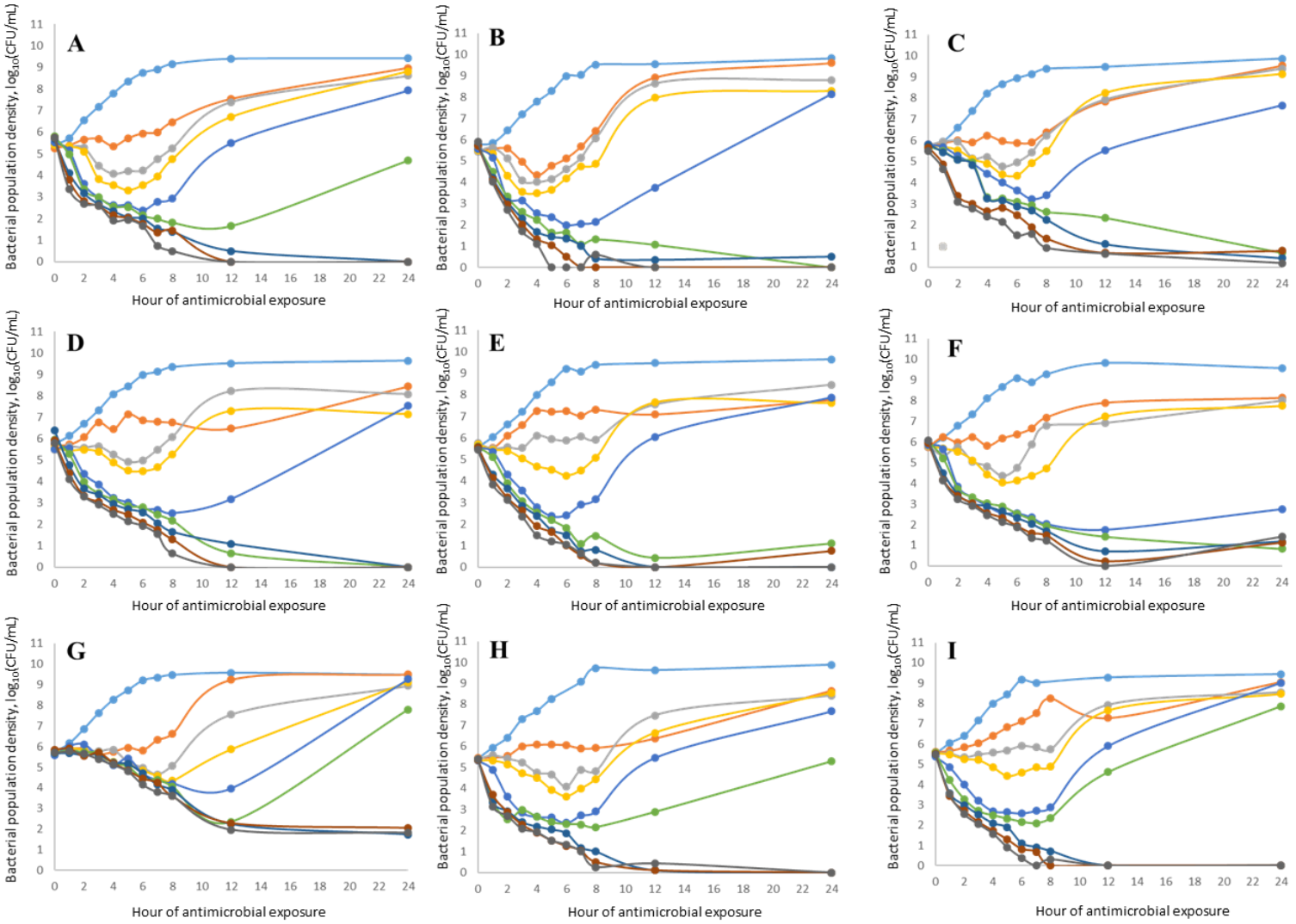
A
B
C
D
E
F
G
H
I
Bacterial population density, log10(CFU/mL)
Hour of antimicrobial exposure

Supplementary Figure 5. Time-kill data for the experiments with ceftriaxone for nontyphoidal *Salmonella enterica* subsp. *enterica* strains. Each dot represents the mean of the data from two to three replicates of the experiment. The drug concentrations used in the experiments are shown by color: light blue – no antimicrobial or control; orange 0.5 MIC; gray 0.75 MIC; yellow 1 MIC; dark blue 2 MIC; green 3 MIC; navy blue 5 MIC; red 8 MIC; and dark gray 10 MIC. MIC – minimum inhibitory concentration of ceftriaxone for the strain. Additional strain characteristics can be referenced in **Table 2**.

a) MIC=38.47 µg/mL; strain 29 **b)** MIC=51.65 µg/mL; strain 32 **c)** MIC=159.84 µg/mL; strain 31 **d)** MIC=160.78 µg/mL; strain 39 **e)** MIC=211.88 µg/mL; strain 36 **f)** MIC=433.13 µg/mL; strain 37 **g)** MIC=630.94 µg/mL; strain 7 **h)** MIC=832.50 µg/mL; strain 35 **i)** MIC=1,260.00 µg/mL; strain 1.

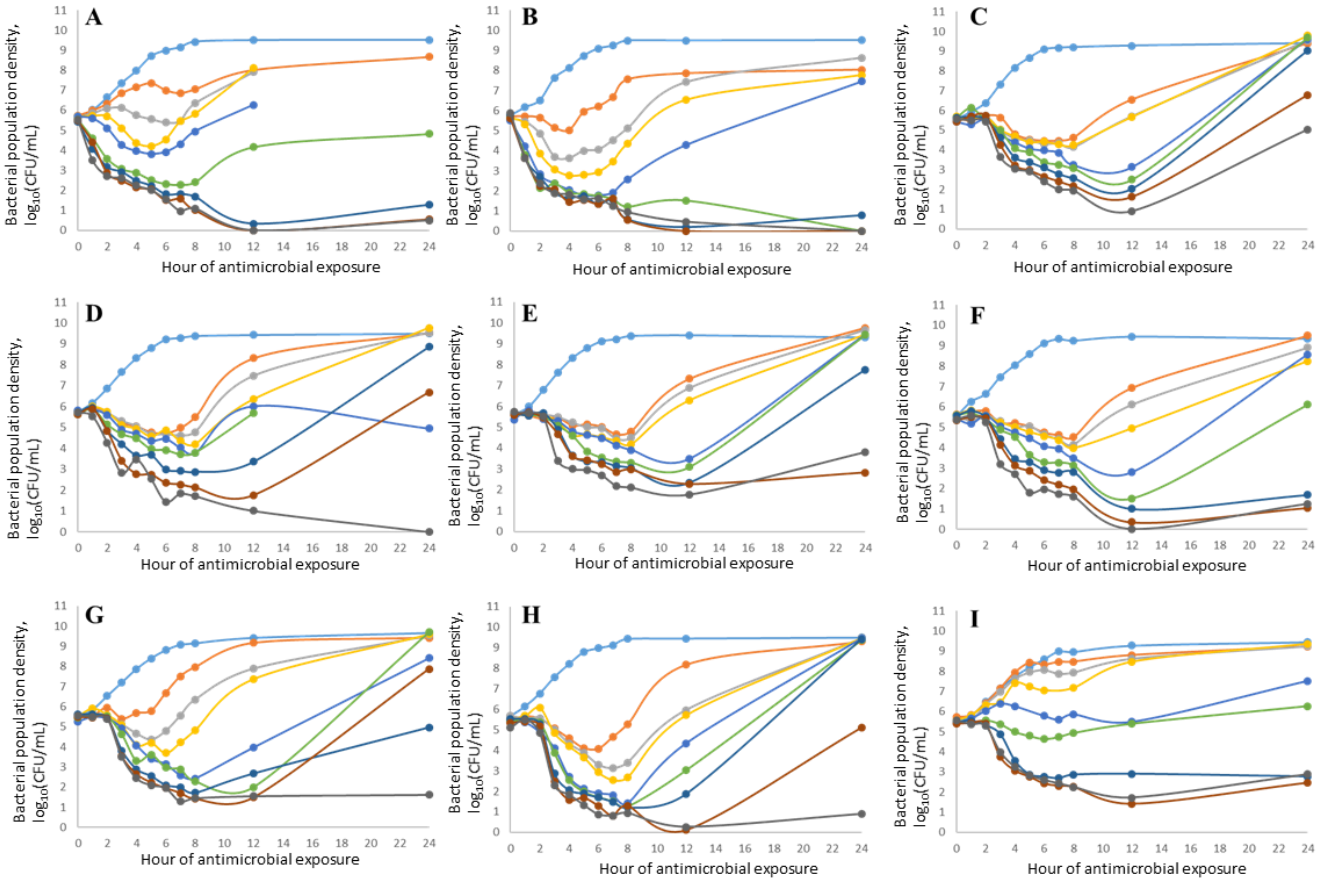

Supplementary Table 1. Relative fit statistics for the six candidate models in capturing the ciprofloxacin pharmacodynamics against *n*=24 strains of nontyphoidal *Salmonella enterica* subsp. *enterica* of diverse serotypes. Results are organized by strain, lowest to highest AIC, and then by highest to lowest adjusted R^2. AIC – Akaike information criterion, a lower value indicates a better model fit. R^2 – coefficient of variation, a higher value indicates a better model fit. The models were 1) inhibitory baseline sigmoid I_{max} model – form 1; 2) inhibitory baseline sigmoid I_{max} model – form 2; 3) inhibitory fractional model; 4) inhibitory fractional sigmoid model; 5) inhibitory fractional I_{max} model; and 6) fractional sigmoid I_{max} model.

Strain ID	Model ID	AIC	Adjusted R^2	Strain ID	Model ID	AIC	Adjusted R^2
9	1	-24.12	0.96	12	1	-15.50	0.90
	6	-24.12	0.96		6	-15.50	0.90
	4	-15.40	0.88		4	-12.81	0.85
	5	-15.40	0.88		5	-12.81	0.85
	3	5.54	-0.24		3	3.73	-0.13
	2	7.33	-0.43		2	5.18	-0.25
13	1	-18.88	0.96	23	1	-38.73	0.99
	6	-18.88	0.96		6	-38.73	0.99
	4	-7.27	0.82		4	-11.61	0.72
	5	-7.27	0.82		5	-11.61	0.72
	3	1.29	0.95		3	-2.93	0.20
	2	11.80	-0.45		2	0.13	-0.12
1	1	-14.88	0.90	14	1	-17.04	0.97
	6	-14.88	0.90		6	-17.04	0.97
	4	-6.22	0.68		4	-10.89	0.92
	5	-6.22	0.68		5	-10.89	0.92
	3	-4.77	1.62		3	11.11	0.31
	2	10.51	-0.51		2	15.81	-0.53
8	1	-20.37	0.92	24	1	-18.65	0.97

	6	-20.37	0.92		6	-18.65	0.97
	4	-14.36	0.82		4	-11.86	0.92
	5	-14.36	0.82		5	-11.86	0.92
	3	-10.20	1.56		3	-9.085	1.32
	2	6.53	-0.49		2	12.87	-0.44
7	1	-20.26	0.97	16	1	-22.13	0.98
	6	-20.26	0.97		6	-22.13	0.98
	4	-6.37	0.83		4	-14.79	0.94
	5	-6.37	0.83		5	-14.79	0.94
	3	9.28	0.38		3	9.53	0.30
	2	14.30	-0.52		2	14.12	-0.51
10	1	-10.36	0.90	18	1	-11.31	0.90
	6	-10.36	0.90		6	-11.31	0.90
	4	-6.11	0.81		4	-1.16	0.63
	5	-6.11	0.81		5	-1.16	0.63
	3	9.81	0.38		3	9.67	0.17
	2	14.59	-0.53		2	13.49	-0.50
5	1	-21.12	0.98	2	1	-22.83	0.95
	6	-21.12	0.98		6	-22.83	0.95
	4	-7.24	0.87		4	-16.07	0.89
	5	-7.24	0.87		5	-16.07	0.89
	3	10.97	0.33		3	2.93	0.037
	2	15.78	-0.53		2	6.13	-0.43
6	6	-37.44	0.98	4	1	-15.46	0.93

	1	-37.44	0.98		6	-15.46	0.93
	5	-25.27	0.90		4	-10.42	0.86
	4	-25.27	0.90		5	-10.42	0.86
	3	-5.44	0.02		3	6.79	0.26
	2	-3.20	-0.23		2	11.22	-0.50
22	1	-12.25	0.91	15	5	-14.04	0.93
	6	-12.25	0.91		4	-14.04	0.93
	4	-4.05	0.73		1	-13.54	0.93
	5	-4.05	0.73		6	-13.54	0.93
	3	8.50	0.23		3	9.09	0.33
	2	12.67	-0.49		2	13.82	-0.51
17	1	-23.74	0.94	3	6	-10.62	0.94
	6	-23.74	0.94		1	-10.62	0.94
	4	-14.85	0.80		4	-3.85	0.85
	5	-14.85	0.80		5	-3.85	0.85
	3	-0.58	-0.098		3	12.87	0.54
	2	0.97	-0.23		2	18.47	-0.54
11	1	-10.75	0.91	19	1	-14.33	0.92
	6	-10.75	0.91		6	-14.33	0.92
	4	0.84	0.59		4	-4.27	0.68
	5	0.84	0.59		5	-4.27	0.68
	3	12.90	-0.29		3	7.41	0.12
	2	14.82	-0.52		2	11.00	-0.47
20	1	-7.10	0.88	21	1	-11.70	0.89

	6	-7.10	0.88		6	-11.70	0.89
	4	2.02	0.61		4	-0.90	0.53
	5	2.02	0.61		5	-0.90	0.53
	3	8.66	0.64		3	8.29	0.17
	2	15.62	-0.49		2	12.14	-0.52

Supplementary Table 2. Relative fit statistics for the six candidate models in capturing the ceftriaxone pharmacodynamics against *n*=29 strains of nontyphoidal *Salmonella enterica* subsp. *enterica* of diverse serotypes. Results are organized by strain, lowest to highest AIC, and then by highest to lowest adjusted R^2. AIC – Akaike information criterion, a lower value indicates a better model fit. R^2 – coefficient of variation, a higher value indicates a better model fit. The models were 1) inhibitory baseline sigmoid I_{max} model – form 1; 2) inhibitory baseline sigmoid I_{max} model – form 2; 3) inhibitory fractional model; 4) inhibitory fractional sigmoid model; 5) inhibitory fractional I_{max} model; and 6) fractional sigmoid I_{max} model.

Strain ID	**Model ID**	**AIC**	**Adjusted R^2**	**Strain ID**	**Model ID**	**AIC**	**Adjusted R^2**
37	4	-28.61	0.9466	45	1	-29.075	0.93
	1	-26.83	0.94		6	-29.07	0.93
	6	-26.83	0.94		4	-21.40	0.80
	3	-13.83	0.85		5	-21.40	0.80
	5	-11.97	0.83		2	-11.85	0.31
	2	-2.17	-0.30		3	-7.40	-0.32
1	6	-23.17	0.91	43	1	-41.50	0.99
	1	-23.17	0.91		6	-41.50	0.99
	4	-19.30	0.86		4	-23.39	0.87
	3	-6.50	0.20		5	-23.39	0.87
	2	-5.75	0.19		2	-9.22	0.19
	5	-4.55	0.05		3	-8.93	0.10
39	4	-29.18	0.97	25	6	-29.52	0.98
	5	-29.18	0.97		1	-29.52	0.98
	1	-27.60	0.96		4	-15.08	0.88
	6	-27.60	0.96		5	-15.08	0.88
	3	-13.02	1.13		3	-8.69	1.34
	2	2.07	-0.39		2	7.56	-0.45

8	1	-34.64	0.94	28	1	-16.27	0.91
	6	-34.64	0.94		6	-16.27	0.91
	5	-34.01	0.93		4	-7.39	0.73
	4	-34.01	0.93		5	-7.40	0.73
	3	-15.47	0.23		3	-5.38	1.30
	2	-15.13	0.23		2	9.28	-0.50
7	1	-28.25	0.96	38	6	-23.96	0.94
	6	-28.250	0.96		1	-23.96	0.94
	4	-22.71	0.91		5	-23.80	0.94
	3	-10.82	0.84		4	-2380	0.94
	5	-9.23	0.50		3	-14.06	1.14
	2	0.13	-0.32		2	2.54	-0.40
29	6	-25.30	0.97	30	1	-31.86	0.99
	1	-25.30	0.97		6	-31.86	0.99
	5	-24.57	0.97		5	-19.08	0.94
	4	-24.57	0.97		4	-19.08	0.94
	3	-10.80	1.25		3	-9.10	1.47
	2	6.66	-0.45		2	9.69	-0.50
27	1	-26.07	0.97	42	1	-29.69	0.95
	6	-26.07	0.97		6	-29.69	0.95
	5	-16.57	0.88		4	-22.71	0.88
	4	-16.57	0.88		5	-22.71	0.88
	3	-9.33	1.21		2	-7.70	0.19
	2	5.69	-0.41		3	-4.57	-0.33

33	1	-21.95	0.96	26	1	-14.63	0.91
	6	-21.95	0.96		6	-14.63	0.91
	4	-7.81	0.76		4	-13.07	0.89
	5	-7.81	0.76		5	-13.07	0.89
	3	-5.24	1.34		3	-10.06	1.60
	2	9.77	-0.48		2	10.98	-0.49
35	4	-18.55	0.90	3	1	-42.07	0.99
	1	-18.43	0.90		6	-42.07	0.99
	3	-10.53	1.23		4	-15.80	0.80
	5	-8.62	1.36		5	-15.80	0.80
	6	3.39	0.30		2	-2.56	-0.00
	2	5.57	-0.46		3	-1.11	-0.33
41	1	-34.18	0.96	40	6	-27.84	0.91
	6	-34.18	0.96		1	-27.84	0.91
	4	-22.17	0.82		4	-24.63	0.86
	5	-22.17	0.82		5	-24.63	0.86
	2	-14.74	0.55		3	-11.63	0.23
	3	-7.43	-0.27		2	-9.66	0.08
2	1	-30.31	0.94	31	1	-18.39	0.95
	6	-30.31	0.94		6	-18.39	0.95
	5	-28.73	0.93		4	-10.75	0.85
	4	-28.73	0.93		5	-10.75	0.85
	2	-8.85	0.10		3	8.47	1.85
	3	-6.54	-0.32		2	11.30	-0.51

36	6	-29.00	0.94	34	5	-37.57	0.98
	1	-29.00	0.94		4	-37.57	0.98
	4	-27.56	0.93		6	-36.39	0.98
	5	-27.56	0.93		1	-36.39	0.98
	3	-14.63	0.88		3	-13.89	0.84
	2	-3.71	-0.20		2	-3.29	-0.22
15	1	-30.20	0.95	47	1	0.99	-61.38
	6	-30.20	0.95		6	0.99	-61.37
	4	-28.18	0.94		4	0.68	-17.33
	5	-28.18	0.94		5	0.68	-17.33
	2	-7.22	0.12		2	0.22	-9.78
	3	-4.62	-0.33		3	-0.33	-6.48
46	1	0.98	-38.27	44	1	0.99	-42.55
	6	0.98	-38.27		6	0.99	-42.55
	4	0.78	-19.72		4	0.87	-25.76
	5	0.78	-19.72		5	0.87	-25.76
	2	0.25	-9.94		2	0.17	-10.99
	3	-0.32	-6.18		3	-0.33	-7.99
32	1	0.97	-23.51	45	1	0.93	-29.07
	6	0.97	-23.51		6	0.93	-29.07
	3	1.57	-5.92		4	0.80	-21.40
	4	0.87	-11.47		5	0.80	-21.40
	5	0.87	-11.47		2	0.31	-11.85
	2	-0.52	12.038		3	-0.32	-7.40

Chapter-3 Mathematical modeling of the "inoculum effect": six applicable models and the MIC advancement point concept

Jessica R. Salas[1], Majid Jaberi-Douraki[2,3,4,*], Xuesong Wen[3,4], Victoriya V. Volkova[1,5*]

[1] Department of Diagnostic Medicine/Pathobiology,

[2] Department of Mathematics,

[3] Institute of Computational Comparative Medicine,

[4] Department of Anatomy and Physiology,

[5] Center for Outcomes Research and Epidemiology,

Kansas State University, Manhattan, KS 66506, USA

* Corresponding author

Phone: +1 (607) 220-8687. e-mail: vv88@vet.k-state.edu (Dr. Victoriya Volkova).

(Published in *FEMS Microbiology Letters* 2020 367(5) fnaa012,

https://doi.org/10.1093/femsle/fnaa012)

Abstract

Antimicrobial treatment regimens against bacterial pathogens are designed using the drug's minimum inhibitory concentration (MIC) measured at the bacterial density of 5.7 $\log_{10}$(colony-forming units (CFU)/mL) *in vitro*. However, MIC changes with pathogen density, which varies among infectious diseases and during treatment. Incorporating this into treatment design requires realistic mathematical models of the relationships. We compared the MIC-density relationships for Gram-negative *Escherichia coli* and nontyphoidal *Salmonella enterica* subsp. *enterica* and Gram-positive *Staphylococcus aureus* and *Streptococcus pneumonia* (for n=4 drug-susceptible strains per (sub)species and 1-8 $\log_{10}$(CFU/mL) densities), for antimicrobial classes with bactericidal activity against the (sub)species: β-lactams (ceftriaxone and oxacillin), fluoroquinolones (ciprofloxacin), aminoglycosides (gentamin), glycopeptides (vancomycin), and oxazolidinones (linezolid). Fitting six candidate mathematical models to the $\log_2$(MIC) *vs.* $\log_{10}$(CFU/mL) curves did not identify one model best capturing the relationships across the pathogen-antimicrobial combinations. Gompertz and logistic models (rather than a previously proposed Michaelis-Menten model) fitted best most often. Importantly, the bacterial density after which the MIC sharply increases (an MIC advancement-point density) and that density's intra-(sub)species range evidently depended on the antimicrobial mechanism of action. Capturing these dependencies for the disease-pathogen-antimicrobial combination could help determine the MICs for which bacterial densities are most informative for treatment regimen design.

Keywords: antimicrobials, antimicrobials, minimum inhibitory concentration (MIC), inoculum effect, antimicrobial pharmacodynamics, *Escherichia coli*, *Salmonella enterica* subsp. *enterica*, non-typhoidal *Salmonella*, *Staphylococcus aureus*, *Streptococcus pneumoniae*

Introduction

Effective antimicrobial treatment regimens for bacterial diseases are essential for prudent use of existing antimicrobial drugs as a limited resource (*2, 8*). Regimens are designed projecting the pharmacodynamics against the pathogen population at the infection site operating with several parameters, most often with the antimicrobial's minimum inhibitory concentration (MIC) measured *in vitro* at the bacterial density of 5.7 $\log_{10}$(colony-forming units (CFU)/mL) (*i.e.*, $5x10^5$ CFU/mL) (*2, 8, 80, 82-85*). Values of the MIC and other pharmacodynamic parameters are assumed to remain constant throughout treatment (*2, 69, 83-87*). However, pathogen density (number of viable bacteria per g or mL) at the infection site varies among pathogen-disease combinations and patients, *e.g.*, densities 3-9 $\log_{10}$(CFU/mL) are reported in human soft tissue and intraabdominal infections (*88-92*) and 3.7-8.5 $\log_{10}$(CFU/mL) in cerebrospinal fluid of humans with meningitis (*93*). During treatment, pathogen density at the infection site can fluctuate in response to the antimicrobial concentration, but overall decreases until the infection is eradicated by the treatment (a.k.a. bacteriological cure) and/or the host immune responses (*13, 94*). Importantly, an antimicrobial's MIC changes with bacterial population density (*95-99*). Accounting for the changes could enable optimizing treatment regimens to maximize the bacteriological cure probability while minimizing antimicrobial drug use (*71, 72*).

The term *inoculum effect* (IE) has been used historically for the MIC-bacterial density relationships (*95-101*). It is believed to be first reported *in vitro* in 1945 (*102*) and *in vivo* in 1952 (*103*). Currently, the phenomenon is considered as a bacterial *collective antimicrobial tolerance* response to antimicrobial exposure (*71*). The phenomenon is documented *in vitro* for bactericidal and bacteriostatic antimicrobial drugs in Gram-negative and Gram-positive bacterial species,

including Enterobacteriaceae, staphylococci, and streptococci (*99, 104-110*). Few mathematical models have been investigated for reflecting the antimicrobial MIC-bacterial density relationships. It has been proposed that a Michaelis-Menten model reflects these relationships, based on data for several antimicrobials and one *Staphylococcus aureus* strain (*99*). We hypothesized that it is unlikely that a single model accurately captures the MIC-density relationships across pathogen-antimicrobial combinations, and that the variety of the relationship's mathematical forms has not been elucidated. The objective for this study was to compare the MIC-density relationships and mathematical models capturing those for exemplar Gram-negative (*Escherichia coli* and nontyphoidal *Salmonella enterica* subsp. *enterica*) and Gram-positive (*Streptococcus pneumoniae* and *S. aureus*) pathogens and focusing on antimicrobials with bactericidal activity against these (sub)species (further- 'species').

Materials and methods

Bacterial isolates. Four isolates from humans and animals of each *E. coli*, *S. enterica* subsp. *enterica* (further – *S. enterica*), *S. aureus*, and *S. pneumoniae* were used. The isolates were classified as susceptible to the antimicrobial drugs tested. The sample size (n=4 isolates per species) was chosen in the absence of prior data on between-isolate variability in the MIC-bacterial density relationships for the antimicrobials and species. Four species isolates were tested throughout the extent of the study, unless stated otherwise. The *Escherichia coli* and *S. enterica* isolates were obtained from farm-animal feces during field studies by the Kansas State University faculty in 2014-2016. The *Salmonella enterica* isolates were of serotypes Anatum, Bovis, Anatum, Give, and Typhimurium (serotyped by the U.S. National Veterinary Services Laboratories, Ames, IA). The *Staphylococcus aureus* isolates obtained from a skin swab, biopsy,

and blood samples from domestic animals in 2016 were provided by the Kansas State Veterinary Diagnostic Laboratory. The *Streptococcus pneumoniae* isolates of serotypes 3 and 19A (serotyped by the U.S. Centers for Disease Control and Prevention) were provided by the CDC and obtained from human blood samples between 2003 and 2009.

Antimicrobials. High purity ceftriaxone, ciprofloxacin, gentamicin, linezolid, oxacillin, and vancomycin forms (Sigma-Aldrich, Inc., St. Louis, MO, U.S.) were used. Stock drug solutions were prepared accounting for the form potency. The stock solutions of ceftriaxone, gentamicin, oxacillin, and vancomycin (10 mg/mL) were prepared by dissolving the drug powder in sterile distilled water; of ciprofloxacin (10 mg/mL) by dissolving the powder in 0.1 N hydrochloric acid solution; and of linezolid (10 mg/mL) by dissolving the powder in dimethyl sulfoxide. The stock solutions were aliquoted, stored at -20°C, and used within 3 months, except for ciprofloxacin stock solutions, which were stored at 4°C and used within 2 weeks. Before each experiment, a stock solution aliquot was diluted to a working solution of desired drug concentration in sterile distilled water.

Determination of antimicrobial MIC for different bacterial densities. Each isolate was incubated overnight at 37°C on tryptic soy agar with 5% sheep blood (BAP, Remel^{TM}, Lenexa, KS, U.S.). For an isolate of *E. coli*, *S. enterica*, or *S. aureus*, bacterial colonies from the BAP plate were suspended in 9 mL of cation-adjusted Mueller-Hinton broth (Ca-MHB, BBL^{TM}, Sparks, MD, U.S.) to visually match the 0.5 McFarland turbidity standard. The suspension was serially diluted in Ca-MHB to each of the expected bacterial densities 10^8, $5x10^7$, 10^7, 10^6, 10^5, 10^4, 10^3, and 10^2 CFU/mL. The densities were confirmed by serially diluting an aliquot of each the 10^8, 10^5, and 10^2 dilutions in a sterile 0.9% saline solution, directly plating the dilutions in duplicate on BAP, incubating the plates at 37°C aerobically for 18-24 hours (until

colonies were visible), and counting the bacterial colonies (*72*). For an isolate of *S. pneumoniae*, bacterial colonies from the BAP were suspended to the expected bacterial density ~$1x10^8$ – $5x10^8$ CFU/mL in 9 mL of Ca-MHB with 5% (v/v) lysed horse blood (Innovative Research, Inc., Novi, MI, U.S.). (For each *S. pneumoniae* isolate, a preparatory experiment was performed to determine the required colony number.) The suspension was serially diluted in Ca-MHB with 5% (v/v) lysed horse blood to the expected densities 10^8 to 10^2 CFU/mL, as for the other bacterial species, and the densities similarly confirmed.

A sterile 96-well plate (Corning, Inc., Lowell, MA, U.S.) was used for one bacterial isolate and one starting drug concentration. A plate row (12 wells) was used for one bacterial density; each well in the row contained 100 µL of the isolate suspension of that density. Eight rows each contained the isolate suspension of one of 10^8, $5x10^7$, 10^7, 10^6, 10^5, 10^4, 10^3, and 10^2 CFU/mL densities. The starting drug concentrations (in different plates) were 1,500, 1,000, 25, and 20 mg/L for all the antimicrobials and species, except linezolid for which those were 1,000, 500, 50, and 40 mg/L for *S. aureus* and *S. pneumoniae*. Of the starting drug concentration solution, 100 µL was loaded into each well in column 1, the bacterial and antimicrobial solutions in column 1 pipetted 10 times, after which 100 µL of each well were loaded from column 1 to column 2 and the pipette tips replaced; this was repeated for columns 2 to 11. Thus, each starting drug concentration and 10 of its sequential two-fold dilutions were tested against each density of the bacterial isolate. Column 12 was the positive control of visible isolate growth in the absence of antimicrobial. The plates were incubated at 37°C aerobically for 18-24 hours; the MIC for each density of the isolate was read as the lowest drug concentration inhibiting visible growth from that density. The experiment for each isolate and each of four starting drug concentrations was performed in duplicate on different dates. For each density of the isolate, if the duplicate

MIC readings were within one 2-fold drug dilution apart, the lowest reading was the result recorded. If the duplicate MIC readings were further apart, a third replicate was performed and the lowest MIC of the readings within one 2-fold drug dilution apart from two of the three replicates was the result recorded.

Mathematical modeling of antimicrobial MIC-bacterial density relationships.

The experimental data were transformed to $\log_2$(MIC) and $\log_{10}$(CFU/mL) to enable a comparative evaluation of the MIC-density relationship forms (Figs. 9-10). Each of six candidate non-linear models was fitted to the transformed data for a representative isolate for each of the antimicrobial-bacterial species combinations. This included the Michaelis-Menten model proposed earlier based on data for several antimicrobials and one *S. aureus* strain (*99*). Each model had at most four parameters to capture the $\log_2$(MIC) vs. $\log_{10}$(CFU/mL) curves. Candidate models with more parameters (*111, 112*) were not considered to avoid model overfitting given the limited number of observations per individual antimicrobial-bacterial species combination.

The investigated six models are detailed below. We defined $y=\log_2$(MIC) and $x=\log_{10}$(CFU/mL) bacterial density.

A Michaelis-Menten model was formulated by:

$$y = \frac{a \times x}{x + b} + c \qquad [1]$$

where

$a + c$ – projects maximum y at high bacterial densities;

b – projects x at which a half maximum y ($(a + c) \times 0.5$) is reached;

c – projects minimum y at low bacterial densities.

The Michaelis-Menten model, however, does not reproduce sigmoid curves, such as those observed for the $\log_2$(MIC) *vs.* $\log_{10}$(CFU/mL) relationships (Figs. 9-10). The Hill-function models, which are also used to describe antimicrobial pharmacodynamics against bacterial populations, can capture such behavior (*74, 113, 114*). Assuming the Hill coefficient value > 0, a Hill-function model was formulated by:

$$y = \frac{a \times x^b}{x^b + c} + d \qquad [2]$$

where

$a + d$ – projects maximum y at high bacterial densities;

b – reflects steepness (steepness of an increase in y with an increase in x) and shape of sigmoid function;

c – projects x^b at which a half maximum y ($(a+d)\times 0.5$) is reached;

d – projects minimum y at low bacterial densities.

A logistic model can also capture a sigmoid curve and was formulated by:

$$y = \frac{a}{b + \exp(-c \times x)} + d \qquad [3]$$

where

$\frac{a}{b} + d$ – projects maximum y at high bacterial densities;

b – represents a shift for the location of $\exp(-c \times x)$ at which a half maximum y ($(\frac{a}{b} + d) \times 0.5$) is reached;

c – reflects steepness of sigmoid function;

$d + \frac{a}{b+1}$ – projects minimum y at low bacterial densities.

Depending on the sigmoid curve shape, a Gompertz model might better capture the shape than Hill or logistic models (*79, 115*). A Gompertz model was formulated by:

$$y = a \times \exp\left[-b \times \exp\left(-c \times x\right)\right] + d \qquad [4]$$

where

$a + d$ – projects maximum y at high bacterial densities;

b – represents a shift for the location of $\frac{\ln(2)}{\exp\left(-c \times x\right)}$ at which a half maximum y ($(a + d) \times 0.5$) is reached;

c – reflects steepness of sigmoid function;

$d + a \times \exp(-b)$ – projects minimum y at low bacterial densities.

A von Bertalanffy model can also capture a sigmoid curve (*116, 117*) and was formulated by:

$$y = a \times \left[1 - \exp\left(-b \times x\right)\right]^{c} + d \qquad [5]$$

where

$a + d$ – projects maximum y at high bacterial densities;

b – reflects steepness of sigmoid function;

c – reflects shape of sigmoid function;

d – projects minimum y at low bacterial densities.

An exponential effect of the bacterial density on the antimicrobial MIC is assumed for modeling the antimicrobial pharmacodynamics against bacterial populations (*118*). We included a bi-exponential model defined as a multilinear approximation of an exponential function by:

$$y = a \times \exp(-b \times x) + c \times \exp(-d \times x) \qquad [6]$$

where

$a + c$ – projects minimum y

b and d – adjust steepness of sigmoid function in approaching maximum y (*i.e.*, control x at which the maximum y is projected).

Each model was fitted using the least-squares method by regressing y on x for a representative isolate for the bacterial-species combination, with the "trust-region" algorithm that efficiently handles large sparse and small dense problems in searching the parameter space (*119*). Model parameter values minimizing mean squared error between the predicted and observed y values across the bacterial densities tested were estimated; model iterations were terminated if the tolerance $< 1 \times 10^{-10}$ change in the mean squared error between successive iterations was met or after 500,000 iterations. No boundaries were imposed on the parameter values except for keeping the value positive or negative per model structure. Using the estimated parameter values, the model projections were generated for the bacterial densities 10^1-10^{12} (CFU/mL). Relative fit of the six models (with parameter values estimated as above) to the representative-isolate data

was evaluated with the adjusted coefficient of determination R^2 (a larger adjusted R^2 indicated a better model fit) and with Akaike's Information Criterion (AIC) obtained using the log-likelihood function penalized by the number of parameters (a smaller AIC indicated a better model fit).

The density x at which there was the maximum positive change in the y slope estimated by the model was defined as the MIC-AP. The curvature (*120, 121*) of the y vs. x curve projected by the model at the density x was defined as:

$$C(x) = \frac{\left|y''(x)\right|}{\left(1+\left(y'(x)^2\right)\right)^{\frac{3}{2}}} \qquad [7]$$

The curvature equations for the six models are included in the supplementary materials. The MIC-AP was:

$$AP = \max_{\text{over all densities } x} C(x) \qquad [8]$$

The modeling was implemented in MATLAB® R2019b (MathWorks Inc., Natick, MA, U.S.). Because of the limited number of isolates tested per bacterial species, statistical evaluations of the intra-species variability and relative magnitudes of the intra- *vs.* inter-species variabilities in the MIC-density relationships within or between antimicrobials were not performed.

Results and discussion

We determined and compared the MIC-bacterial density relationships for two Gram-negative (*E. coli* and nontyphoidal *S. enterica*) and two Gram-positive (*S. aureus*, *S. pneumoniae*) bacterial species and bactericidal antimicrobials from these drug classes: β-lactams

(oxacillin and ceftriaxone), fluoroquinolones (ciprofloxacin), aminoglycosides (gentamicin), and glycopeptides (vancomycin) (*122, 123*). We added the bacteriostatic oxazolidinone linezolid as one of newest antimicrobials introduced to tackle infections by strains resistant to older antimicrobials (*124, 125*). For an antimicrobial, the MIC-density relationship curve varied among the bacterial species; likewise, for a species, it varied among the antimicrobials (Figs. 9-10). These results agreed with earlier *in vitro* data, *e.g.*, for *Haemophilus influenzae* type b isolates a stronger IE is observed for the *β*-lactams penicillin and ampicillin than for chloramphenicol (*93*). For a *Staphylococcus aureus* strain (one tested), the IE is strongest for oxacillin, followed by gentamicin, and lowest for vancomycin and linezolid (*99*). Based on our results, for a given antimicrobial species combination, the MIC-density relationship could be similar across isolates classified as susceptible to the antimicrobial (Figs. 9-10 and Table 5).

Mathematical modeling of antimicrobial MIC-bacterial density relationships. Six mathematical models were compared in fitting the MIC-density relationship curve for each of the antimicrobial-bacterial species combinations. The candidate model set was chosen based on the observed $\log_2$(MIC) *vs.* $\log_{10}$(CFU/mL) curves (Figs. 9-10). The models were based on the exponential, logistic, Gompertz, von Bertalanffy, Hill, and Michaelis-Menten functions. The Gompertz, logistic, von Bertalanffy, and exponential models most often demonstrated the best-fit to the data across the antimicrobial-species combinations. These trends could be seen in Figs. 11-12 (the model parameter values and fit statistics for each antimicrobial-bacterial species combination are given in Supplementary Table 1).

The “classical” microbiological methods used did not allow reproducible (within one 2-fold drug dilution) MIC measurements at the densities beyond ~8.5-8.7 $\log_{10}$(CFU/mL). We conjuncture that similar goodness-of-fit of multiple models to a $\log_2$(MIC) *vs.* $\log_{10}$(CFU/mL)

curve was due to the limited observation of the relationship curve. The models captured the curve's observed part. It is unclear which model would be followed for a wider range of densities. This is demonstrated theoretically by the model predictions for the densities 10^1 to 10^{12} (CFU/mL) in Figs. 11-12. Identifying mathematical models that capture the MIC-IE relationship could reveal the relationship's clinically important specifications, including the density beyond which the MIC increases sharply, which we term the MIC advancement-point; the steepness of the subsequent MIC increase; and whether and at which density an inflection (deceleration in the MIC increase) occurs or the MIC levels-off. For example, predictions of two "best-fit" models for higher-than-tested bacterial densities diverged in some (Fig. 11 a, c, d) but not in other (Fig. 11c, Fig. 12h) cases. The divergent predictions showed that, *e.g.*, the oxacillin MIC would increase steeper at high densities of *S. aureus* or *S. pneumoniae* (Fig. 11 c-d), or the gentamicin MIC would level-off at a higher value for *S. pneumoniae* (Fig. 4f), if the relationship follows an exponential rather than logistic model. The ceiling prediction example is that the gentamicin MIC for *S. aureus* was projected to level-off from ~8 $\log_{10}$(CFU/mL) (Fig. 12e) but the ceftriaxone MIC to not level-off until >12 $\log_{10}$(CFU/mL) (Fig. 12a).

Location and range of the antimicrobial MIC-AP. We focus further discussion on specifications and implications of the MIC-AP bacterial density. Antimicrobial treatment regimens are currently designed utilizing the MIC for the density 5.7 $\log_{10}$(CFU/mL). Such a regimen would likely achieve bacteriological cure only if both of the following conditions are true: (1) the antimicrobial MIC-AP across the antimicrobial-susceptible pathogen strains is >5.7 $\log_{10}$(CFU/mL) (*e.g.*, 6.5-8 $\log_{10}$(CFU/mL) for the β-lactam ceftriaxone in *E. coli*, *S. enterica*, and *S. aureus*, Figs. 9 a-b and 10a); and (2) the pathogen density at the infection site(s) is below the MIC-AP. A regimen designed utilizing the MIC for the density 5.7 $\log_{10}$(CFU/mL) would

less likely achieve bacteriological cure if the MIC-AP is lower (*e.g.*, for gentamicin in *E. coli* and *S. enterica*, Figs. 9 e-f, and linezolid in *S. aureus*, Fig. 10i) and the pathogen density at the infection site(s) reaches the MIC-AP. The full MIC-density curve and MIC-AP have not been considered in the design and interpretation of *in vivo* experiments. For example, that clinical efficacy of a *β*-lactam treatment regimen is apparently not sensitive to the infectious inoculum density for *E. coli* or *Klebsiella* spp. (*126*) but is sensitive for *Streptococcus pyogenes* (*127*) could be because the MIC-AP density differs for these antimicrobial-bacterial species combinations (*i.e.*, whether the inocula densities were below or above the MIC-AP for each combination). For illustration, the ceftriaxone MIC-AP for *S. enterica* (Fig. 9b) is ≥1 $\log_{10}$(CFU/mL) higher than for *S. pneumoniae* (Fig. 10b).

Both how consistent the MIC–AP location was among bacterial species and its intra-species between-isolate range apparently depended on the antimicrobial's mechanism of action (Figs. 9-10 and Table 5). The AP location was relatively consistent across the species for an antimicrobial that disrupts bacterial cell-wall synthesis (for the mechanisms of action see (*128-131*)). Specifically, for the *β*-lactam ceftriaxone the AP location was at medium-to-high densities among *E. coli, S. enterica, S. aureus*, and *S. pneumoniae* isolates (Table 5). For the *β*-lactam oxacillin, the location was at lower densities for both *S. aureus* and *S. pneumoniae*. The vancomycin AP for *S. aureus* (single species tested) was at medium to high densities for three of four isolates tested. The AP location was also relatively consistent across the species for the fluoroquinolone ciprofloxacin that inhibits bacterial DNA replication (*29, 128, 132*), but was at lower densities in *E. coli, S. enterica,* and *S. pneumoniae* compared to antimicrobials with different mechanisms of action. In contrast, the AP location varied widely among the species for the aminoglycoside gentamicin and oxazolidinone linezolid which inhibit bacterial protein

synthesis (*128*, *133*, *134*). The gentamicin AP occurred over a range of low to high densities among the 4 different species. This large inter-species range was also observed for linezolid with *S. aureus* and *S. pneumoniae*.

In terms of the intra-species range of the MIC–AP density among the four isolates tested (Figs. 9-10, Table 5), comparatively wide ranges were observed for antimicrobials disrupting bacterial cell-wall synthesis. For the *β*-lactam ceftriaxone the range was 1.1-1.5 $\log_{10}$(CFU/mL) in *E. coli*, *S. enterica*, *S. aureus*, and *S. pneumoniae*. For example, the range of 1.5 $\log_{10}$(CFU/mL) corresponds to the MIC-AP at the densities 5.0 to 6.5 $\log_{10}$(CFU/mL) across *S. pneumoniae* isolates (Fig. 10). The AP range for vancomycin MIC for *S. aureus* was 2.9 $\log_{10}$(CFU/mL). For ciprofloxacin that inhibits bacterial DNA replication, the MIC–AP ranges were also wide: 2.7 $\log_{10}$(CFU/mL) in *E. coli*, 1.9 $\log_{10}$(CFU/mL) in *S. enterica*, and 1.8 $\log_{10}$(CFU/mL) in *S. pneumoniae* (Table 1). In contrast, the MIC-AP ranges intra-species were narrow, <1 $\log_{10}$(CFU/mL), for antimicrobials inhibiting bacterial protein synthesis. For the aminoglycoside gentamicin the range was 0.6-0.9 $\log_{10}$(CFU/mL) in *E. coli*, *S. enterica*, *S. aureus*, and *S. pneumoniae*. For the oxazolidinone linezolid, the range was 1.1 $\log_{10}$(CFU/mL) in *S. aureus* and 0.7 $\log_{10}$(CFU/mL) in *S. pneumoniae*.

The observed differences in the overall location and intra-species range of the MIC-AP density among antimicrobials with different modes of action could relate to IE mechanisms. For antimicrobials disrupting bacterial cell-wall synthesis, the IE is attributed to reduced availability of the target membrane proteins due to the reduced population growth (*127*) and accumulation of drug-degrading enzymes (*126*) at high bacterial densities. For antimicrobials inhibiting bacterial protein synthesis, the IE is attributed to a population growth instability due to the drug-induced

ribosome degradation (*135*). Drug loss due to binding to non-target bacterial structures is proposed as a general mechanism of the IE (*99*).

Our results suggest that the clinical significance of the IE likely systematically varies among antimicrobial drug classes for a bacterial species depending on their action mechanism, which determines the MIC –AP and its intra-species variability. We observed this for bacterial strains susceptible to the antimicrobials. Mathematical models of the MIC-bacterial density relationships could capture such clinically relevant specifications as the MIC-AP density and steepness and ceiling of the subsequent MIC increase.

Overall, across all mechanisms of action and bacteria species, the Gompertz model fit the data best (Table 6, supplementary materials). This evaluation was based on the following criteria: One point was assigned to a model with an adjusted R^2 within 5% of the highest adjusted R^2 obtained for all of the models of that antimicrobial-bacterial species combination. Another point was assigned to the model if it projected the advancement point within the range shown in Table 1. To obtain the model ranking, these awarded "points" for each model were summed and the percentages were calculated based on different comparisons (Tables 6-8 in the supplementary materials). This resulted in Gompertz being within 5% of the highest adjusted R^2 of the model in 81% of cases and within the advancement point range for the bacterial-antimicrobial species combinations in 69% of cases. Similarly, Logistic and von Bertalanffy fit this combined criteria in 69% of the cases, making them other possible fits for different bacterial species-antimicrobials for future studies. Such models should be considered for rational optimization of treatment regimens.

Acknowledgments

We thank microbiologists of the U.S. CDC for providing the *Streptococcus pneumoniae* isolates, and of the Kansas State Veterinary Diagnostic Laboratory for providing the *Staphylococcus aureus* isolates. XW was supported by the Kansas Bioscience Authority via funding for the Institute of Computational Comparative Medicine, Kansas State University. JS and VVV were supported by the National Institute of General Medical Sciences of the U.S. National Institutes of Health (NIH) under award number R15GM126503. The manuscript content is solely the responsibility of the authors and does not represent the NIH official views.

Author contributions

VVV conceived and designed the study. JS and XW performed the experiments. MJD performed the modeling. JS and VVV interpreted the microbiological results and MJD, JS, and VVV the modeling results. VVV and JS wrote the manuscript and MJD contributed.

Conflicts of interest

None declared.

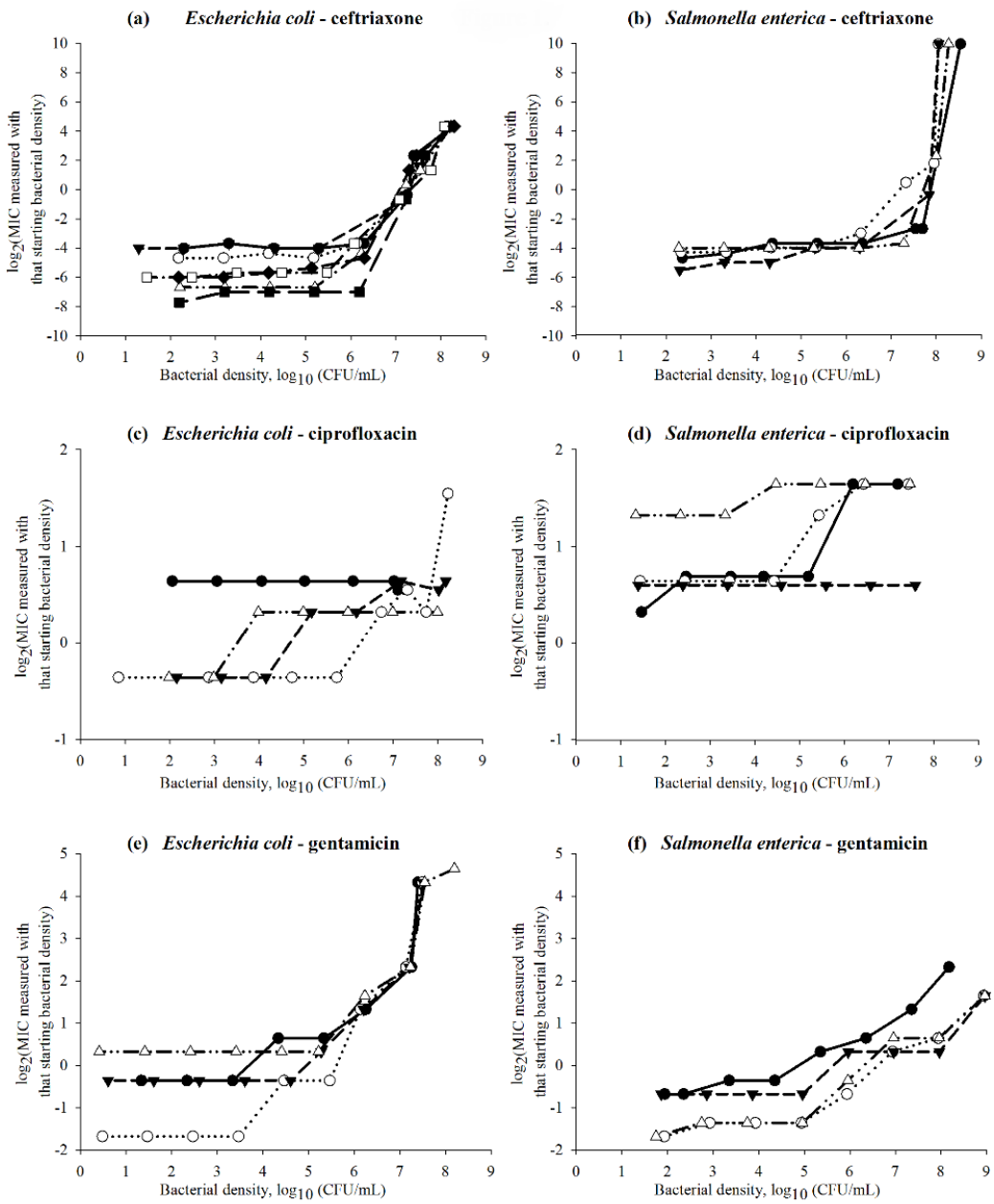

Figure 8: Experimental data on the antimicrobial's minimum inhibitory concentration (MIC) dependency on the bacterial density for Gram-negative *Escherichia coli* (*n*=4 isolates except for ceftriaxone *n*=8 isolates) and nontyphoidal *Salmonella enterica* subsp. *enterica* (*n*=4 isolates).

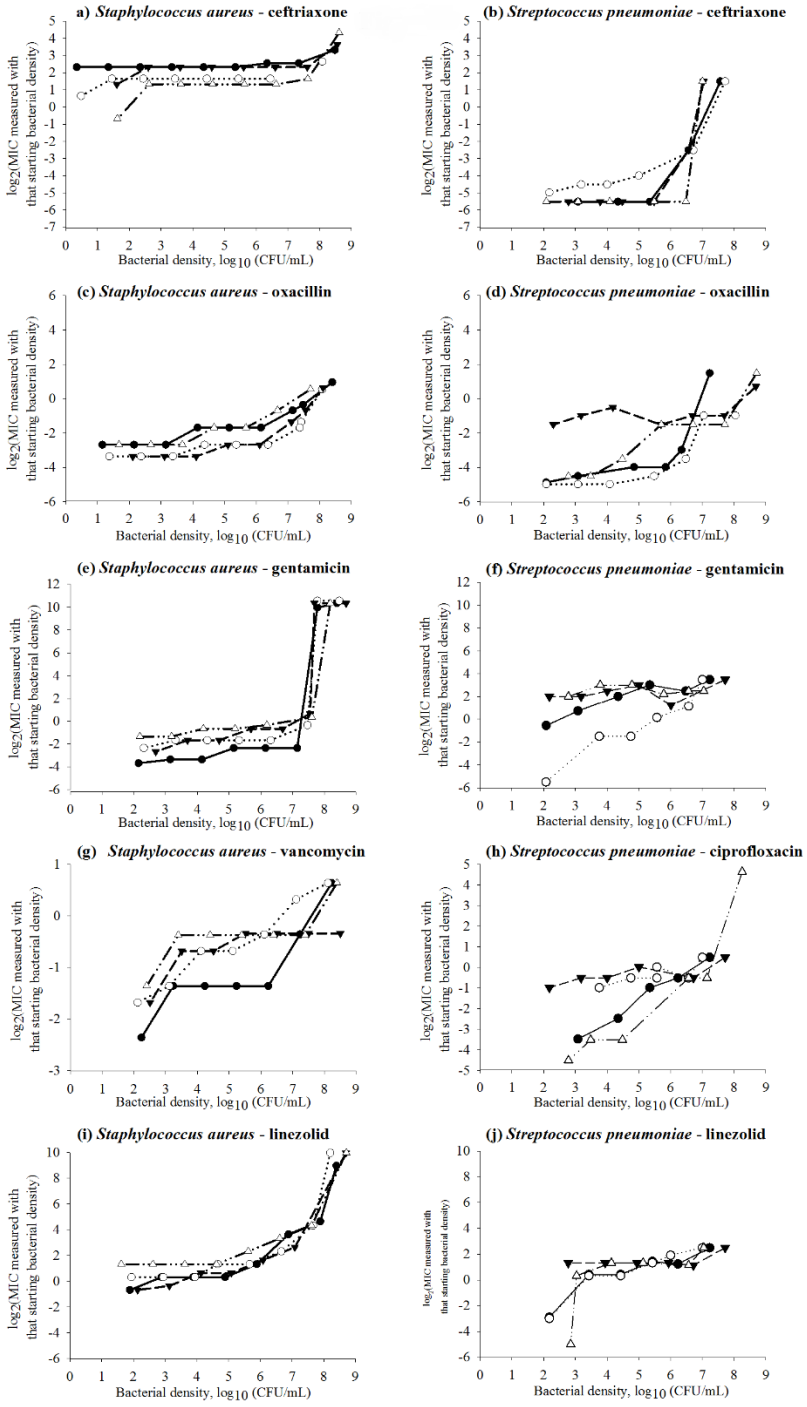

Figure 9: Experimental data on the antimicrobial's minimum inhibitory concentration (MIC) dependency on the bacterial density for Gram-positive *Staphylococcus aureus* (*n*=4 isolates) and *Streptococcus pneumoniae* (*n*=4 isolates).

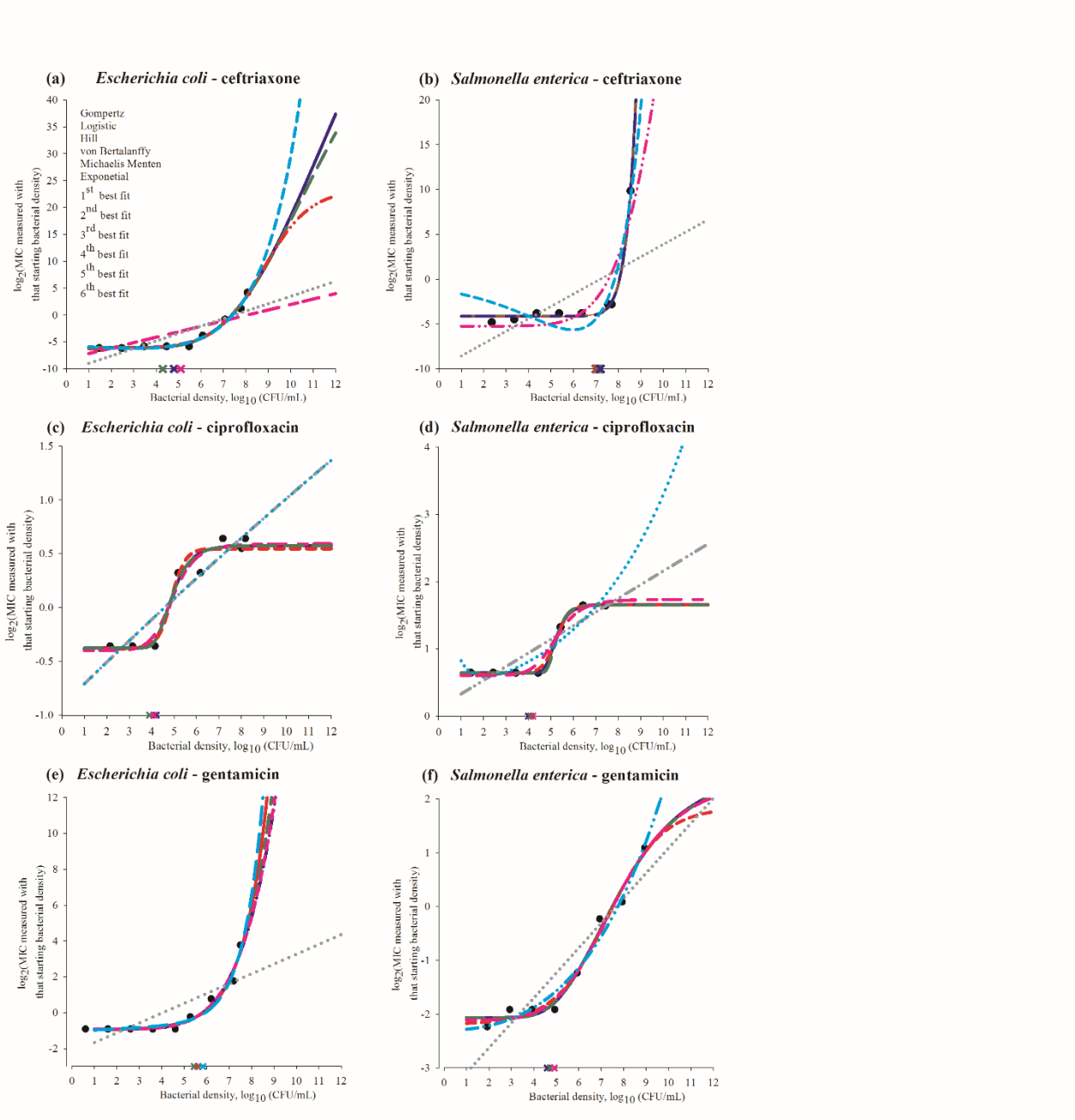

Figure 10: Predictions of candidate mathematical models of the $\log_2$(MIC) vs. $\log_{10}$(CFU/mL) density relationship curve for a representative isolate for each tested antimicrobial in Gram-negative *Escherichia coli* and nontyphoidal *Salmonella enterica* subsp. *enterica*. In each panel, the experimental data for the representative isolate for the bacterial (sub)species and antimicrobial combination are shown by black circles. Each of six candidate models was fitted to the data using the least-squares method. Best-fit parameter values for each of the six models were estimated and used to make the model predictions of $\log_2$(MIC) for 1 to 12 $\log_{10}$(CFU/mL) bacterial densities. The predictions are shown by lines: blue – von Bertalanffy, dark green – Gompertz, red – logistic, pink – Hill, gray – Michaelis-Menten, and cyan – exponential model. The line increment indicates the relative fit of the six models (each with best-fit parameter

values) to the data for the representative isolate. Specifically, predictions of the model with highest adjusted R^2 are shown by a solid line; predictions of the other models are shown in the order of decreasing adjusted R^2 of the model by a long dashed, short-long dashed, short dashed, dashed-dotted-dotted, and dotted lines. The cross shows the MIC advancement-point density estimated using the curvature analysis of the predicted curve for each of the three models with highest adjusted R^2; the cross is of the same color as the line showing the curve predicted by the model. MIC – minimum inhibitory concentration of the antimicrobial. CFU – colony forming units of the bacterial population.

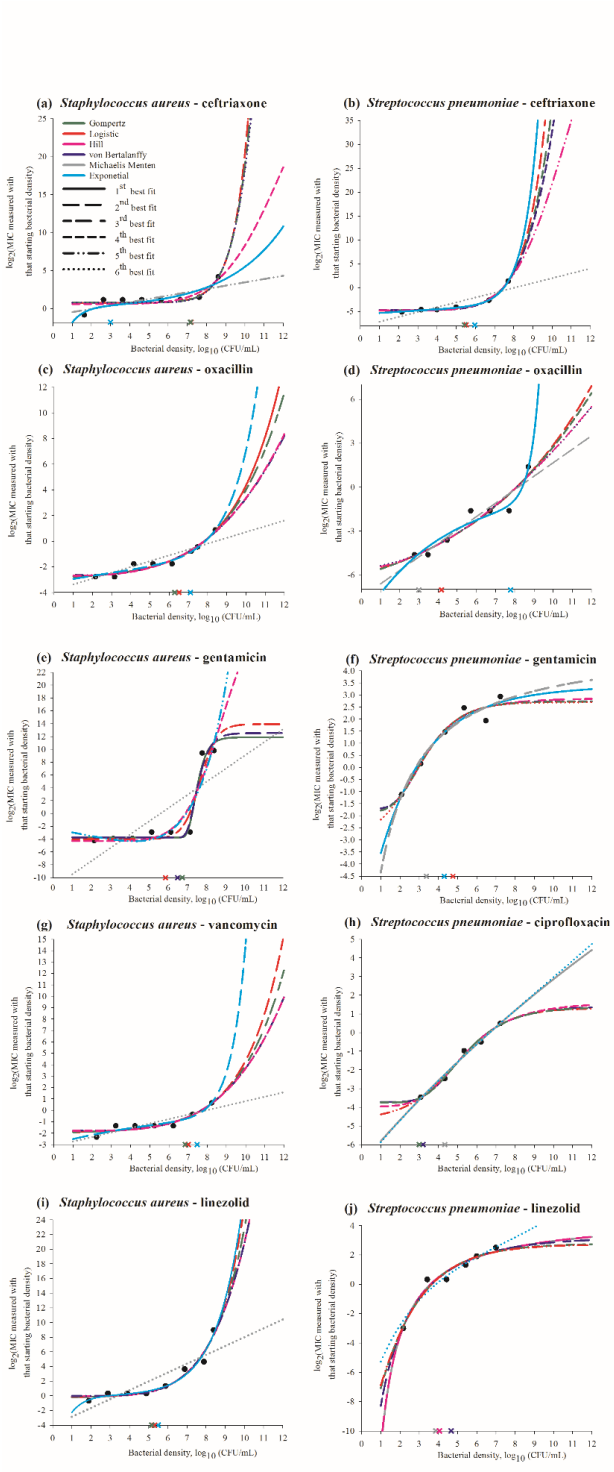

Figure 11: Predictions of candidate mathematical models of the $\log_2$(MIC) *vs.* $\log_{10}$(CFU/mL) density relationship curve for a representative isolate for each tested antimicrobial in Gram-positive *Staphylococcus aureus* and *Streptococcus pneumoniae*. In each panel, the experimental data for the representative isolate for the bacterial (sub)species and antimicrobial combination are shown by black circles. Each of six candidate models was fitted to the data using the least-

squares method. Best-fit parameter values for each of the six models were estimated and used to make the model predictions of $\log_2$(MIC) for 1 to 12 $\log_{10}$(CFU/mL) bacterial densities. The predictions are shown by lines: blue – von Bertalanffy, dark green – Gompertz, red – logistic, pink – Hill, gray – Michaelis-Menten, and cyan – exponential model. The line increment indicates the relative fit of the six models (each with best-fit parameter values) to the data for the representative isolate. Specifically, predictions of the model with highest adjusted R^2 are shown by a solid line; predictions of the other models are shown in the order of decreasing adjusted R^2 of the model by a long dashed, short-long dashed, short dashed, dashed-dotted-dotted, and dotted lines. The cross shows the MIC advancement-point density estimated using the curvature analysis of the predicted curve for each of the three models with highest adjusted R^2; the cross is of the same color as the line showing the curve predicted by the model. MIC – minimum inhibitory concentration of the antimicrobial. CFU – colony forming units of the bacterial population.

Table 7. Location and between-isolate range of the antimicrobial's MIC advancement-point bacterial density (AP), after which the MIC sharply increased, observed for each of the antimicrobial-bacterial (sub)species combinations**.**

Mechanism of antibacterial action: Antimicrobial drug	**The antimicrobial drug MIC's AP observed across *n*=4 isolates of the bacterial (sub)species, $\log_{10}$(colony forming units (CFU)/mL)**			
	Escherichia coli	Nontyphoidal *Salmonella enterica* subsp. *enterica*	*Staphylococcus aureus*	*Streptococcus pneumoniae*
Inhibiting cell-wall synthesis:				
Ceftriaxone	5.2 - 6.3 (range 1.1)	6.2 - 7.3 (range 1.1)	6.4 - 7.6 (range 1.2)	5.0 - 6.5 (range 1.5)
Oxacillin			3.2 - 4.1 (range 0.9)	3.5 - 5.5 (range 2.0)
Vancomycin			4.5 - 7.4 (range 2.9)	
Inhibiting DNA replication:				
Ciprofloxacin	3.0 - 5.7 (range 2.7)	3.3 - 5.2 (range 1.9)		2.2 - 4.0 (range 1.8)
Inhibiting protein synthesis:				
Gentamicin	4.6 - 5.5 (range 0.9)	4.4 -5.0 (range 0.6)	6.7 - 7.6 (range 0.9)	2.1 - 2.8 (range 0.7)
Linezolid			4.6 - 5.7 (range 1.1)	2.2 - 2.9 (range 0.7)

Supplementary Materials

Supplementary Table 3. Parameter values and goodness-of-fit statistics of six candidate mathematical models fitted using the least-squares method to the $\log_2$(MIC) vs. $\log_{10}$(CFU/mL) data for a representative isolate of the bacterial (sub)species for each of the tested antimicrobial-(sub)species combinations. The model equations and parameter definitions are given in the materials and methods section of the manuscript.

Mechanism of action	**Bacterial (sub)species**	**Model**	**Adjusted R^2**	**AIC**	Parameter value (95% confidence interval)			
					a	*b*	*c*	*d*
Inhibiting cell-wall synthesis: Ceftriaxone	*Escherichia coli*	von Bertalanffy	0.98	1.51	108.64 (0; 922.12)	0.23 (0; 1.27)	14.57 (0; 84.49)	-6.07 (-6.94; -5.20)
		Gompertz	0.98	1.50	76.35 (0; 608.57)	22.04 (0; 88.90)	0.29 (0; 1.08)	-6.07 (-6.96; -5.19)
		Hill	0.98	1.48	80.36 (0; 717.47)	6.03 (0; 13.43)	2.10×10^{6} ($0; 1.20\times10^{7}$)	-6.13 (-7.04; -5.21)
		Exponential	0.98	1.47	0.12 (0; 1.01)	-0.58 (-1.35; 0)	-5.77 (-7.77; -3.77)	-0.06 (-0.33; 0)
		Logistic	0.97	1.43	0.01 (0; 0.06)	2.00×10^{-4} ($0; 1.00\times10^{-3}$)	0.96 (0; 2.11)	-6.22 (-7.33; -5.10)
		Michaelis Menten	0.63	4.09	1.32×10^{6} ($0; 8.59\times10^{6}$)	9.53×10^{5} ($0; 4.82\times10^{6}$)	-10.34 (-20.40; -0.29)	-
	Nontyphoidal *Salmonella enterica* subsp. *enterica*	Logistic	0.99	1.79	0 (2.07×10^{-9}; 8.30×10^{-9})	0 (2.07×10^{-9}; 8.31×10^{-9})	2.52 (2.01×10^{-13}; 5.22×10^{-12})	-4.15 (-4.54; -3.76)
		Gompertz	0.99	1.78	1.15×10^{7} ($0; 1.00\times10^{8}$)	60.98 (0; 590.60)	0.18 (0; 1.53)	-4.13 (-4.80; -3.46)
		von Bertalanffy	0.99	1.77	1.89×10^{5} ($0; 1.46\times10^{6}$)	0.22 (0; 14.17)	59.07 (0; 442.29)	-4.12 (-4.78; -3.46)
		Exponential	0.83	3.20	0.05 (0; 0.24)	-0.76 (-3.91; 0)	-1.23 (-4.60; 0)	-0.36 (-2.27; 0)
		Hill	0.70	4.00	138.47 ($0; 1.34\times10^{3}$)	7.42 (0; 54.88)	8.38×10^{7} ($0; 4.59\times10^{8}$)	-5.22 (-10.00; -0.40)
		Michaelis Menten	0.16	5.27	1.16×10^{7} (5.34×10^{6}; 1.80×10^{7})	8.43×10^{6} ($0; 6.24\times10^{7}$)	-9.93 (-25.82; 0)	-
	Staphylococcus aureus	Exponential	0.66	0.50	0.19 (0; 0.70)	-0.34 (-0.68; 0)	-10.00 (-7.20; -10.00)	1.58 (0; 3.32)
		Logistic	0.65	0.48	6.10×10^{5} ($0; 3.38\times10^{4}$)	0 (1.66×10^{-14}; 4.01x10-^{14})	1.27 (0; 3.51)	0.78 (0; 1.75)

Mechanism of action	**Bacterial (sub)species**	**Model**	**Adjusted R^2**	**AIC**	Parameter value (95% confidence interval)			
					a	*b*	*c*	*d*
		Gompertz	0.56	0.43	2.34×10^6 ($0; 2.27 \times 10^7$	30.81 (0; 168.58)	0.10 (0; 0.94)	0.81 (0; 2.11)
		von Bertalanffy	0.56	0.40	1.08×10^5 ($0; 2.40 \times 10^5$)	0.09 (0; 0.82)	17.54 (0; 36.25)	0.83 (0; 2.04)
		Hill	0.52	-0.15	43.30 (0; 188.78)	6.54 (0; 57.49)	1.70×10^7 ($0; 1.26 \times 10^9$)	0.66 (0; 2.16)
		Michaelis Menten	0.47	1.35	3.30×10^5 ($0; 2.95 \times 10^6$)	7.59×10^5 ($0; 2.52 \times 10^6$)	-0.87 (-5.55; 0)	-
	Streptococcus pneumoniae	Exponential	0.99	2.07	2.17×10^{-4} ($0; 1.71 \times 10^{-3}$)	-1.31 (-2.16; -0.45)	-5.58 (-7.15; -4.01)	0.05 (0; 0.14)
		Logistic	0.99	2.03	3.00×10^{-3} (0; 0.02)	0 (1.64×10^{-14}; 3.86×10^{-14})	0.97 (0.54; 1.40)	-4.82 (-5.36; -4.28)
		Gompertz	0.98	2.02	4.79×10^5 ($0; 1.07 \times 10^6$)	21.35 (0; 111.67)	0.08 (0; 0.46)	-4.77 (-6.20; -3.35)
		von Bertalanffy	0.97	2.00	1.02×10^5 ($0; 6.02 \times 10^5$)	0.05 (0; 0.48)	8.94 (0; 79.72)	-4.70 (-5.89; -3.52)
		Hill	0.97	1.99	85.80 (0; 749.37)	6.85 (0; 37.20)	1.59×10^7 ($0; 1.54 \times 10^8$)	-4.77 (-6.02; -3.51)
		Michaelis Menten	0.62	2.00	2.68×10^6 ($0; 2.57 \times 10^7$)	2.64×10^6 ($0; 1.85 \times 10^7$)	-8.15 (-21.04; 0)	-
Oxacillin	*Staphylococcus aureus*	Logistic	0.95	1.95	0.11 (0; 0.36)	0 (1.68×10^{-14}; 3.95×10^{-14})	0.42 (0.16; 0.68)	-2.93 (-3.69; -2.17)
		Exponential	0.95	1.97	3.99×10^{-3} (0; 0.04)	-0.77 (-1.73; 0)	-3.20 (-4.31; -2.10)	0.08 (0; 0.23)
		Gompertz	0.93	1.94	1.75×10^5 ($0; 3.91 \times 10^5$)	14.84 (0; 77.64)	0.04 (0; 0.21)	-2.87 (-4.91; -0.83)
		Hill	0.92	1.92	4.06×10^3 ($0; 3.54 \times 10^4$)	3.29 (0; 10.63)	1.31×10^6 ($0; 1.27 \times 10^7$)	-2.69 (-3.39; -2.00)
		von Bertalanffy	0.92	1.92	1.58×10^4 ($0; 9.31 \times 10^4$)	0.01 (0; 0.01)	3.46 (0; 23.60)	-2.67 (-3.41; -1.92)
		Michaelis Menten	0.79	0.78	1.06×10^7 ($0; 1.02 \times 10^8$)	2.35×10^7 ($0; 1.64 \times 10^8$)	-3.82 (-5.01; -2.64)	-
	Streptococcus pneumoniae	Exponential	0.90	1.67	0 ($0; 1.28 \times 10^{-7}$)	-2.13 (-11.39; 0)	-9.17 (-18.54; 0)	0.23 (0; 0.50)
		Logistic	0.86	1.00	2.43 (0; 19.60)	0 (2.43×10^{-14}; 1.55×10^{-13})	0.15 (0; 0.71)	-8.38 (-30.17; 0)
		Michaelis Menten	0.84	-2.45	1.02×10^5 ($0; 6.93 \times 10^5$)	1.11×10^5 ($0; 5.71 \times 10^5$)	-7.51 (-15.62; 0)	-
		Gompertz	0.81	0.99	4.33×10^3 ($0; 2.26 \times 10^4$)	7.75 (0; 54.22)	0.03 (0; 0.07)	-7.85 (-40.94; 0)

Mechanism of action	**Bacterial (sub)species**	**Model**	**Adjusted R^2**	**AIC**	Parameter value (95% confidence interval)			
					a	*b*	*c*	*d*
		Hill	0.80	0.95	7.55 x10^4 (0; 3.08 x10^5)	1.74 (0; 292.58)	5.17 x10^5 (0; 1.49 x10^6)	-5.55 (-26.04; 0)
		von Bertalanffy	0.80	0.94	1.26 x10^3 (0; 6.83 x10^3)	0.01 (0; 0.02)	1.81 (0; 7.68)	-5.48 (-29.09; 0)
Vancomycin	*Staphylococcus aureus*	Exponential	0.84	1.96	2.70x10^{-5} (0; 6.00x10^{-5})	-1.32 (-6.03; 0)	-2.95 (-6.66; 0)	0.16 (0; 0.53)
		Logistic	0.83	1.91	0.04 (0; 0.30)	0 (4.28x10^{-15}; 2.82x10^{-14})	0.51 (0; 1.26)	-1.98 (-3.26; -0.70)
		Gompertz	0.77	1.91	4.81 x10^5 (0; 2.83 x10^6)	16.96 (0; 152.26)	0.04 (0; 0.36)	-1.94 (-6.19; 0)
		Hill	0.75	1.90	599.23 (0; 4.62 x10^3)	4.23 (0; 32.15)	1.85 x10^6 (0; 1.17 x10^8)	-1.81 (-3.20; -0.41)
		von Bertalanffy	0.75	1.90	4.10 x10^4 (0; 3.53 x10^5)	0.02 (0; 0.09)	4.55 (0; 12.68)	-1.78 (-3.32; -0.25)
		Michaelis Menten	0.69	1.33	2.50 x10^5 (0; 1.59 x10^6)	6.28 x10^5 (0; 2.39 x10^6)	-3.13 (-7.13; 0)	-
Inhibiting DNA replication: Ciprofloxacin	*Escherichia coli*	von Bertalanffy	0.93	2.07	0.95 (0.64; 1.26)	1.77 (0; 3.99)	4.10 x10^3 (0; 2.60 x10^4)	-0.38 (-0.61; -0.15)
		Gompertz	0.93	2.07	0.95 (0.64; 1.26)	4.10 x10^3 (0; 3.93 x10^4)	1.77 (0; 3.99)	-0.38 (-0.61; -0.15)
		Hill	0.92	2.06	0.99 (0.59; 1.39)	9.72 (0; 23.90)	5.47 x10^6 (2.51 x10^6; 8.43 x10^6)	-0.40 (-0.67; -0.13)
		Logistic	0.92	2.06	0 (0; 7.28x10^{-7})	0 (0; 6.08x10^{-7})	3.26 (0; 7.73)	-0.38 (-0.65; -0.12)
		Michaelis Menten	0.84	1.73	30.62 (0; 223.05)	148.92 (0; 895.94)	-0.91 (-2.22; 0)	-
		Exponential	0.80	2.04	9.06 (0; 80.90)	-4.00x10^{-3} (-0.03; 0)	-9.98 (-33.11; 0)	0.02 (0; 0.06)
	Nontyphoidal *Salmonella enterica* subsp. *enterica*	Gompertz	0.99	2.08	1.01 (0.99; 1.03)	1.69 x10^7 (0; 1.62, x10^8)	3.24 (1.36; 5.13)	0.64 (0.63; 0.65)
		von Bertalanffy	0.99	2.08	1.02 (0.97; 1.06)	2.66 (1.22; 4.11)	7.57 x10^5 (0; 6.65 x10^6)	0.64 (0.62; 0.66)
		Logistic	0.99	2.08	0 (0; 3.55x10^{-7})	0 (0; 4.42x10^{-7})	3.24 (2.20; 4.28)	0.63 (0.56; 0.70)
		Hill	0.95	2.07	1.13 (0.60; 1.66)	9.65 (0; 22.64)	8.86 x10^6 (4.06 x10^6; 1.37 x10^7)	0.61 (0.40; 0.81)
		Exponential	0.75	2.03	0.32 (0; 0.88)	-0.23 (-0.50; 0)	2.27 (0; 20.26)	1.68 (0; 5.56)

Mechanism of action	**Bacterial (sub)species**	**Model**	**Adjusted R^2**	**AIC**	Parameter value (95% confidence interval)			
					a	*b*	*c*	*d*
		Michaelis Menten	0.70	1.69	4.19 x10^4 (0; 3.06 x10^5)	2.07 x10^5 (0; 1.24 x10^6)	0.13 (0; 1.21)	-
	Streptococcus pneumoniae	Michaelis Menten	0.97	1.74	55.55 (0; 2.99 x10^3)	46.46 (0; 132.34)	-6.98 (-15.52; 0)	-
		von Bertalanffy	0.96	2.05	5.12 (0; 39.35)	0.63 (0; 2.55)	19.56 (0; 3.28 x10^3)	-3.72 (-15.23; 0)
		Gompertz	0.96	2.05	5.12 (0; 39.56)	21.43 (0; 184.06)	0.64 (0; 2.40)	-3.75 (-16.85; 0)
		Hill	0.96	2.05	5.61 (0; 53.55)	4.29 (0; 9.58)	1.37 x10^3 (0; 7.16 x10^3)	-3.96 (-18.73; 0)
		Logistic	0.95	2.05	0.14 (0; 1.31)	0.02 (0; 0.16)	0.77 (0; 7.66)	-4.66 (-41.76; 0)
		Exponential	0.94	2.04	2.87 (0; 25.09)	-0.08 (-0.70; 0)	-10.00 (-96.85; 0)	0.11 (0; 1.03)
Inhibiting protein synthesis: Gentamicin	*Escherichia coli*	Logistic	0.96	1.88	0.01 (0; 0.02)	0 (1.81x10^{-14}; 4.03 x10^{-14})	0.92 (0.42; 1.41)	-0.96 (-1.43; -0.49)
		Exponential	0.95	1.87	1.00 x10^{-3} (0; 0.03)	-1.12 (-2.32; 0)	-1.04 (-2.11; 0)	0.07 (0; 0.51)
		Gompertz	0.94	1.87	1.08 x10^5 (0; 7.85 x10^5)	18.84 (0; 153.80)	0.08 (0; 0.50)	-0.95 (-1.62; -0.27)
		Hill	0.94	1.86	691.06 (0; 4.49 x10^3)	6.01 (0; 18.34)	2.91 x10^7 (0; 1.47 x10^8)	-0.92 (-1.47; -0.37)
		von Bertalanffy	0.94	1.86	7.67 x10^4 (0; 7.59 x10^5)	0.04 (0; 0.20)	6.83 (0; 19.21)	-0.92 (-1.49; -0.34)
		Michaelis Menten	0.54	2.20	1.36 x10^7 (0; 5.70 x10^7)	2.48 x10^7 (0; 9.00 x10^7)	-2.22 (-4.25; -0.19)	-
	Nontyphoidal *Salmonella enterica* subsp. *enterica*	von Bertalanffy	0.97	2.03	4.55 (0; 10.09)	0.48 (0; 1.22)	27.48 (0; 141.18)	-2.07 (-2.47; -1.67)
		Gompertz	0.97	2.03	4.49 (0; 9.59)	30.79 (0; 143.11)	0.49 (0; 1.17)	-2.07 (-2.48; -1.66)
		Hill	0.96	2.03	4.52 (0; 10.39)	5.36 (0; 11.77)	5.72 x10^4 (0; 5.00 x10^5)	-2.11 (-2.57; -1.66)
		Logistic	0.96	2.02	0.01 (0; 0.07)	2.00 x10^{-3} (0; 1.60 x10^{-2})	0.83 (0; 1.83)	-2.19 (-2.84; -1.54)
		Exponential	0.95	2.01	7.70 (0; 74.49)	-0.15 (-1.43; 0)	-10.00 (-54.72; 0)	-0.12 (-1.12; 0)
		Michaelis Menten	0.84	1.30	3.92 x10^5 (0; 3.76 x10^6)	8.45 x10^5 (0; 5.91x10^5)	-3.56 (-6.14; -0.98)	-
	Staphylococcus aureus	Gompertz	0.94	2.23	15.62 (8.18; 23.06)	9.75x10^8 (0; 8.52 x10^9)	2.80 (0; 6.32)	-3.73 (-5.56; -1.91)
		von Bertalanffy	0.92	2.71	16.29 (0; 55.53)	2.40 (0; 18.07)	5.14 x10^7 (0; 3.96 x10^8)	-3.75 (-5.86; -1.64)

Mechanism of action	**Bacterial (sub)species**	**Model**	**Adjusted R^2**	**AIC**	Parameter value (95% confidence interval)			
					a	*b*	*c*	*d*
		Logistic	0.84	3.65	0 (0; 3.64x10^{-6})	0 (0; 7.55x10^{-8})	2.30 (0.36; 4.24)	-4.01 (-7.21; -0.81)
		Hill	0.76	4.13	41.72 (0; 403.40)	8.11 (0; 42.36)	5.55 x10^{7} (0; 3.04 x10^{8})	-4.29 (-9.07; 0)
		Exponential	0.75	4.21	0.51 (0; 2.24)	-0.51 (-2.21; 0)	-2.95 (-0.77; -5.13)	-0.26 (-1.41; 0)
		Michaelis Menten	0.41	5.35	2.86 x10^{6} 1.31 x10^{6}; 4.41 x10^{6})	1.39 x10^{6} (0; 1.03 x10^{7})	-11.53 (-42.26; 0)	-
	Streptococcus pneumoniae	Exponential	0.92	1.93	3.07 (0; 24.24)	-0.01 (-0.01; -3.00 x10^{-3})	-10.00 (-7.40; -10.00)	0.41 (0; 2.24)
		Michaelis Menten	0.92	1.58	17.73 (0; 79.15)	1.17 (0; 9.12)	-12.53 (-80.38; 0)	-
		Hill	0.89	1.94	4.70 (0; 17.87)	3.65 (0; 20.07)	84.20 (0; 808.37)	-1.82 (-11.13; 0)
		von Bertalanffy	0.89	1.94	4.45 (0; 18.08)	0.79 (0; 4.22)	9.45 (0; 28.43)	-1.71 (-13.02; 0)
		Gompertz	0.89	1.94	4.57 (0; 21.66)	9.93 (0; 533.81)	0.81 (0; 4.17)	-1.84 (-16.67; 0)
		Logistic	0.89	1.94	0.46 (0; 3.32)	0.08 (0; 0.47)	0.91 (0; 5.35)	-3.11 (-22.64; 0)
Linezolid	*Staphylococcus aureus*	Exponential	0.95	1.06	0.02 (0; 0.06)	-0.74 (-1.06; -0.42)	-10.00 (-7.08; -10.00)	1.47 (0; 2.93)
		Logistic	0.94	0.76	0.03 (0; 0.13)	0 (1.12x10^{-14}; 3.34x10^{-14})	0.69 (0.23; 1.15)	-0.24 (-1.66; 0)
		Gompertz	0.93	0.61	6.81 x10^{5} (3.12 x10^{5}; 1.05 x10^{6})	18.35 (0; 135.78)	0.06 (0; 0.15)	-0.17 (-0.27; -0.08)
		Hill	0.92	0.33	2.15 x10^{3} (0; 1.92 x10^{4})	5.31 (0; 19.82)	2.01 x10^{7} (0; 6.82 x10^{7})	-0.04 (-0.34; 0)
		von Bertalanffy	0.92	0.26	1.10 x10^{5} (0; 9.30 x10^{5})	0.03 (0.01; 0.05)	6.00 (0; 99.00)	3.00 x10^{-3} (0; 0.01)
		Michaelis Menten	0.68	3.32	8.53 x10^{5} (0; 5.55 x10^{6})	7.07 x10^{5} (0; 3.57 x10^{6})	-4.07 (-14.32; 0)	-
	Streptococcus pneumoniae	Michaelis Menten	0.94	1.52	326.71 (0; 701.40)	0.05 (0; 0.47)	-322.10 (-691.50; 0)	-
		Hill	0.94	1.88	208.28 (0; 1.79 x10^{3})	1.00 (0.37; 1.37)	0.08 (0; 0.31)	-203.63 (-1.75 x10^{3}; 0)
		von Bertalanffy	0.895	1.86	358.59 (0; 1.87 x10^{3})	0.34 (0; 2.38)	0.03 (0; 0.07)	-355.42 (-1.85 x10^{3}; 0)
		Gompertz	0.89	1.83	536.35	0.30	0.48	-533.58

Mechanism of action	**Bacterial (sub)species**	**Model**	**Adjusted R^2**	**AIC**	Parameter value (95% confidence interval)			
					a	*b*	*c*	*d*
					(0; 2.03 x10^3)	(0; 170.00)	(0; 2.86)	(-2.02 x10^3; 0)
		Logistic	0.88	1.83	369.50 (0; 1.99 x10^4)	4.52 (0; 12.86)	0.51 (0; 1.53)	-79.11 (-13.84; -144.38)
		Exponential	0.86	1.76	1.05 (0; 2.34)	-0.15 (-0.34; 0)	-10.00 (-50.68; 0)	0.43 (0; 2.26)

CFU – colony-forming units of the bacterial population. R^2 – coefficient of determination of the model. AIC – Akaike Information Criterion. A zero indicates a value ≤1 x 10^{-23}.

Supplementary Table 4. Relative fit and performance of the six mathematical models fitted using the least-squares method to the $\log_2$(MIC) vs. $\log_{10}$(CFU/mL) data for a representative isolate of each of the antimicrobial-bacterial (sub)species combinations. The studied combinations are detailed in Supplementary Table 1. The fit and performance are summarized across the four bacterial (sub)species by the mechanism of action of the antimicrobial drugs.

Mechanism of action	**Model**	**Fit: The adjusted R^2 is the highest or within 0.05 of the highest**	**Performance: The model-based estimate of the antimicrobial drug MIC's advancement-point density is within the observed range (the range for n=4 isolates per antimicrobial-(sub)species combination)**
Inhibiting cell wall synthesis	Gompertz	4/7 57%	4/7 57%
	Logistic	7/7 100%	5/7 71%
	von Bertalanffy	4/7 57%	3/7 43%
	Exponential	6/7 86%	1/7 14%
	Hill	3/7 43%	3/7 43%
	Michaelis Menten	0/7 0%	0/7 0%
Inhibiting DNA replication	Gompertz	3/3 100%	3/3 100%
	Logistic	3/3 100%	2/3 67%
	von Bertalanffy	3/3 100%	3/3 100%
	Exponential	1/3 33.333%	2/3 67%
	Hill	3/3 100%	3/3 100%
	Michaelis Menten	1/3 33%	1/3 33%
Mechanism of action	**Model**	**Fit: The adjusted R^2 is the highest or within 0.05 of the highest**	**Performance: The model-based estimate of the antimicrobial drug MIC's advancement-point density is within the observed range (the range for n=4 isolates per antimicrobial-(sub)species combination)**
Inhibiting protein synthesis	Gompertz	5/6 83%	4/6 67%
	Logistic	4/6 67%	1/6 17%
	von Bertalanffy	6/6 100%	3/6 50%

	Exponential	4/6 67%	1/6 17%
	Hill	5/6 83%	3/6 50%
	Michaelis Menten	2/6 33%	0/6 0%

CFU – colony-forming units of the bacterial population. R^2 – coefficient of determination of the model.

Supplementary Table 5. Relative fit and performance of the six mathematical models fitted using the least-squares method to the $\log_2$(MIC) vs. $\log_{10}$(CFU/mL) data for a representative isolate of each of the antimicrobial-bacterial (sub)species combinations. The studied combinations are detailed in Supplementary Table 1. The fit and performance are summarized across all the antimicrobial drugs for each of the bacterial (sub)species. CFU – colony-forming units of the bacterial population. R^2 – coefficient of determination of the model

Bacterial (sub)species	Model	Fit: The adjusted R^2 is the highest or within 0.05 of the highest	Performance: The model-based estimate of the antimicrobial drug MIC's advancement-point density is within the observed range (the range for n=4 isolates per antimicrobial-(sub)species combination)
Escherichia coli	Gompertz	3/3 100%	2/3 67%
	Logistic	3/3 100%	1/3 33%
	von Bertalanffy	3/3 100%	2/3 67%
	Exponential	2/3 67%	1/3 33%
	Hill	3/3 100%	2/3 67%
	Michaelis Menten	0/3 0%	1/3 33%
Nontyphoidal *Salmonella enterica* subsp. *enterica*	Gompertz	3/3 100%	3/3 100%
	Logistic	3/3 100%	2/3 67%
	von Bertalanffy	3/3 100%	3/3 100%
	Exponential	1/3 33%	0/3 0%
	Hill	2/3 67%	2/3 67%
	Michaelis Menten	0/3 0%	0/3 0%
Bacterial (sub)species	**Model**	**Fit: The adjusted R^2 is the highest or within 0.05 of the highest**	**Performance: The model-based estimate of the antimicrobial drug MIC's advancement-point density is within the observed range (the range for n=4 isolates per antimicrobial-(sub)species combination)**
Staphylococcus aureus	Gompertz	3/5 60%	3/5 60%
	Logistic	4/5 80%	3/5 60%
	von Bertalanffy	3/5 60%	3/5 60%
	Exponential	4/5 80%	1/5 20%
	Hill	2/5 40%	4/5 80%
	Michaelis Menten	0/5 0%	1/5 20%
Streptococcus pneumoniae	Gompertz	4/5 80%	2/5 40%
	Logistic	4/5 80%	2/5 40%
	von Bertalanffy	4/5 80%	2/5 40%
	Exponential	4/5 80%	2/5 40%
	Hill	4/5 80%	2/5 40%
	Michaelis Menten	3/5 60%	0/5 0%

Supplementary Table 6. Relative fit and performance of the six mathematical models fitted using the least-squares method to the $\log_2$(MIC) *vs.* $\log_{10}$(CFU/mL) data for a representative isolate of each of the antimicrobial-bacterial (sub)species combinations. The fit and performance are summarized across all the antimicrobial-bacterial (sub)species combinations studied. The combinations are detailed in Supplementary Table 1.

Model	**Fit: The adjusted R^2 is the highest or within 0.05 of the highest**	**Performance: The model-based estimate of the antimicrobial drug MIC's advancement-point density is within the observed range (the range for *n*=4 isolates per antimicrobial-(sub)species combination)**	**Overall model ranking (sum of the fit and performance rankings)**
Gompertz	13/16 81%	11/16 69%	24/32 75%
Logistic	14/16 88%	8/16 50%	22/32 69%
von Bertalanffy	13/16 81%	9/16 56%	22/32 69%
Hill	11/16 69%	9/16 56%	20/32 63%
Exponential	11/16 69%	3/16 19%	14/32 44%
Michaelis Menten	2/16 13%	1/16 6%	3/32 9%

CFU – colony-forming units of the bacterial population. R^2 – coefficient of determination of the model.

Curvature based definition of the MIC advancement-point bacterial density for the $\log_2$(MIC) *vs.* $\log_{10}$(CFU/mL) curve

We define $y = \log_2(\text{MIC})$ and $x = \log_{10}(\text{CFU/mL})$. Where MIC – minimum inhibitory concentration of the antimicrobial drug for the bacterial population density x, and CFU – colony-forming units of the bacterial population. We regress y on x (y and x are from experimental data for a bacterial isolate) using a non-linear mathematical model, we then use the fitted model to project the y vs. x curve. Conceptually, the advancement point (AP) is the density x after which the MIC increases most sharply. The advancement-point can be defined as the density x at which there is the maximum positive change in the y slope, and estimated using the curvature of the y *vs.* x curve projected by the fitted non-linear mathematical model. The curvature C (*120, 121*) at a density x is defined by: $C(x) = \frac{|y''(x)|}{\left(1+(y'(x))^2\right)^{\frac{3}{2}}}$. Then the MIC advancement-point density is:

$AP = \max_{\text{over all densities } x} C(x)$.

Curvature definitions for the curves projected by the six mathematical models

The model equations and parameter definitions are given in the materials and methods section of the manuscript.

Curvature for the Michaelis-Menten model:

$$C(x) = \frac{2\left|-\frac{a}{(x\ +\ b)^2} + \frac{ax}{(x\ +\ b)^3}\right|}{\left(1\ +\ \left(\frac{a}{x\ +\ b} - \frac{xz}{(x\ +\ b)^2}\right)^2\right)^{\frac{3}{2}}}$$

Curvature for the Hill-function based model:

$$C(x) = \frac{\left|\frac{ax^b b^2}{x^2(x^b + c)} - \frac{ax^b b}{x^2(x^b + c)} - \frac{3a(x^b)^2 b^2}{x^2(x^b + c)^2} + \frac{2a(x^b)^3 b^2}{(x^b + c)^3 x^2} + \frac{a(x^b)^2 b}{x^2(x^b + c)^2}\right|}{\left(1 + \left(\frac{ax^b b}{x(x^b + c)} - \frac{a(x^b)^2 b}{(x^b + c)^2 x)}\right)^2\right)^{\frac{3}{2}}}$$

Curvature for the logistic model:

$$C(x) = \frac{\left|\frac{2ac^2(\exp(-cx))^2}{(b + \exp(-cx))^3} - \frac{ac^2 \exp(-cx)}{(b + \exp(-cx))^2}\right|}{\left(1 + \frac{a^2c^2(\exp(-cx))^2}{(b + \exp(-cx))^4}\right)^{\frac{3}{2}}}$$

Curvature for the Gompertz model:

$$C(x) = \frac{|(-abc^2 \exp(-cx)\exp(-b\exp(-cx)) + ab^2c^2(\exp(-cx))^2 \exp(-b\exp(-cx))|}{(1 + a^2b^2c^2(\exp(-cx))^2(\exp(-b\exp(-cx)))^2)^{\frac{3}{2}}}$$

Curvature for the von Bertalanffy model:

$$C(x) = \frac{\left|\frac{a(1 - \exp(-bx))^c(\exp(-bx))^2(c^2b^2 - cb^2)}{(1 - \exp(-bx))^2} - \frac{a(1 - \exp(-bx))^c cb^2 \exp(-bx)}{1 - \exp(-bx)}\right|}{\left(1 + \frac{a^2((1 - \exp(-bx))^c)^2c^2b^2(\exp(-bx))^2}{(1 - \exp(-bx))^2}\right)^{\frac{3}{2}}}$$

Curvature for the exponential model:

$$C(x) = \frac{|ab^2 \exp(-bx) + cd^2 \exp(-dx)|}{(1 + (-ab\exp(-bx) - cd\exp(-dx))^2)^{\frac{3}{2}}}$$

References

1. CDC, "Antibiotic resistance threats in the United States.," (U.S. Department of Health and Human Services, Atlanta, Georgia, 2019).
2. M. G. Papich, Pharmacokinetic–pharmacodynamic (PK–PD) modeling and the rational selection of dosage regimes for the prudent use of antimicrobial drugs. *Veterinary Microbiology* **171**, 480-486 (2014).
3. CDC, Antibiotic resistance threats in the United States, 2013., (2013).
4. R. Aminov, History of antimicrobial drug discovery: Major classes and health impact. *Biochem Pharmacol* **133**, 4-19 (2017).
5. J. Davies, D. Davies, Origins and evolution of antibiotic resistance. *Microbiol Mol Biol Rev* **74**, 417-433 (2010).
6. R. I. Aminov, A brief history of the antibiotic era: lessons learned and challenges for the future. *Front Microbiol* **1**, 134 (2010).
7. R. Gehring, J. E. Riviere, Limitations of MIC as the sole criterion in antimicrobial drug dosage regimen design: the need for full characterization of antimicrobial pharmacodynamic profile especially for drug-resistant organisms. . *Veterinary Journal* **198**, 15-18 (2013).
8. P. L. Toutain, J. R. E. del Castillo, A. Bousquet-Mélou, The pharmacokinetic–pharmacodynamic approach to a rational dosage regimen for antibiotics. *Res in Vet Sci* **73**, 105-114 (2002).
9. X. Wen, R. Gehring, A. Stallbaumer, J. E. Riviere, V. V. Volkova, Limitations of MIC as sole metric of pharmacodynamic response across the range of antimicrobial susceptibilities within a single bacterial species. *Scientific Reports* **6**, 37907 (2016).
10. World Health Organization, Highest Priority Critically Important Antimicrobials. (2019).
11. W. H. Organization, "Antimicrobial Resistance Global Report on Surveillance," (World Health Organization World Health Organization, 2014).
12. CDC, "Surveillance for Foodborne Disease Outbreaks, United States, 2011, Annual Report," (US Department of Health and Human Services, Atlanta, Georgia, 2011).
13. P. Ankomah, B. R. Levin, Exploring the collaboration between antibiotics and the immune response in the treatment of acute, self-limiting infections. *Proceedings of the National Academy of Sciences of the United States of America* **111**, 8331-8338 (2014).
14. J. M. Munita, C. A. Arias, Mechanisms of Antibiotic Resistance. *Microbiol Spectr* **4**, (2016).
15. J. Strahilevitz, G. A. Jacoby, D. C. Hooper, A. Robicsek, Plasmid-mediated quinolone resistance: A multifaceted threat. *Clin. Microbiol. Rev.* **22**, 664−689 (2009).
16. R. A. Bonomo, β-Lactamases: A Focus on Current Challenges. *Cold Springs Harbor Perspectives in Medicine*, (2016).
17. R. R. Uchil, G. S. Kohli, V. M. Katekhaye, O. C. Swam, Strategies to Combat Antimicrobial Resistance. *J Clin Diagn Res.* **8**, (2014).
18. D. J. Morgan, I. N. Okeke, R. Laxminarayan, E. N. Perencevich, S. Weisenberg, Non-prescription antimicrobial use worldwide: a systematic review. *Lancet Infect Dis* **11**, 692-701 (2011).
19. N. K. Ganguly *et al.*, Rationalizing antibiotic use to limit antibiotic resistance in India. *Indian J Med Res.* **134**, 281-294 (2011).
20. Z. C. Conley, T. J. Bodine, A. Chou, L. Zechiedrich, Wicked: The untold story of ciprofloxacin. *PLOS Pathogens* **14**, (2018).

21. A.B. Khodursky, E.L. Zechiedrich, N.R. Cozzarelli (Proc Natl Acad Sci U S A . , 2020), vol. 92, pp. 11801-11805.
22. Kreuzer KN, C. NR., E*scherichia coli* mutants thermosensitive for deoxyribonucleic acid gyrase subunit A: effects on deoxyribonucleic acid replication, transcription, and bacteriophage growth. Journal of Bacteriology **140,** 424-435 (1975).
23. X. Zhao, H. Y., K. Drlica, Moving forward with reactive oxygen species involvement in antimicrobial lethality. *Journal of Antimicrobial Chemotherapy* **70**, 639-642 (2015).
24. R. Davis, A. Markham, J. A. Balfour, Ciprofloxacin. An updated review of its pharmacology, therapeutic efficacy and tolerability. *Drugs* **51**, 1019-1074 (1996).
25. P. Heisig, Type II topoisomerases—inhibitors, repair mechanisms and mutations. *Mutagenesis* **24**, 465-469 (2009).
26. K. J. Aldred, R. J. Kerns, N. Osherof, Mechanism of Quinolone Action and Resistance. *Current Topics in Biochemistry* **53**, 1565−1574 (2014).
27. K. J. Aldred, R. J. Kerns, N. Osherof, Mechanism of Quinolone Action and Resistance. *Current Topics in Biochemistry* **53**, 1565−1574 (2014).
28. K. Drlica *et al.*, Quinolones: Action and resistance updated. *Curr. Top. Med. Chem* **9**, 981−998 (2009).
29. D. C. Hooper, Mode of action of fluoroquinolones. *Drugs* **58 Suppl 2**, 6-10 (1999).
30. D. C. Hooper, Mechanisms of action of antimicrobials: Focus on fluoroquinolones. *Clin. Infect. Dis* **32**, S9−S15 (2001).
31. V. E. Anderson, N. Osheroff, Type II topoisomerases as targets for quinolone antibacterials: Turning Dr. Jekyll into Mr. Hyde. *Curr. Pharm. Des.* **7**, 337−353 (2001).
32. B. Fournier, X. Zhao, T. Lu, K. Drlica, D. C. Hooper, Selective targeting of topoisomerase IV and DNA gyrase in Staphylococcus aureus: Different patterns of quinolone-induced inhibition of DNA synthesis. *Antimicrob. Agents Chemother.* **44**, 2160−2165 (2000).
33. L. B. Price *et al.*, In vitro selection and characterization of Bacillus anthracis mutants with high-level resistance to ciprofloxacin. *Antimicrob. Agents Chemother* **47**, 2362−2365 (2003).
34. S. K. Morgan-Linnell, L. Becnel Boyd, D. Steffen, L. Zechiedrich, Mechanisms accounting for fluoroquinolone resistance in Escherichia coli clinical isolates. *Antimicrob. Agents Chemother.* **53**, 235−241 (2009).
35. K. Drlica, X. Zhao, DNA gyrase, topoisomerase IV, and the 4-quinolones. *Microbiol. Mol. Biol. Rev.* **61**, 377−392 (1997).
36. Z. Li *et al.*, Alteration in the GyrA subunit of DNA gyrase and the ParC subunit of DNA topoisomerase IV in quinolone-resistant clinical isolates of Staphylococcus epidermidis. *Antimicrob. Agents Chemother* **42**, 3293−3295 (1998).
37. A. Robicsek *et al.*, Fluoroquinolone-modifying enzyme: A new adaptation of a common aminoglycoside acetyltransferase. *Nat. Med.* **12**, 83-88 (2006).
38. T. Guillard *et al.*, Ciprofloxacin treatment failure in a murine model of pyelonephritis due to an AAC(6′)-Ib-cr-producing Escherichia coli strain susceptible to ciprofloxacin in vitro. *Antimicrob. Agents Chemother.* **57**, 5830-5835 (2013).
39. L. Martinez-Martinez, A. Pascual, G. A. Jacoby, Quinolone resistance from a transferable plasmid. *Lancet Infect Dis* **351**, 797−799 (1998).
40. M. Wang *et al.*, Plasmid-mediated quinolone resistance in clinical isolates of Escherichia coli from Shanghai, China. *Antimicrob. Agents Chemother* **47**, 2242−2248 (2003).

41. A. Robicsek, G. A. Jacoby, D. C. Hooper, The worldwide emergence of plasmid-mediated quinolone resistance. *Lancet Infect. Dis* **6**, 629−640 (2006).
42. J. H. Tran, G. A. Jacoby, Mechanism of plasmidmediated quinolone resistance. *Proc. Natl. Acad. Sci. U.S.A* **99**, 5638−5642 (2002).
43. X. Xiong, E. H. Bromley, P. Oelschlaeger, D. N. Woolfson, J. Spencer, Structural insights into quinolone antibiotic resistance mediated by pentapeptide repeat proteins: Conserved surface loops direct the activity of a Qnr protein from a Gram-negative bacterium. *Nucleic Acids Res.* **39**, 3917−3927 (2011).
44. J. H. Tran, G. A. Jacoby, D. C. Hooper, Interaction of the plasmid-encoded quinolone resistance protein Qnr with Escherichia coli DNA gyrase. *Antimicrob. Agents Chemother.* **49**, 118−125 (2005).
45. J. H. Tran, G. A. Jacoby, D. C. Hooper, Interaction of the plasmid-encoded quinolone resistance protein QnrA with Escherichia coli topoisomerase IV. *Antimicrob. Agents Chemother.* **49**, (2005).
46. K. Yamane *et al.*, New plasmid-mediated fluoroquinolone efflux pump, QepA, found in an Escherichia coli clinical isolate. *Antimicrob. Agents Chemother.* **51**, 3354-3360 (2007).
47. V. Cattoir, L. Poirel, P. Nordmann, Plasmid mediated quinolone resistance pump QepA2 in an Escherichia coli isolate from France. *Antimicrob. Agents Chemother.* **52**, 3801−3804 (2008).
48. D. M. Richards, R. C. Heel, R. N. Brogden, T. M. Speight, G. S. Avery, Ceftriaxone. A review of its antibacterial activity, pharmacological properties and therapeutic use. *Drugs* **27**, 469-527 (1984).
49. Sandoz. (Sandoz Inc., Princeton, NJ, 2013) https://www.accessdata.fda.gov/drugsatfda_docs/label/2014/065169s022lbl.pdf.
50. Sigma, "Biofiles- Inhibition of Cell Wall Biosynthesis by Antibiotics," *Biofiles* https://www.sigmaaldrich.com/technical-documents/articles/biofiles/how-antibiotics-work.html (2006).
51. K. Bush, Bench-to-bedside review: The role of β-lactamases in antibiotic-resistant Gram-negative infections. *Critical Care* **14**, (2010).
52. E. P. Abraham, E. Chain, An enyzme from bacteria able to destroy penicillin. *Nature* **146**, (1940).
53. J. G. Bush K, Medeiros AA, A functional classification scheme for β-lactamases and its correlation with molecular structure. *Antimicrob Agents Chemother* **39**, 1211-1233 (1995).
54. K. Bush, G. A. Jacoby, An updated functional classification of β-lactamases. *Antimicrob Agents Chemother* **54**, 969-976 (2010).
55. R.P. Ambler, The structure of β-lactamases. *Philos Trans R Soc Lond B Biol Sci* **289**, 321-331 (1980).
56. B. Jaurin, T. Grundstrom, ampC cephalosporinase of Escherichia coli K-12 has a diff erent evolutionary origin from that of β-lactamases of the penicillinase type. *Proc Natl Acad Sci USA* **78**, 4897-4901 (1981).
57. P. Huovinen, S. Huovinen, G. A. Jacoby, Sequence of PSE-2 beta-lactamase. *Antimicrob Agents Chemother* **32**, 134-136 (1988).
58. G. A. Jacoby, B-Lactamase Nomenclature. *Antimicrobial Agents and Chemotherapy* **50**, 1123-1129 (2006).

59. K. M. Papp-Wallace, A. Endimiani, M. A. Taracila, R. A. Bonomo, Carbapenems: Past, present, and future. *Antimicrob Agents Chemother* **55**, 4943-4960 (2011).
60. S. M. Drawz, R. A. Bonomo, Three decades of β-lactamase inhibitors. *Clin Microbiol Rev* **23**, 160-201 (2010).
61. J. Bigger, Treatment of staphylococcal infections with penicillin by intermittent sterilisation. . *Lancet Infect Dis* **244**, 497-500 (1944).
62. J. Kester, S. Fortune, Persisters and beyond: Mechanisms of phenotypic drug resistance and drug tolerance in bacteria. *Critical Reviews in Biochemistry and Molecular Biology* **49**, 91-101 (2014).
63. N. Q. Balaban, J. Merrin, R. Chait, L. Kowalik, S. Leibler, Bacterial persistence as a phenotypic switch. *Science* **305**, 1622-1625 (2004).
64. B. Levin, J. Concepcion-Acevedo, K. Udekwu, Persistence: a copacetic and parsimonious hypothesis for the existence of non-inherited resistance to antibiotics. *Curr Opin Microbiol*, (2014), pp. 18-21.
65. I. Levin-Reisman, N. Q. Balaban, Quantitative Measurements of Type I and Type II Persisters Using ScanLag. *Methods in Molecular Biology* **1333**, (2016).
66. H. Luidalepp, A. Jõers, N. Kaldalu, T. Tenson, Age of inoculum strongly influences persister frequency and can mask effects of mutations implicated in altered persistence. *J. Bacteriol* **193**, 3598–3605 (2011).
67. P. J. Johnson, B. R. Levin, Pharmacodynamics, population dynamics, and the evolution of persistence in Staphylococcus aureus. *PLoS Genet* **9**, e1003123 (2013).
68. B. W. Kwan, J. A. Valenta, M. J. Benedik, T. K. Wood, Arrested protein synthesis increases persister-like cell formation. *Antimicrob. Agents Chemother.* **57**, 1468–1473 (2013).
69. P. L. Toutain, P. Lees, Integration and modelling of pharmacokinetic and pharmacodynamic data to optimize dosage regimens in veterinary medicine. *J Vet Pharmacol Ther* **27**, 467-477 (2004).
70. G. L. Drusano, Antimicrobial pharmacodynamics:critical interactions of 'bug and drug'. *Nature Reviews-Microbiology* **2**, 289-300 (2004).
71. H. R. Meredith, J. K. Srimani, A. J. Lee, A. J. Lopatkin, L. You, Collective antibiotic tolerance: mechanisms, dynamics and intervention. *Nat Chem Biol* **11**, 182-188 (2015).
72. R. R. Regoes *et al.*, Pharmacodynamic functions: a multiparameter approach to the design of antibiotic treatment regimens. *Antimicrobial Agents and Chemotherapy* **48**, 3670-3676 (2004).
73. H. Eagle, R. Fleischman, M. Levy, Continuous vs. Discontinuous Therapy with Penicillin — The Effect of the Interval between Injections on Therapeutic Efficacy. *N Engl J Med* **248**, 481-488 (1953).
74. S. Goutelle *et al.*, The Hill equation: a review of its capabilities in pharmacological modelling. *Fundamental and Clinical Pharmacology* **22**, 633-648 (2008).
75. X. Wen *et al.*, Variation in fluoroquinolone pharmacodynamic parameter values among isolates of two bacterial pathogens of bovine respiratory disease. *Scientific Reports* **8**, 10553 (2018).
76. P. Ankomah, P. J. Johnson, B. R. Levin, The pharmaco -, population and evolutionary dynamics of multi-drug therapy: experiments with S. aureus and E. coli and computer simulations. *PLOS Pathogens* **9**, (2013).

77. D. Czock, F. Keller, Mechanism-based pharmacokinetic-pharmacodynamic modeling of antimicrobial drug effects. *J Pharmacokinet Pharmacodyn* **34**, 727-751 (2007).
78. A. Ahmad *et al.*, Pharmacodynamic modelling of in vitro activity of tetracycline against a representative, naturally occurring population of porcine Escherichia coli. *Vet Scand Acta* **57**, (2015).
79. F. Keller, M. Giehl, D. Czock, D. Zellner, PK-PD curve-fitting problems with the Hill equation? Try one of the 1-exp functions derived from Hodgkin, Douglas or Gompertz. *International Journal of Clinical Pharmacology and Therapeutics* **40**, 23-29 (2002).
80. CLSI, Methods for dilution antimicrobial susceptibility tests for bacteria that grow aerobically; Approved standard - 10th ed. (CLSI document M07-A10) Clinical and Laboratory Standards Institute, 940 West Valley Road, Suite 1400, Wayne, PA, USA. (2015).
81. A. J. Lee *et al.*, Robust, linear correlations between growth rates and beta-lactam-mediated lysis rates. *Proceedings of the National Academy of Sciences of the United States of America* **115**, 4069-4074 (2018).
82. L. S. Garcia, Clinical microbiology procedures handbook. 3rd ed. Edited by L. S. Garcia. Volume 2, Chapter 5. Antimicrobial Susceptibility Testing. ASM Press. Washington, DC, USA. (2010).
83. M. E. Levison, Pharmacodynamics of antimicrobial drugs. *Infectious disease clinics of North America* **18**, 451-465, vii (2004).
84. P. Lees, F. Shojaee Aliabadi, Rational dosing of antimicrobial drugs: animals versus humans. *International journal of antimicrobial agents* **19**, 269-284 (2002).
85. M. Mueller, A. de la Pena, H. Derendorf, Issues in pharmacokinetics and pharmacodynamics of anti-infective agents: kill curves versus MIC. *Antimicrobial Agents and Chemotherapy* **48**, 369-377 (2004).
86. J. M. Blondeau, G. Hansen, K. Metzler, P. Hedlin, The role of PK/PD parameters to avoid selection and increase of resistance: mutant prevention concentration. *Journal of chemotherapy* **16 Suppl 3**, 1-19 (2004).
87. D. G. McClary *et al.*, Relationship of *in vitro* minimum inhibitory concentrations of tilmicosin against *Mannheimia haemolytica* and *Pasteurella multocida* and *in vivo* tilmicosin treatment outcome among calves with signs of bovine respiratory disease. *Journal of the American Veterinary Medical Association* **239**, 129-135 (2011).
88. P. Mastroeni, A. Grant, O. Restif, D. Maskell, A dynamic view of the spread and intracellular distribution of *Salmonella enterica*. *Nature reviews. Microbiology* **7**, 73-80 (2009).
89. J. Chastre *et al.*, Evaluation of bronchoscopic techniques for the diagnosis of nosocomial pneumonia. *American journal of respiratory and critical care medicine* **152**, 231-240 (1995).
90. C. Konig, H. P. Simmen, J. Blaser, Bacterial concentrations in pus and infected peritoneal fluid--implications for bactericidal activity of antibiotics. *The Journal of antimicrobial chemotherapy* **42**, 227-232 (1998).
91. M. Sheppard *et al.*, Dynamics of bacterial growth and distribution within the liver during *Salmonella* infection. *Cellular Microbiology* **5**, 593-600 (2003).
92. H. Smith, Questions about the behaviour of bacterial pathogens in vivo. *Philos Trans R Soc Lond B Biol Sci* **355**, 551-564 (2000).

93. W. E. Feldman, Concentrations of bacteria in cerebrospinal fluid of patients with bacterial meningitis. *Journal of Pediatrics* **88**, 549-552 (1976).
94. A. F. Read, T. Day, S. Huijben, The evolution of drug resistance and the curious orthodoxy of aggressive chemotherapy. *Proceedings of the National Academy of Sciences of the United States of America* **108 Suppl 2**, 10871-10877 (2011).
95. I. Brook, Inoculum effect. *Reviews of Infectious Diseases* **11**, 361-368 (1989).
96. K. L. LaPlante, M. J. Rybak, Impact of high-inoculum Staphylococcus aureus on the activities of nafcillin, vancomycin, linezolid, and daptomycin, alone and in combination with gentamicin, in an in vitro pharmacodynamic model. *Antimicrob Agents Chemother* **48**, 4665-4672 (2004).
97. D. S. Burgess, R. G. Hall, 2nd, In vitro killing of parenteral beta-lactams against standard and high inocula of extended-spectrum beta-lactamase and non-ESBL producing Klebsiella pneumoniae. *Diagnostic microbiology and infectious disease* **49**, 41-46 (2004).
98. E. Bidlas, T. Du, R. J. Lambert, An explanation for the effect of inoculum size on MIC and the growth/no growth interface. *International journal of food microbiology* **126**, 140-152 (2008).
99. K. I. Udekwu, N. Parrish, P. Ankomah, F. Baquero, B. R. Levin, Functional relationship between bacterial cell density and the efficacy of antibiotics. *The Journal of antimicrobial chemotherapy* **63**, 745-757 (2009).
100. A. S. Kesteman *et al.*, Influence of inoculum size and dosing regimen on the selection of marbofloxacin resistant mutants in experimental rat Klebsiella pneumoniae lung infection. *J Vet Pharmacol Ther* **32**, 63-63 (2009).
101. R. Singh *et al.*, Pharmacodynamics of moxifloxacin against a high inoculum of Escherichia coli in an in vitro infection model. *The Journal of antimicrobial chemotherapy* **64**, 556-562 (2009).
102. W. M. Kirby, Bacteriostatic and lytic actions of penicillin on sensitive and resistant *Staphylococci*. *J Clin Invest* **24**, 165-169 (1945).
103. H. Eagle, Experimental approach to the problem of treatment failure with penicillin. I. Group A streptococcal infection in mice. *Am J Med* **13**, 389-399 (1952).
104. A. Bryskier, Roxithromycin: review of its antimicrobial activity. *The Journal of antimicrobial chemotherapy* **41 Suppl B**, 1-21 (1998).
105. R. C. Tilton, L. Lieberman, E. H. Gerlach, Microdilution antibiotic susceptibility test: examination of certain variables. *Applied microbiology* **26**, 658-665 (1973).
106. V. H. Tam, K. R. Ledesma, K. T. Chang, T. Y. Wang, J. P. Quinn, Killing of *Escherichia coli* by beta-lactams at different inocula. *Diagnostic microbiology and infectious disease* **64**, 166-171 (2009).
107. J. F. Chantot, A. Bryskier, J. C. Gasc, Antibacterial activity of roxithromycin: a laboratory evaluation. *J Antibiot (Tokyo)* **39**, 660-668 (1986).
108. K. S. Thomson, E. S. Moland, Cefepime, piperacillin-tazobactam, and the inoculum effect in tests with extended-spectrum beta-lactamase-producing Enterobacteriaceae. *Antimicrob Agents Chemother* **45**, 3548-3554 (2001).
109. T. Butler, Effect of increased inoculum of *Salmonella typhi* on MIC of azithromycin and resultant growth characteristics. *The Journal of antimicrobial chemotherapy* **48**, 903-906 (2001).
110. T. Butler, R. W. Frenck, R. B. Johnson, R. Khakhria, *In vitro* effects of azithromycin on *Salmonella typhi*: early inhibition by concentrations less than the MIC and reduction of

MIC by alkaline pH and small inocula. *The Journal of antimicrobial chemotherapy* **47**, 455-458 (2001).
111. F. Muhammad, M. Jaberi-Douraki, D. P. de Sousa, J. E. Riviere, Modulation of chemical dermal absorption by 14 natural products: a quantitative structure permeation analysis of components often found in topical preparations. *Cutan Ocul Toxicol* **36**, 237-252 (2017).
112. J. F. Andrews, A mathematical model for the continuous culture of microorganisms utilizing inhibitory substrates. *Biotechnology and Bioengineering* **10**, 707-723 (1968).
113. D. Czock, C. Markert, B. Hartman, F. Keller, Pharmacokinetics and pharmacodynamics of antimicrobial drugs. *Expert Opinion on Drug Metabolism and Toxicology* **5**, 475-487 (2009).
114. M. I. Stefan, N. Le Novere, Cooperative binding. *PLoS Computational Biology* **9**, e1003106 (2013).
115. M. Peleg, M. G. Corradini, Microbial growth curves: what the models tell us and what they cannot. *Critical reviews in food science and nutrition* **51**, 917-945 (2011).
116. J. L. Maino, M. R. Kearney, The universality of the von Bertalanffy growth curve: Comment on: "Physics of metabolic organization" by Marko Jusup et al. *Physics of Life Reviews* **20**, 63-65 (2017).
117. A. J. Fabens, Properties and fitting of the bon Bertalanffy growth curve. *Growth* **29**, 265-289 (1965).
118. J. Karslake, J. Maltas, P. Brumm, K. B. Wood, Population density modulates drug inhibition and gives rise to potential bistability of treatment outcomes for bacterial infections. *PLoS Comput Biol* **12**, e1005098 (2016).
119. G. A. Shultz, R. B. Schnabel, R. H. Byrd, A family of trust-region-based algorithms for unconstrained minimization with strong global convergence properties. *SIAM Journal on Numerical Analysis* **22**, 47-67 (1985).
120. S. Sternberg, *Curvature in mathematics and physics*. Dover Books on Mathematics (Dover Publications, Inc., New York, NY, U.S., 2012).
121. J. Stewart, *Single variable calculus: Early transcendentals, 8th ed.*, (Cengage Learning, Boston, MA, U.S., 2015).
122. M. A. Kohanski, D. J. Dwyer, B. Hayete, C. A. Lawrence, J. J. Collins, A common mechanism of cellular death induced by bactericidal antibiotics. *Cell* **130**, 797-810 (2007).
123. M. A. Lobritz *et al.*, Antibiotic efficacy is linked to bacterial cellular respiration. *Proceedings of the National Academy of Sciences of the United States of America* **112**, 8173-8180 (2015).
124. S. M. Swaney, H. Aoki, M. C. Ganoza, D. L. Shinabarger, The oxazolidinone linezolid inhibits initiation of protein synthesis in bacteria. *Antimicrob Agents and Chemotherapy* **42**, 3251-3255 (1998).
125. L. D. Dresser, M. J. Rybak, The pharmacologic and bacteriologic properties of oxazolidinones, a new class of synthetic antimicrobials. *Pharmacotherapy* **18**, 456-462 (1998).
126. W. A. Craig, S. M. Bhavnani, P. G. Ambrose, The inoculum effect: fact or artifact? *Diagnostic microbiology and infectious disease* **50**, 229-230 (2004).
127. D. L. Stevens, S. Yan, A. E. Bryant, Penicillin-binding protein expression at different growth stages determines penicillin efficacy *in vitro* and *in vivo*: an explanation for the inoculum effect. *J Infect Dis* **167**, 1401-1405 (1993).

128. B. A. Espedido, I. B. Gosbell, Chromosomal mutations involved in antibiotic resistance in Staphylococcus aureus. *Front Biosci (Schol Ed)* **4**, 900-915 (2012).
129. C. Watanakunakorn, Mode of action and *in-vitro* activity of vancomycin. *The Journal of antimicrobial chemotherapy* **14 Suppl D**, 7-18 (1984).
130. D. J. Waxman, R. R. Yocum, J. L. Strominger, Penicillins and cephalosporins are active site-directed acylating agents: evidence in support of the substrate analogue hypothesis. *Philos Trans R Soc Lond B Biol Sci* **289**, 257-271 (1980).
131. D. J. Waxman, J. L. Strominger, Penicillin-binding proteins and the mechanism of action of beta-lactam antibiotics. *Annu Rev Biochem* **52**, 825-869 (1983).
132. C. C. Sanders, Ciprofloxacin: *in vitro* activity, mechanism of action, and resistance. *Reviews of Infectious Diseases* **10**, 516-527 (1988).
133. M. P. Mingeot-Leclercq, Y. Glupczynski, P. M. Tulkens, Aminoglycosides: activity and resistance. *Antimicrob Agents Chemother* **43**, 727-737 (1999).
134. D. M. Livermore, Linezolid *in vitro*: mechanism and antibacterial spectrum. *The Journal of antimicrobial chemotherapy* **51 Suppl 2**, ii9-16 (2003).
135. C. Tan *et al.*, The inoculum effect and band-pass bacterial response to periodic antibiotic treatment. *Mol Syst Biol* **8**, 617 (2012).